A Method to Discriminate Between Flicker Sources

by

Daniel Lee Geiger II

A dissertation submitted to the Graduate Faculty of
Auburn University
in partial fulfillment of the
requirements for the Degree of
Doctor of Philosophy

Auburn, Alabama
August 1, 2015

Keywords: Flickermeter, RMS Flicker Calculation
Impedance Estimation, Flicker Distinguisher, Flicker Discriminator

Approved by

S. Mark Halpin, Chair, Alabama Power Company Distinguished Professor of Electrical and Computer Engineering
R. Mark Nelms, Professor and Chair of Electrical and Computer Engineering
Charles A. Gross, Professor Emeritus of Electrical and Computer Engineering
John Hung, Professor of Electrical and Computer Engineering

Abstract

This work is a discussion on discriminating between multiple flicker producing sources that are connected electrically close together in the power system. IEC 61000-4-15 provides a thorough description on how to build a device that measures voltage fluctuations and outputs a number that corresponds to customer irritation to the amount of voltage fluctuation present in the power system. IEEE has adopted IEC 61000-4-15 in IEEE 1453. The input to the flicker measuring device (flickermeter) is time sampled voltage data. It will be shown that it is acceptable to use full cycle RMS values as the input to the flickermeter when the voltage fluctuations are of a relatively low frequency. The RMS values will be held constant on the input of the meter for a full cycle. If the sampling frequency of the voltage is 64 samples per cycle, then the full cycle RMS value would be held constant to the flickermeter input for 64 samples. This allows the flickermeter to operate such that it does not matter to the meter whether the input values are time sampled or RMS values; the flickermeter treats the data as time sampled data.

Flicker sources that are connected electrically close together could significantly impact the voltage at the terminals of each other. The flickermeter can determine the amount of flicker that is present in the power system via voltage measurements, but it is not able to determine the amount of flicker that a particular flicker producing source is generating. It will be shown that it is possible to calculate the equivalent voltage at the load of interest which corresponds to the voltage that the load would have if the other

flicker producing sources were not connected to the power system. This will be accomplished by measuring the load's voltage and current to determine the complex power that is being absorbed by the load. A power flow is performed using the load's complex power to calculate the equivalent load voltage. The calculated voltage is an RMS value, valid for a full cycle, and is used as the input to the flickermeter. By using this equivalent voltage with the flickermeter, it is possible to determine the amount of flicker sensation that is due to a particular flicker producing source while ignoring flicker sensation that is produced by other flicker producing sources that are electrically close.

The power flow that is performed to determine the equivalent voltage at the load is a two bus power flow where the source is treated as the slack bus. It is necessary to know what the Thévenin impedance is at the load to be able to calculate a valid voltage for the load using the power flow. If the impedance that is utilized is wrong, then the resulting voltage that is calculated will be incorrect. There is an approximate impedance that is known by the utility company, but this impedance will fluctuate based on the present power system operation. A method for determining the Thévenin impedance will be discussed such that it will be possible to perform the two bus power flow and calculate an accurate voltage.

Demonstration of the concepts required at each step of the design process will be provided that validate the approach described in building a device that can determine the amount of voltage flicker being produced by a load when other flicker producing loads are connected electrically close together. Measurement results will also be provided from a device that has been implemented in hardware that utilizes the discussed concepts to measure the amount of flicker sensation that is due to a particular load of interest when

there are multiple flicker producing loads connected. The measurement results consist of months of data that was collected at multiple sites that will substantiate the claims associated with the steps involved in building the flicker discriminating device.

In summary, a methodology that describes how to determine the amount of flicker sensation that is being created by a flicker producing source that is in parallel with other flicker producing sources will be presented. This will be accomplished by utilizing the flickermeter defined in IEEE 1453 with either a half cycle or full cycle RMS input signal. The RMS values will be calculated from a two bus power flow problem that uses an estimated Thévenin impedance between the source and load. A justification for the acceptability of RMS inputs to the flickermeter in IEEE 1453 is presented. The output of the flickermeter will be the amount of flicker sensation that is being produced by the load of interest, even though there are other flicker producing loads connected electrically close together. A device that implements these design concepts has been built. There will be months of flicker data provided that the device collected at multiple sites. This provided data will validate the concepts that are provided in each stage of the device design.

Acknowledgments

First and foremost I would like to thank my Lord and Savior Jesus Christ for providing me with my capabilities. It is because of Him that all things exist. "For from him and through him and to him are all things. To him be glory forever. Amen." – Romans 11:36 ESV. I also want to thank my wife Tabitha for her patience, endurance, love, and support as I pursued my academic goals. She was always available to offer words of support and affirmation during times of frustration. I also want to thank my parents as well for their love and support of my family in encouraging me to pursue an advanced education and for teaching me to keep my eyes on Christ who is the ultimate treasure. Thank you to my advisor Dr. Mark Halpin for providing me the opportunity to pursue this degree. His words of wisdom in life and engineering are greatly appreciated. Also, thank you for reading my plethora of various paper drafts and for teaching me the importance of making a positive impact in the power system field. I would also like to thank my committee members Dr. Charles Gross, Dr. John Hung, and Dr. Mark Nelms for their help and time that they invested in me as I pursued my degree. Also, thank you to my friends and family who provided words of encouragement to my wife and I as we made this journey together.

Table of Contents

Abstract ii

Acknowledgments v

List of Tables viii

List of Figures ix

List of Abbreviations xiii

Chapter 1: Introduction 1

Chapter 2: Impedance Estimation 8

2.1: Real Time Impedance Estimation Technique 15

2.2: Impedance Estimation Technique Implementation with Theoretical Data 18

2.3: Impedance Estimation Technique Implementation with Measured System Data 23

Chapter 3: Applicability of using RMS values with the Flickermeter 28

3.1: IEEE Std 1453 28

3.2: Flickermeter with RMS Input 30

3.3: Flickermeter Field Measurements 34

3.4: RMS Input Operation Conditions 37

3.4.1: RMS Fluctuations due to RMS Window Location 39

3.4.2: Repeating RMS Fluctuations of AM Signal 43

3.4.3: Signal Aliasing due to the RMS Calculation 47

3.4.4: Short Term Flicker for Complex Modulations 53

3.5: Summary of Issues....54
Chapter 4: Calculating the Equivalent Load Voltage....56
Chapter 5: Device Implementation with Theoretical Data....58
5.1: Example 1....58
5.2: Example 2....64
5.3: Example 3....70
5.4: Example 4....77
5.5: Examples Summary....82
Chapter 6: Device Implementation with Field Measurements....83
6.1: Flicker Discriminator connected to EAF 1 and EAF 2....84
6.2: Second Test Location with EAF 3 and EAF 4....88
6.3: Flicker Discriminator connected to EAF 3....89
6.4: Flicker Discriminator connected to EAF 4....96
6.5: Flicker Discriminator with Field Data Conclusions....103
Chapter 7: Conclusion....105
References....108

List of Tables

Table II-I: R and X results for Dataset 1 23

Table II-II: R and X results for Dataset 2 24

Table III-I: Short-Term and Long-Term Flicker Compatibility Levels 29

Table III-II: Flicker Test Points 31

Table III-III: Flicker Test Points with RMS Input from [9] 31

Table III-IV: Flicker Test Points with RMS Input 33

Table III-V: Flicker Test Points with RMS Input 38

Table III-VI: FFT Results of the RMS Signal in Fig. 3-7 49

Table III-VII: FFT Results of the RMS Signal in Fig. 3-13 51

Table V-I: Flicker Results for the Parallel Loads 70

Table V-II: Flicker Results for Load 2 74

Table V-III: Flicker Results for Load 1 76

Table V-IV: Flicker Results for the Parallel Loads 81

Table V-V: Flicker Results for Load 2 82

Table VI-I: 95% Flicker Results for the EAF 87

List of Figures

Figure 1-1. Multiple Steel Furnaces Connected Electrically Close Together 2

Figure 1-2. Equivalent Circuit for Calculating the Load's Flicker Level.....5

Figure 2-1. System Equivalent Circuit.....9

Figure 2-2. Single Line Diagram 12

Figure 2-3. Single Line Diagram 13

Figure 2-4. Positive Sequence Circuit 15

Figure 2-5. Impedance Estimation Flow Chart.....18

Figure 2-6. Theoretical Test Circuit for the Impedance Estimation Technique 19

Figure 2-7. Thévenin Estimated Resistance at Load 2 20

Figure 2-8. Thévenin Estimated Reactance at Load 2 20

Figure 2-9. Thévenin Estimated Resistance at Load 2 21

Figure 2-10. Thévenin Estimated Reactance at Load 2 22

Figure 2-11. Per-Unit Equivalent Resistant Estimates for Dataset 1.....25

Figure 2-12. Per-Unit Equivalent Reactance Estimates for Dataset 1 25

Figure 2-13. Per-Unit Equivalent Resistant Estimates for Dataset 2.....26

Figure 2-14. Per-Unit Equivalent Reactance Estimates for Dataset 2 26

Figure 3-1. Example RMS Input to the Flickermeter 32

Figure 3-2. Residential and Industrial Load 35

Figure 3-3. DC Arc Furnace 36

Figure 3-4. Welder Loads 37
Figure 3-5. Amplitude Modulated Signal 40
Figure 3-6. AM Signal with 9 Hz Sinusoidal Modulation 44
Figure 3-7. RMS of AM Signal with 9 Hz Sinusoidal Modulation 44
Figure 3-8. AM Signal with 20 Hz Sinusoidal Modulation 45
Figure 3-9. RMS of AM Signal with 20 Hz Sinusoidal Modulation 45
Figure 3-10. AM Signal with 7 Hz Sinusoidal Modulation 46
Figure 3-11. RMS of AM Signal with 7 Hz Sinusoidal Modulation 46
Figure 3-12. AM Signal with 40 Hz Square Wave Modulation 50
Figure 3-13. RMS of AM Signal with 40 Hz Square Wave Modulation 51
Figure 4-1. Thévenin Equivalent Circuit for the Load of Interest 56
Figure 5-1. Thévenin Equivalent Circuit for the Load of Interest 58
Figure 5-2. Voltage at the Parallel Load's Terminals 59
Figure 5-3. Thévenin Estimated Resistance at Load 2 60
Figure 5-4. Thévenin Estimated Reactance at Load 2 61
Figure 5-5. Load 2 Calculated Equivalent Voltage 62
Figure 5-6. Load 2 Calculated Equivalent Voltage at Steady State 62
Figure 5-7. Load 1 Calculated Equivalent Voltage 63
Figure 5-8. Adjusted View of Load 1 Calculated Equivalent Voltage 64
Figure 5-9. Voltage at the Parallel Load's Terminals 65
Figure 5-10. Thévenin Estimated Resistance at Load 2 66
Figure 5-11. Thévenin Estimated Reactance at Load 2 66
Figure 5-12. Load 2 Calculated Equivalent Voltage 67

Figure 5-13. Load 2 Calculated Equivalent Voltage at Steady State....68
Figure 5-14. Load 1 Calculated Equivalent Voltage....69
Figure 5-15. Adjusted View of Load 1 Calculated Equivalent Voltage....69
Figure 5-16. Voltage at the Parallel Load's Terminals....71
Figure 5-17. Thévenin Estimated Resistance at Load 2....72
Figure 5-18. Thévenin Estimated Reactance at Load 2....72
Figure 5-19. Load 2 Calculated Equivalent Voltage....73
Figure 5-20. Load 2 Calculated Equivalent Voltage at Steady State....74
Figure 5-21. Load 1 Calculated Equivalent Voltage....75
Figure 5-22. Adjusted View of Load 1 Calculated Equivalent Voltage....76
Figure 5-23. Voltage at the Parallel Load's Terminals....77
Figure 5-24. Voltage at the Parallel Load's Terminals....78
Figure 5-25. Thévenin Estimated Resistance at Load 2....79
Figure 5-26. Thévenin Estimated Reactance at Load 2....79
Figure 5-27. Load 2 Calculated Equivalent Voltage....81
Figure 6-1. Power System Single Line Diagram of EAF Locations....84
Figure 6-2. Discriminated Flicker Results for EAF 1....85
Figure 6-3. Discriminated Flicker Results for EAF 2....86
Figure 6-4. Discriminated Flicker Results for EAF 1 for 3 Week Data Set....87
Figure 6-5. Power System Single Line Diagram of EAF Locations....88
Figure 6-6. Total Demand Power for each EAF for the First Operating Condition....90
Figure 6-7. Flicker Levels Measured at EAF 3 for the First Operating Condition....91
Figure 6-8. Total Demand Power for each EAF for the Second Operating Condition....92

Figure 6-9. Flicker Levels Measured at EAF 3 for the Second Operating Condition 92

Figure 6-10. Total Demand Power for each EAF for the Third Operating Condition.....93

Figure 6-11. Flicker Levels Measured at EAF 3 for the Third Operating Condition 94

Figure 6-12. Total Demand Power for each EAF for the Fourth Operating Condition.....95

Figure 6-13. Flicker Levels Measured at EAF 3 for the Fourth Operating Condition 95

Figure 6-14. Single Line Diagram of Transformer Connecting EAF 4 to 115 kV Bus.....96

Figure 6-15. Total Demand Power for each EAF for the First Operating Condition 98

Figure 6-16. Flicker Levels Measured at EAF 4 for the First Operating Condition.....98

Figure 6-17. Background Flicker Levels Measured at EAF 4 99

Figure 6-18. Total Demand Power for each EAF for the Third Operating Condition.....100

Figure 6-19. Flicker Levels Measured at EAF 4 for the Third Operating Condition 101

Figure 6-20. Total Demand Power for each EAF for the Fourth Operating Condition...102

Figure 6-21. Flicker Levels Measured at EAF 3 for the Fourth Operating Condition 102

List of Abbreviations

AM	Amplitude Modulation
CPM	Changes Per Minute
EAF	Electric Arc Furnaces
GCD	Greatest Common Devisor
HV	High Voltage
KVL	Kirchhoff's Voltage Law
LPF	Low Pass Filter
LV	Low Voltage
PCC	Point of Common Coupling

Chapter 1: Introduction

IEEE is the standards governing body in North America for the electrical power system. This organization provides standards to the electric power industry suppliers and consumers that must be followed to prevent undesirable operation of the electric power system. Unfortunately, it can be difficult to make the necessary measurements to determine if the utility and/or customer are operating within the requirements of a particular standard. This is especially true for IEEE Std 1453, which is the standard that applies to voltage fluctuations in the power system.

Voltage fluctuations in the power system that result in customer irritation are called voltage flicker. It can be either voltage surges or sags that change the light output of an incandescent light bulb such that a customer becomes annoyed. General Electric did work in the early 20th century in determining various voltage fluctuation magnitudes and frequencies that are necessary for half of the population to become irritated. The results of the work were plotted and the resulting figure is referred to as the "GE Flicker Curve" [1]. This curve was used in industry for several decades, but it is lacking because it is difficult to determine how actual voltage fluctuations correspond to the curve. IEC 61000-4-15 is a standard that documents how to build a flicker measuring device or flickermeter and was adopted by IEEE in Std 1453 [1]. A flickermeter makes voltage measurements and determines the amount of voltage fluctuation or flicker for a determined amount of time, typically 10 minutes. The flickermeter outputs a number that

is called the "short-term flicker severity" or P_{st} and it numerically represents the amount of voltage fluctuation present at the measurement point. A P_{st} result of 1.0 corresponds to the "GE Flicker Curve" in that half of the customers are expected to experience irritation due to the voltage fluctuations [1]. The flickermeter is advantageous because flicker irritation can be measured independently of the fluctuating voltage waveform shape.

A flickermeter measures time sampled voltage data at its connection point and is able to determine the amount of flicker present by processing the time sampled data. Electric arc welders, steel furnaces, and starting motors are a few of the many different pieces of equipment that can produce flicker in the power system. Unfortunately, it is not possible to determine the source of flicker issues when there are multiple flicker producing loads connected electrically near to each other. This is because each flicker producing load could significantly impact the voltage at the terminals of other loads. An example of this issue is when there are two steel furnaces connected electrically close together as illustrated in Fig. 1-1.

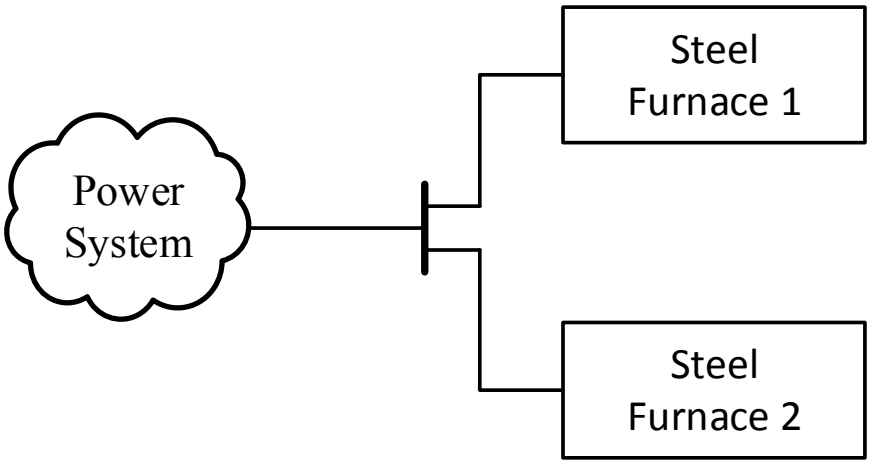

Figure 1-1. Multiple Steel Furnaces Connected Electrically Close Together

Any voltage fluctuations that are produced by either steel furnace will be experienced by the other steel furnace. It may be that the first steel furnace has installed a flicker mitigating device to reduce the amount of voltage fluctuations that are produced to prevent undesirable operation of the power system, but the second steel furnace has not installed any such equipment. This means that any flicker that is produced by the second steel furnace will be experienced by the first steel furnace because they are connected electrically near to each other. A flicker issue may be reported by the first steel furnace and the utility company can connect a flickermeter to assess the flicker level. It may be that the measured flicker level is high, but there is not a way to identify which steel furnace is causing the flicker issue. The second steel furnace is expected to produce the majority of the flicker level because of the lack of a flicker mitigating device, but the flickermeter can only measure the total level in the area. A device that can accurately measure the flicker level for the second steel furnace is desirable because then it would be possible to identify the second steel furnace as the primary flicker source.

The goal of this research is to identify a method that is able to accurately determine the amount of flicker produced by a load when there are multiple loads connected electrically close together. As previously discussed, the flickermeter is not able to determine which load is producing flicker in the power system; it is only able to measure the total flicker that is present in the area. If it is possible to determine what the equivalent voltage would be at a load by ignoring all of the other loads that are electrically close by, then that equivalent voltage could be used as the input to the flickermeter. The flickermeter result then would be based on only the load of interest,

thus the amount of flicker due to that one load could be determined even though there are multiple loads connected.

There are three primary steps that will need to be managed in order to calculate the amount of flicker that is produced by one load of interest when multiple loads are connected electrically close together. These steps apply to the equivalent system circuit provided in Fig. 1-2, where it is desired to calculate the flicker level of the load. The steps are as follows:

1. An online method to determine the power system Thévenin impedance at the load is necessary because the impedance will fluctuate as the power system changes.
2. It is necessary to show that it is acceptable to use cycle-by-cycle RMS values as the input to the flickermeter for low frequency voltage fluctuations.
3. The power flow is going to be used to determine the equivalent voltage at the load of interest based on voltage and current measurements for that load with the estimated Thévenin impedance from step 1. RMS values are used in the power flow calculation, thus the need for verifying the acceptable use of RMS values as the input to the flickermeter from step 2.

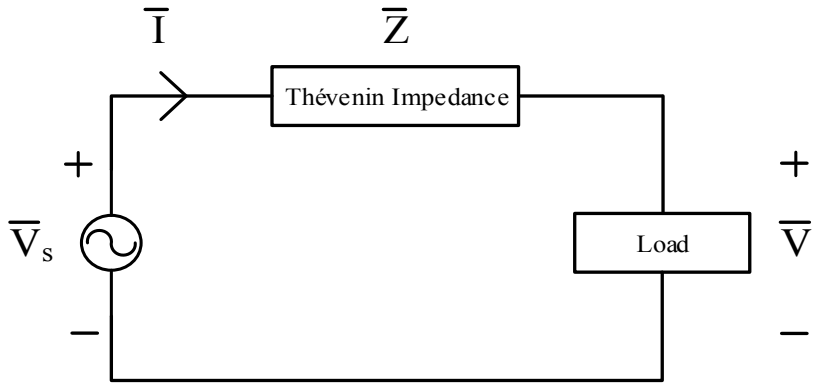

Figure 1-2. Equivalent Circuit for Calculating the Load's Flicker Level

The first step in calculating the equivalent load voltage for the flickermeter involves determining the Thévenin equivalent impedance of the power system at the load, as illustrated in Fig. 1-2. It is assumed that the power system Thévenin impedance at the load is going to be relatively constant from cycle to cycle. If the source voltage is assumed to be constant from cycle to cycle, then it is possible to calculate an impedance from two adjacent cycles of RMS voltage and current measurements. Unfortunately, this method breaks down when the current does not change much between cycles. Thus it is necessary to set a condition such that the invalid impedance values are ignored and only valid impedance results are considered. A method will be presented that calculates a valid Thévenin equivalent impedance that can be used in the power flow calculation to determine the equivalent voltage at the load.

The second step involves justifying that it is acceptable to utilize RMS values as the input to the flickermeter in the place of time sampled voltage data. Modulation magnitude and frequency information for an amplitude modulated (AM) signal is provided in IEEE Std 1453 to create various time domain fluctuating voltage waveforms that will produce a P_{st} result of 1. These waveforms are to be applied to the input of the

flickermeter to test and make sure that the meter operates correctly. If the meter outputs a P_{st} result of 1 for the test point, then the meter passes that test point. All of the test points describe time domain functions and each of the test points must be passed in order for the flickermeter to be authorized for use. Notice that the waveforms are all time domain expressions and not RMS values which are obtained from the power flow calculation. It is possible to calculate RMS values from the time domain expression for every full cycle of the fundamental frequency. This is accomplished by calculating the RMS value for a full cycle and then making that RMS value constant for the duration of time for which it was calculated. The RMS values are obtained from the power flow equation, but the flickermeter needs a time domain function. A hybrid time domain function of RMS values can be created by holding the RMS value constant for a whole cycle at the flickermeter input. It will be shown that for low frequency fluctuations, it is possible to use the RMS time domain function as the input to the flickermeter and have proper operation. Unfortunately, the method of holding an RMS value constant to the input of the flickermeter is not valid for high frequency fluctuations. Typically this is not an issue because the flicker produced by most flicker producing loads is in the low frequency range. Additionally, this is a huge advancement to the field because it allows for offline processing of data that is collected by voltage recorders. Voltage recorders are cheap and being able to process the collected data offline is extremely advantageous.

The third step involves the use of the power flow calculation to determine the equivalent voltage at the load in Fig. 1-2. It is known that the voltage is the same for loads that are connected in parallel. In order to determine the amount of flicker that a load is producing, it is necessary to be able to determine the equivalent voltage at the load

terminals. The equivalent load voltage is possible to calculate by using the power flow calculation. Voltage and current measurements for the load are made and then the complex power of the load is calculated and used in the power flow calculation. A two bus power flow is performed where the source is the slack bus at bus 1, the load is connected to bus 2, and the power system Thévenin equivalent impedance is connected between the two buses. An equivalent voltage for the load is calculated that is representative of what the load voltage would be if there was not anything else connected in parallel. This equivalent voltage is an RMS value that is utilized with the flickermeter to calculate the flicker that is being produced by the load.

Successful implementation of the previous three steps will result in the ability to determine the amount of flicker that is produced by a load of interest while it is connected in parallel to other flicker producing loads. This is desirable because it is presently not possible to determine how much flicker is being produced by an individual load; it is only possible to measure the total flicker of all of the parallel loads. By being able to discriminate between flicker producing loads, it will be possible to determine which load is in excess of its flicker limit.

Chapter 2: Impedance Estimation Techniques

The actual power system impedance is necessary in order to calculate the correct voltage for the load from the power flow calculation. Existing work has been done in determining the impedance of the power system. One of the approaches is to use some type of external stimulus to produce voltage and current transients in an active shunt filter. A continuous wavelet transform is used to capture the complex voltage and current. The formula for the continuous wavelet transform is provided in (2-1) and the main wavelet function Ψ(s,τ,t) is provided in (2-2). The main wavelet function also utilizes an analyzing wavelet that is given in (2-3).

$$C(S,\tau) = \int_{-\infty}^{\infty} f(t)\Psi^*(S,\tau,t)dt \tag{2-1}$$

$$\Psi(\mathrm{S},\tau,\mathrm{t}) = \frac{1}{\sqrt{|S|}}\Psi\left(\frac{\mathrm{t}-\tau}{\mathrm{S}}\right) \tag{2-2}$$

$$\Psi(x) = \sqrt{\pi f_b}e^{-\frac{x^2}{f_b}}e^{j\omega_c x} \tag{2-3}$$

The following variable definitions apply for (2-1) – (2-3):

S: the scale parameter of the wavelet,

τ: translation parameter of the wavelet,

t: time,

f_b: bandwidth parameter, and

ω_c: wavelet center frequency.

By applying (2-1) to the transient voltage and current data it is possible to calculate the system impedance in the wavelet domain by using (2-4).

$$\bar{Z}_W(\tau - S) = \frac{\bar{V}_W(\tau - S)}{\bar{I}_W(\tau - S)} \tag{2-4}$$

After utilizing (2-4), it is necessary to convert from the wavelet domain back to the frequency domain by using (2-5).

$$f_s = \frac{f_c}{S \cdot \Delta t} \tag{2-5}$$

Unfortunately, this method does not allow for real time evaluation of the impedance because of the need to produce a transient via an active shunt filter [2].

Another method that can be used to determine the Thévenin impedance of the power system is based on changes in the power system. A Kirchhoff's Voltage Law (KVL) equation can be written for the system equivalent circuit that is provided in Fig. 2-1 and is provided in (2-6).

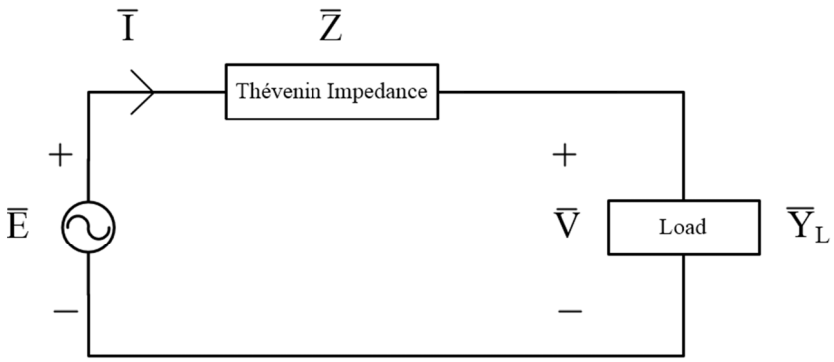

Figure 2-1. System Equivalent Circuit

$$\bar{E} = \bar{I}\bar{Z} + \bar{V} \tag{2-6}$$

Consider the condition if there is a small perturbation to each of the variables in (2-6) except for the Thévenin impedance. Then (2-6) will be written as (2-7) for the perturbation.

$$(\bar{E} + \Delta\bar{E}) = (\bar{I} + \Delta\bar{I})\bar{Z} + (\bar{V} + \Delta\bar{V}) \tag{2-7}$$

It is possible to derive (2-8) by assuming that $\Delta\bar{\mathrm{E}} = 0$ and then subtracting (2-6) from (2-7).

$$\bar{Z} = \frac{-Mean[\Delta\bar{V}\Delta\bar{Y}]}{Mean[\Delta\bar{I}\Delta\bar{Y}]} \tag{2-8}$$

Equation (2-8) is very easy to utilize if the necessary information is available, but the load impedance information is typically unknown which makes this approach difficult to implement [3].

Other methods use synchronized voltage and current measurements at each end of a power line to calculate the impedance of the line [4] - [5]. In [4], the ABCD parameters are found by making two sets of synchronized voltage and current measurements at both the sending and receiving ends of the transmission line. These sets of measurements are used with (2-9) – (2-12) to calculate the ABCD parameters for the model of the transmission line.

$$A = \frac{\bar{V}_s}{\bar{V}_r} \tag{2-9}$$

$$B = \frac{\bar{V}_s}{\bar{I}_r} \tag{2-10}$$

$$C = \frac{\bar{I}_s}{\bar{V}_r} \tag{2-11}$$

$$D = \frac{\bar{I}_s}{\bar{I}_r} \tag{2-12}$$

It was found that the measured ABCD parameters are more accurate than values given by computer model software tools. This was found by measuring power flows at the transmitting and receiving ends of the transmission line and comparing these measurements to power flows that were calculated by using the ABCD parameters from computer software tools and the measured ABCD parameters [4].

Another transmission line impedance method estimates the positive sequence impedance of the transmission line by making synchronized voltage and current measurements at both ends of the transmission line. Two sets of measurements are made and then used to calculate the ABCD parameters that are presented in (2-13) and (2-14) for short and medium length lines. If a line is longer than 200 km, then it is necessary to use (2-15) in addition to (2-13) and (2-14) to calculate the series positive sequence impedance of the transmission line. The variables in (18) are defined where "γ" is the propagation constant of the line and "l" is the length of the line in kilometers [5].

$$\bar{E}_s = A\bar{E}_R + B\bar{I}_R \tag{2-13}$$

$$\bar{I}_s = C\bar{E}_R + D\bar{I}_R \tag{2-14}$$

$$\bar{Z} = B\frac{\gamma l}{sinh(\gamma l)} \tag{2-15}$$

Unfortunately the Thévenin equivalent impedance is not determined using the techniques described in [4] and [5]. The techniques in [4] and [5] are important because they make it possible to set the zone impedances for breaker relays properly. But the techniques are not applicable for the flicker discriminator application because the techniques do not provide the required Thévenin impedance.

The impedance method provided in [6] does allow for the calculation of the Thévenin impedance if the load is connected to an on-load tap changer. When the taps are changed

on the on-load tap changer, then it is possible to use the voltage and current measurements from the primary side of the transformer to calculate the Thévenin impedance. This is accomplished by measuring the voltage and current both before and after the tap changes state. These measurements are used with (2-16) to calculate the Thévenin impedance of the power system as seen at the primary side of the on-load tap changer. Equation (2-16) assumes that the Thévenin impedance and source voltages are constant for the single line diagram in Fig. 2-2. The following variable definitions apply for (2-16): the source voltage $\bar{E}$ is at Bus 1, the Thévenin impedance $\bar{Z}_{TH}$ is connected between Bus 1 and Bus 2, the transformer primary voltage $\bar{V}_p$ is at Bus 2, and the transformer primary current $\bar{I}_p$ flows into Bus 2 [6].

$$\bar{Z}_{TH} = -\frac{\Delta \bar{V}_p}{\Delta \bar{I}_p} \tag{2-16}$$

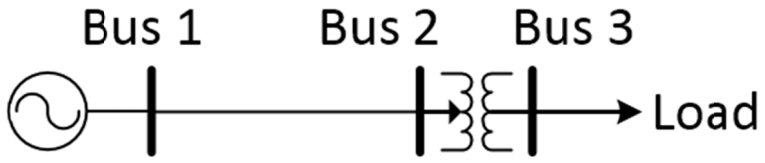

Figure 2-2. Single Line Diagram

The methods that are presented in [2] – [6] are able to calculate the impedance of portions of the power system and/or the Thévenin equivalent impedance of the power system for a particular load. Unfortunately they require special circumstances in order to be able to calculate an accurate impedance in real time. An impedance estimation technique that is able to determine the Thévenin equivalent impedance in real time for

any load of interest that is connected electrically close to other loads in the power system is necessary for the flicker discriminator application.

It is necessary to utilize a method that can estimate the Thévenin impedance in real time and only uses measurements at the load of interest. A method is presented in [7] that attempts estimate the Thévenin impedance in real time and only makes measurements at the point of common coupling (PCC). Voltage and current measurements are made at the load bus for the single line diagram presented in Fig. 2-3. By applying KVL to the circuit in Fig. 2-3 it is possible to derive the equation presented in (2-17).

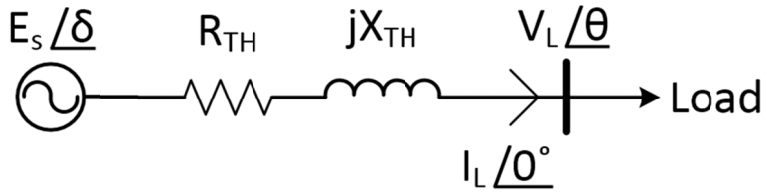

Figure 2-3. Single Line Diagram

$$E_s \angle \delta = (R_{TH} + jX_{TH}) I_L \angle 0° + V_L \angle \theta \tag{2-17}$$

The KVL equations for two sets of voltage and current measurements that are taken at the load bus are provided in (2-18) and (2-19) where the subscripts 1 and 2 denote the first and second set of data respectively.

$$E_s \angle \delta_1 = (R_{TH} + jX_{TH}) I_{L,1} \angle 0° + V_{L,1} \angle \theta_1 \tag{2-18}$$

$$E_s \angle \delta_2 = (R_{TH} + jX_{TH}) I_{L,2} \angle 0° + V_{L,2} \angle \theta_2 \tag{2-19}$$

If we assume that the source voltage is constant from the first set of measurements to the second, then it is possible to derive (2-20) by setting (2-18) equal to (2-19) and solving for the Thévenin impedance.

$$\bar{Z}_{TH} = R_{TH} + jX_{TH} = -\frac{V_{L,1}\angle\theta_1 - V_{L,2}\angle\theta_2}{I_{L,1}\angle 0° - I_{L,2}\angle 0°} = -\frac{\Delta\bar{V}}{\Delta\bar{I}} \tag{2-20}$$

It is stated that this method will work in theory, but it is based on the assumption that the source voltage angle δ_1 is equal to δ_2. This is typically an invalid assumption because of the fluctuating frequency of the power source, thus it is necessary to use a third set of data. There will be six unknowns in the three sets of data: E_s, δ_1, δ_2, δ_3, R_{TH}, and X_{TH}. Each of the KVL equations for each set of data can be separated into the real and imaginary equations. This results in six equations for the six unknowns that can be easily solved. Unfortunately there are several issues that are experienced in the field that make this approach difficult to implement successfully. It was found that valid results could be calculated by using a least square fitting approach with six or more measurement points. The measured data is used in (2-21) which is (2-17) rewritten with the real and imaginary portions separated and where "i" is the i^{th} measurement set of a total of "n" sets. It is suggested that the data should be collected with a sampling rate of 256 samples per cycle and that it should be processed in a three to five second window. The complete set of data that is developed using the voltage and current measurements and (2-21) is solved by using the Gauss-Newton algorithm for non-linear least squares problems [7].

$$\begin{bmatrix} E_s\cos(\delta_i) \\ E_s\sin(\delta_i) \end{bmatrix} = \begin{bmatrix} R_{TH} & 0 \\ 0 & X_{TH} \end{bmatrix}\begin{bmatrix} I_{L,i} \\ I_{L,i} \end{bmatrix} + \begin{bmatrix} V_L\cos(\theta_i) \\ V_L\sin(\theta_i) \end{bmatrix}, \quad i = 1, \dots, n \tag{2-21}$$

The approach taken in [7] utilizes a least squares approach to attempt to reduce the error due to measurement error and assumption inaccuracies. The least squares method

has costs associated with the amount of time necessary to perform the calculations and it tends to break down (e.g. errors remain large) when real system data is utilized. These costs will prevent a successful real time implementation.

2.1: Real Time Impedance Estimation Technique

A Thévenin impedance estimation approach that can be easily implemented for any load type that is not dependent on any type of error minimization techniques should be utilized to avoid the algorithm breakdowns that [7] experiences. An approach that calculates the Thévenin impedance when the change in load power reaches a threshold along with a moving average to mitigate calculation error should be utilized. Consider the positive sequence equivalent system circuit that is provided in Fig. 2-4 for a positive phase sequence power system.

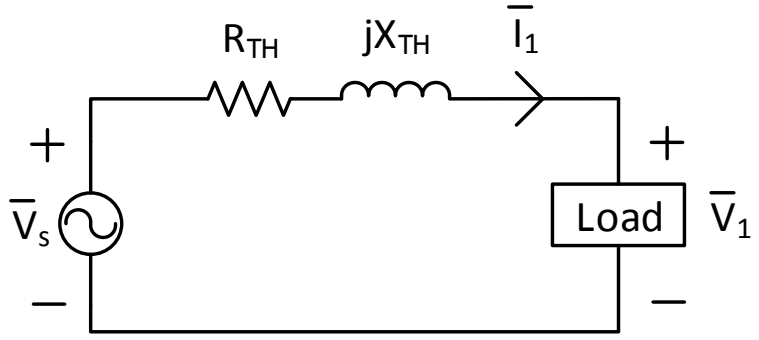

Figure 2-4. Positive Sequence Circuit

The load voltage $\bar{V}_1$ and current $\bar{I}_1$ are the measured three-phase load voltages and currents converted to sequence variables. If the source voltage, $\bar{V}_s$, and the Thévenin impedance, $\bar{Z} = R_{TH} + jX_{TH}$, is assumed to be constant for sequential cycles, k-1 to k, then it is possible to derive (2-22) via KVL.

$$\bar{V}_s = \bar{Z}\bar{I}_{1,k-1} + \bar{V}_{1,k-1}$$
$$\bar{V}_s = \bar{Z}\bar{I}_{1,k} + \bar{V}_{1,k} \tag{2-22}$$

By subtracting the first equation from the second equation it is possible to derive (2-23) because the unknown source voltage is the same for each cycle [8].

$$\bar{Z} = -\frac{\bar{V}_{1,k} - \bar{V}_{1,k-1}}{\bar{I}_{1,k} - \bar{I}_{1,k-1}} = -\frac{\Delta\bar{V}_1}{\Delta\bar{I}_1} \tag{2-23}$$

The equations presented in (2-22) will be linearly dependent unless the voltage and current relationship is unique between the consecutive cycles (i.e. there is sufficient excitation in the system). This is particularly important in (2-23) where if the current between cycles is very similar then a divide-by-zero will occur that will amplify measurement error. It has been found that checking for unique differences between the load voltages and currents for each cycle is accomplished by checking for a change in real power between the cycles. A threshold is established such that (2-23) is evaluated anytime the change in real power exceeds the chosen threshold value. The load power for the cycle of interest is calculated by using (2-24) and if (2-25) is satisfied, then it is appropriate to calculate a new Thévenin impedance via (2-23).

$$P_{1,k} = V_{1,k}I_{1,k}\cos\left(\theta_{V1,k} - \theta_{I1,k}\right) \tag{2-24}$$

$$\left|\Delta P_{1,k}\right| = \left|P_{1,k} - P_{1,k-1}\right| > Threshold \tag{2-25}$$

If the threshold is large, then more excitation is required before the impedance will be calculated. This will result in a more reliable impedance calculation than if the threshold were lower because the Thévenin impedance will not be calculated for cycles where the assumptions (e.g. the system voltage is not constant) are not met. However, a larger

threshold will result in fewer impedance calculations which will lead to the possibility that changes in the system impedance could go completely undetected [8].

The assumptions associated with (2-23) will not always be met when the equality in (2-25) states that it is appropriate to calculate a new Thévenin impedance. It is likely that the power system is not perfectly balanced, that the source voltage is not constant between the two cycles of interest, and that there is measurement error in the voltage and current measurements. These issues will lead to inaccurate impedance calculations that will have to be managed in the impedance estimation algorithm. A moving average is utilized to mitigate the error associated with impedance calculations that are made when the assumptions are not valid because it is known that the Thévenin impedance will not drastically change over a short period of time. A first-order LPF with a time constant of τ is used with R_{TH} and X_{TH}. The most recent outputs of the LPF are used as the input to the filter in the event that the system is not excited enough for a new impedance calculation. This method is more desirable than a least squares approach because it is computationally less intensive and the moving-average will prevent a single bad result from affecting the estimated impedance. A summary of the threshold and moving average approach in estimating the Thévenin impedance of the source is provided in Fig. 2-5 [8]. It is appropriate to consider how this Thévenin equivalent impedance estimation technique performs when processing theoretical data.

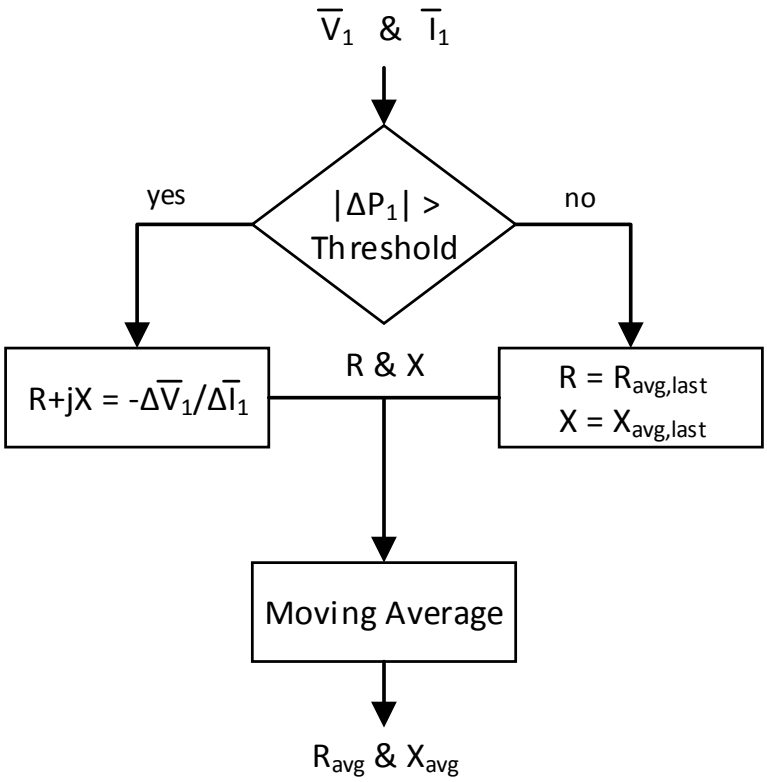

Figure 2-5. Impedance Estimation Flow Chart

2.2: Impedance Estimation Technique Implementation with Theoretical Data

The algorithm described in the flow chart presented in Fig. 2-5 was implemented in software and used to estimate the Thévenin equivalent impedance at the load terminals of a test system. This test system involves two parallel loads that are connected to the power system through an impedance. A circuit diagram of the test circuit is provided in Fig. 2-6. Both of the loads in the test system are modeled as impedances, where the first load is a constant impedance of 1+j0.3 per-unit and the second load fluctuates between 1+j0.3 per-unit and some fraction of the base impedance for some number of changes per minute (CPM). The impedance estimation technique will be used to calculate the Thévenin equivalent impedance at the terminals of the second load because it is the load

that is fluctuating. The Thévenin equivalent impedance at the terminals of the second load for each of the following two examples will be the parallel combination of the line equivalent impedance (0.01+j0.05) and the first load impedance (1+j0.3), which results in an impedance of 0.0118+j0.0484 per-unit.

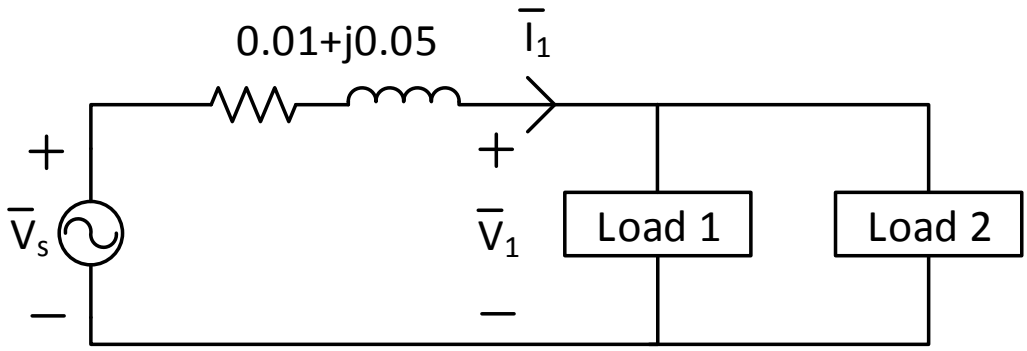

Figure 2-6. Theoretical Test Circuit for the Impedance Estimation Technique

The first test involves fluctuating the impedance of the second load from 1+j0.3 per-unit to 0.5+j0.15 per-unit at 20 CPM or 0.167 Hz. The initial condition for the impedance estimation technique was chosen to be 0.01+j0.04 per-unit. A plot of the estimated resistance is provided in Fig. 2-7 and a plot of the estimated reactance is provided in Fig. 2-8. The time constant and power threshold were chosen as 5 seconds and 0.2 per-unit, respectively. Notice that the impedance estimation algorithm tracks the analytical Thévenin impedance at the terminals of the second load.

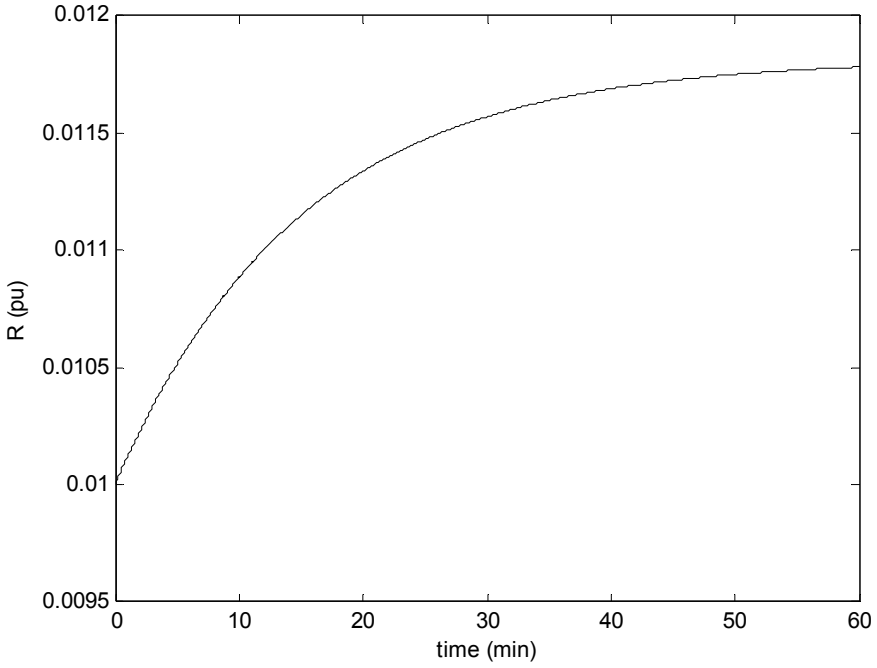

Figure 2-7. Thévenin Estimated Resistance at Load 2

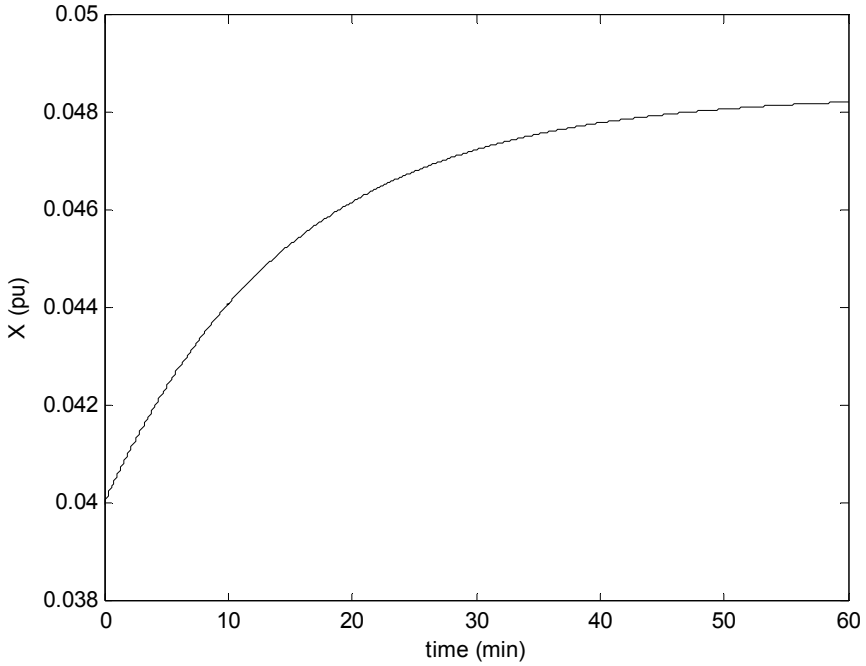

Figure 2-8. Thévenin Estimated Reactance at Load 2

The second test involves fluctuating the impedance of the second load from 1+j0.3 per-unit to 0.75+j0.225 per-unit at 240 CPM or 2 Hz. The initial condition values for the impedance estimation technique in the previous test were also used in this test. The time constant and power threshold were chosen to be the same as the previous example and are 5 seconds and 0.2 per-unit, respectively. A plot of the estimated resistance is provided in Fig. 2-9 and a plot of the estimated reactance is provided in Fig. 2-10. Notice that the impedance estimation algorithm tracks the analytical Thévenin impedance at the terminals of the second load.

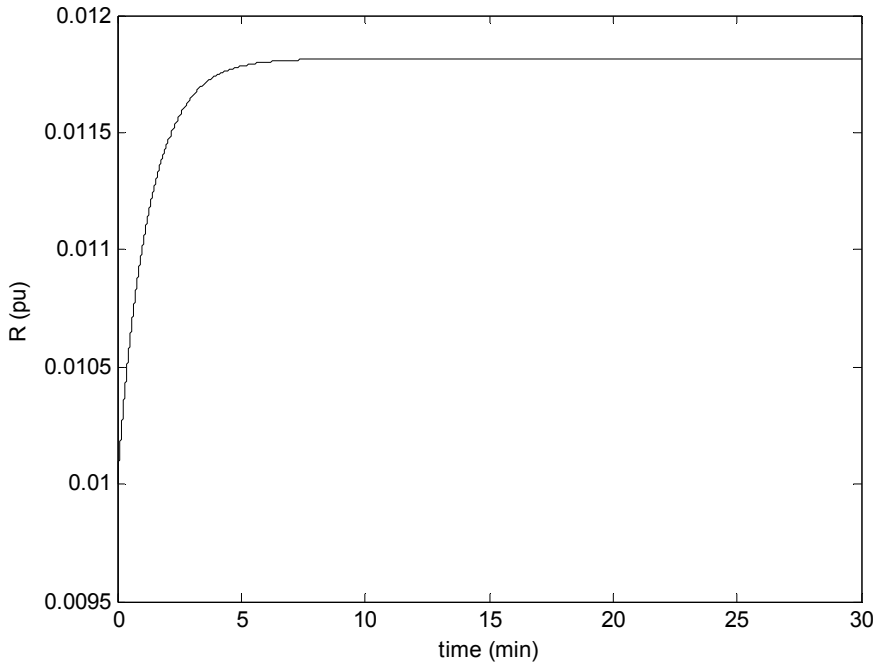

Figure 2-9 Thévenin Estimated Resistance at Load 2

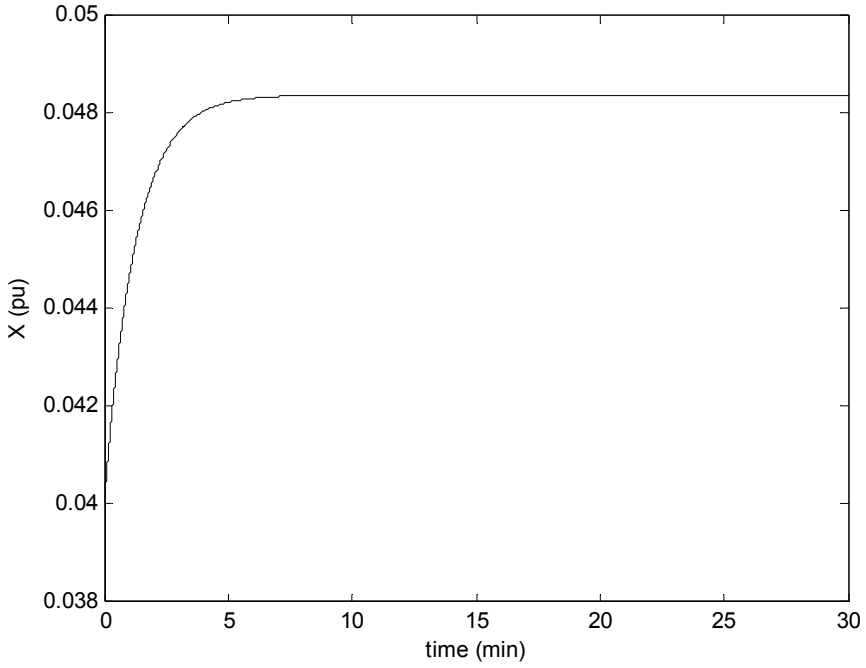

Figure 2-10. Thévenin Estimated Reactance at Load 2

The Thévenin equivalent impedance technique reaches the analytical Thévenin impedance at the terminals of the second load in each of the tests. It takes the algorithm longer to reach the analytical impedance in the first test than it does in the second test. This is due to the number of fluctuations of the second load that will allow for a valid impedance calculation. The second test involves fluctuations that occur twelve times more often than in the first example, which will result in more impedance calculations in the second test than the first test for the same amount of time. The estimated impedance results in each of the tests support valid operation of the Thévenin impedance estimation algorithm that is presented in Fig. 2-5. It is appropriate to utilize the approach with measured power system data to determine if the Thévenin impedance estimation algorithm still functions properly.

2.3: Impedance Estimation Technique Implementation with Measured System Data

Two sets of three-phase voltages and currents were collected from two different locations in the power system to process with the Thévenin impedance estimation algorithm. Both of the data sets were sampled at 32 samples per cycle or 1920 Hz. There is approximately 6 hours of data in the first set and 16.5 hours of data in the second set. The impedance estimation algorithm that is summarized in the flow chart in Fig. 2-5 was applied to these two sets of data with different real power thresholds and different LPF time constants.

The initial conditions for dataset 1 and dataset 2 were specified to be 0.00117+j0.01432 and 0.00112+j0.01401, respectively. A time for each dataset was picked that represented approximately when the tracking algorithms reached a steady-state value. Then the mean and standard deviation of all the R's and X's from the selected point in time to the end of the data file were calculated. The results for each data file are provided in Table II-I and Table II-II.

TABLE II-I.
R AND X RESULTS FOR DATASET 1

Set	$\lvert\Delta P_{1,k}\rvert >$	τ	R_{mean}	R_{σ}	X_{mean}	X_{σ}
#1	0.2	12 sec	0.0042	2.32E-4	0.0139	3.24E-4
#2	0.3	1 sec	0.0053	3.54E-4	0.0148	8.40E-4
#3	0.3	2 sec	0.0052	2.95E-4	0.0146	6.11E-4
#4	0.3	5 sec	0.0051	2.06E-4	0.0145	3.69E-4
#5	0.3	12 sec	0.0049	1.45E-4	0.0144	2.42E-4
#6	0.4	1 sec	0.0052	2.92E-4	0.0146	4.94E-4
#7	0.4	2 sec	0.0051	2.18E-4	0.0146	3.53E-4
#8	0.4	5 sec	0.0049	1.59E-4	0.0146	2.06E-4
#9	0.4	12 sec	0.0042	2.47E-4	0.0146	9.71E-5
#10	0.5	1 sec	0.0047	1.65E-4	0.0150	3.65E-4

TABLE II-II.
R AND X RESULTS FOR DATASET 2

Set	$\lvert\Delta P_{1,k}\rvert >$	τ	R_{mean}	R_{σ}	X_{mean}	X_{σ}
#1	0.2	12 sec	0.0056	2.08E-4	0.0128	2.45E-4
#2	0.3	1 sec	0.0054	5.21E-4	0.0130	4.39E-4
#3	0.3	2 sec	0.0054	4.16E-4	0.0130	3.63E-4
#4	0.3	5 sec	0.0054	2.94E-4	0.0130	2.95E-4
#5	0.3	12 sec	0.0054	2.06E-4	0.0130	2.46E-4
#6	0.4	1 sec	0.0052	4.85E-4	0.0132	4.72E-4
#7	0.4	2 sec	0.0052	3.70E-4	0.0132	3.96E-4
#8	0.4	5 sec	0.0052	2.47E-4	0.0132	2.86E-4
#9	0.4	12 sec	0.0050	2.30E-4	0.0132	1.58E-4
#10	0.5	1 sec	0.0050	3.22E-4	0.0135	1.84E-4

The experimental results for four of the sets that represented the best trade-offs are provided in Fig. 2-11 through Fig. 2-14. The largest variation at any point in time between any of the steady-state values of these four sets occurs around minute 635 in dataset 2, between sets #4 and #10. At this time the per-unit impedances are 0.005494+j0.1285 and 0.00517+j0.01379, respectively, and correspond to impedance magnitudes of 0.01390 and 0.01473. The percent difference between these is 5.38%, a negligible difference for most power system analyses requiring the equivalent system impedance. Upon close inspection of the trends, either set #5 (smaller, reasonable threshold with larger time constant) or set #8 (larger, reasonable threshold with smaller time constant) would offer the best tradeoff between tracking and estimation variation [8].

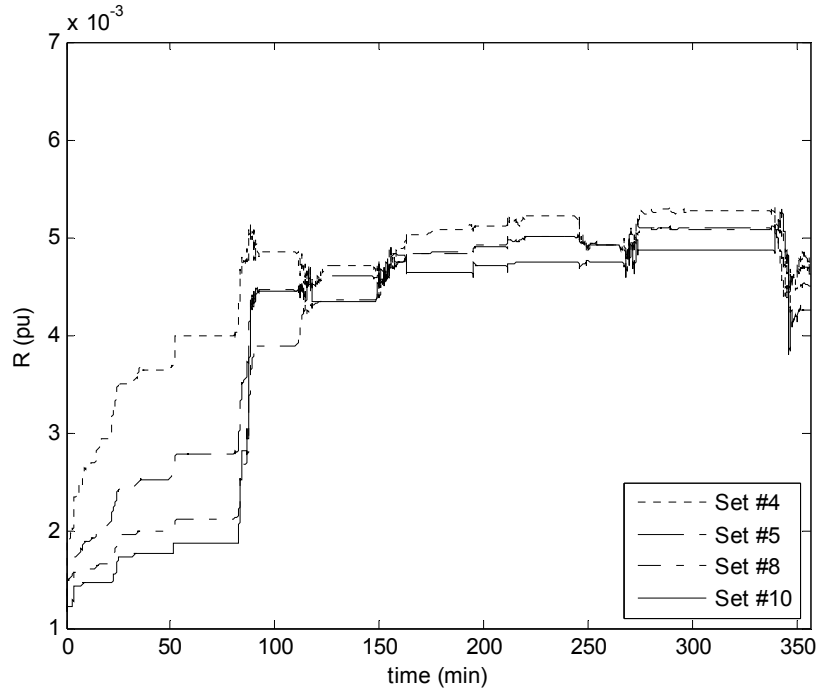

Figure 2-11. Per-Unit Equivalent Resistant Estimates for Dataset 1

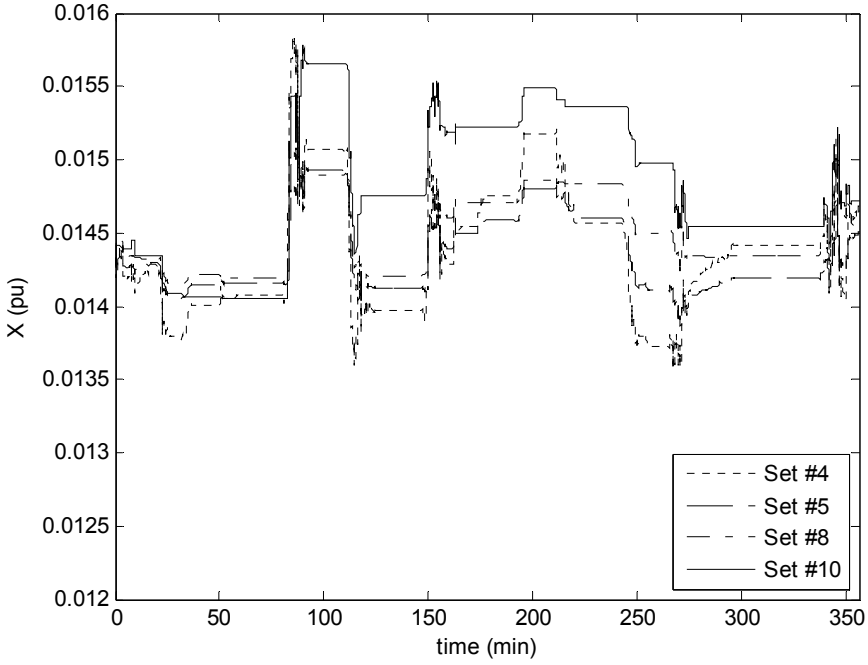

Figure 2-12. Per-Unit Equivalent Reactance Estimates for Dataset 1

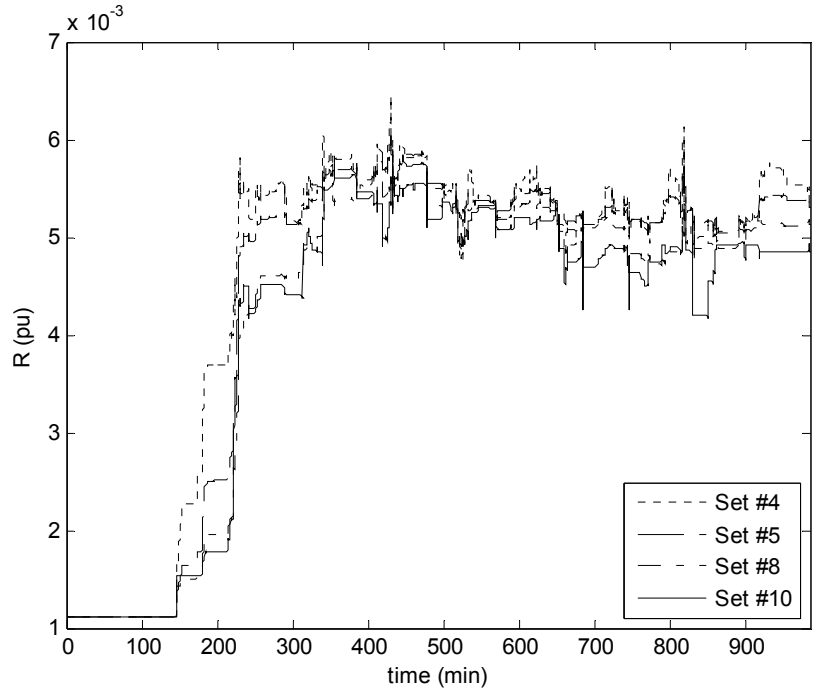

Figure 2-13. Per-Unit Equivalent Resistant Estimates for Dataset 2

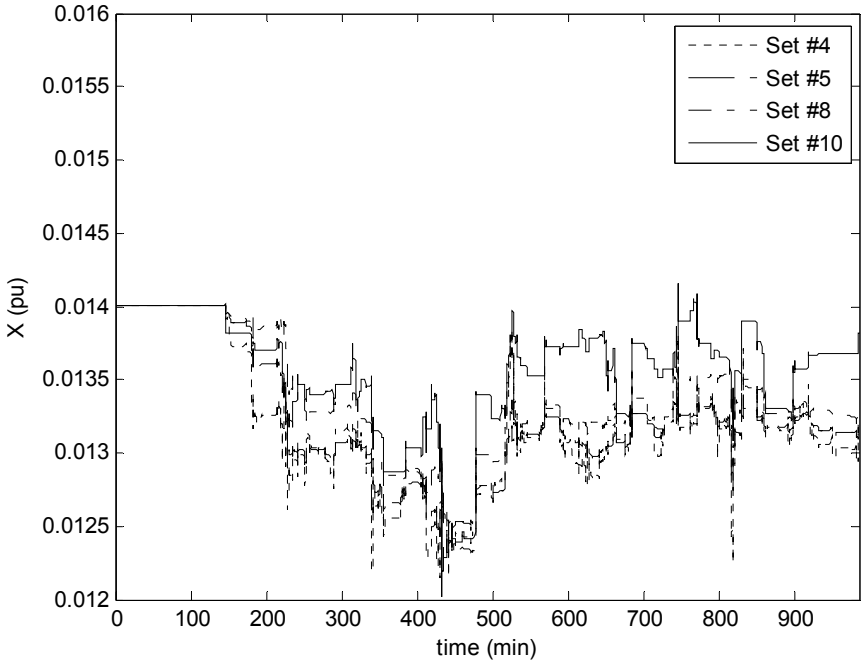

Figure 2-14. Per-Unit Equivalent Reactance Estimates for Dataset 2

An algorithm that is able to estimate the Thévenin equivalent impedance at the load terminals has been presented. This impedance will be used in the power flow problem with the load's measured real and reactive power to calculate the load's equivalent voltage. This voltage will be calculated on a cycle-by-cycle basis and then processed by the flickermeter. It is necessary to consider the acceptability of utilizing these RMS voltage values with the flickermeter.

Chapter 3: Applicability of RMS values with the Flickermeter

It is necessary to consider if it is acceptable to utilize RMS values as the input to the flickermeter because the flickermeter input is specified to be time sampled voltage data in [1]. A power flow calculation is going to be performed every cycle to calculate an equivalent voltage at the load terminals. This is going to result with a cycle-by-cycle time series of RMS voltage values. These RMS voltage values will be processed by the flickermeter to calculate the load's flicker level. It is appropriate to review the flickermeter implementation requirements for a basic understanding of the device operation. This will aid in extending the input from time sampled voltage data to cycle-by-cycle RMS voltage data.

3.1: IEEE Std 1453

Device requirements to build a flickermeter that will measure any voltage fluctuations in the power system and provide the corresponding flicker severity for the fluctuations are provided in IEEE Std 1453. The device specifications in IEEE 1453 are provided in 5 different sections or blocks and describe how to build the flickermeter. Block 1 describes the input voltage adapter which normalizes the input voltage signal by the output of a 1st order low pass filter. This allows the flicker level to be determined independent of the actual voltage level of the power system. The voltage adapter processes half cycle RMS values through a 1st order low pass resistance and capacitance filter that utilizes a time

constant of 27.3 seconds. Block 2 is the squaring multiplier that simulates a light bulb's behavior. Block 3 comprises a 6th order low pass butterworth filter with a cutoff frequency of 42 Hz for a 60 Hz power system and a 1st order high pass filter with a cutoff frequency of 0.05 Hz to remove any dc content and the doubled mains frequency content from block 2; it then uses a weighting filter to simulate the human visual system. Block 4 is composed of a squaring multiplier and a first-order low pass filter with an RC time constant of 300 milliseconds and the output is defined as the instantaneous flicker sensation, P_{inst}. Block 5 is an online statistical analysis that determines the short-term flicker severity, P_{st}, that is typically calculated for 10 minute intervals. In some instances, it may be necessary to calculate the flicker severity over a period of time that is longer than what the P_{st} result provides. Thus, a long-term flicker severity assessment is calculated using (3-1) and some determined number (usually 12) of the previous P_{st} results.

$$P_{lt} = \sqrt[3]{\frac{\sum_{i=1}^{N} P_{sti}^3}{N}} \tag{3-1}$$

Compatibility levels for short-term and long-term flicker severity correspond to when customers will typically complain about the flicker sensation and are only defined for LV systems. These compatibility levels are provided in Table III-I [1].

TABLE III-I.
SHORT-TERM AND LONG-TERM FLICKER COMPATIBILITY LEVELS

	Compatibility Levels
P_{st}	1.0
P_{lt}	0.8

A summary of IEEE Std 1453 has been provided that briefly describes the flickermeter operation. IEEE 1453 specifies that the input to the flickermeter is time sampled voltage data. Also, the output of the flickermeter is a number that describes the flicker severity for all loads that are connected electrically near to the measurement point and it is only based on the voltage measurement. Because of this it is not possible to determine the amount of flicker that is being produced by a particular load of interest when there are multiple loads connected electrically near to each other. Additional work is required to be able to determine how much of the flicker that is present at the measurement point is being produced by a particular load.

3.2: Flickermeter with RMS Input

A flickermeter implementation that meets the requirements specified in IEEE 1453 is necessary to be able to assess the validity of using cycle-by-cycle RMS values as the input to the flickermeter. There are required time domain test points provided in [1] that must be passed in order to state that the flickermeter operates properly. Each of these test points defines a magnitude and frequency for the modulating portion of an AM signal, where the frequency is calculated from a defined number of fluctuation CPM. Each of the input test signals is processed by the flickermeter and the P_{st} result for each signal is calculated. Each P_{st} result for the test points must be 1.0 +- 5% in order to pass all of the tests. The results for each test point for the software flickermeter implementation are provided in Table III-II.

Prior work has been done in partially verifying that RMS voltage values applied to the input of the flickermeter pass the required test points. It has been found in [9] that it

is permissible to use cycle-by-cycle RMS voltage data as the input to the flickermeter for low frequency fluctuations. The digital implementation of the flickermeter was designed to accept the sampling rate associated with having one data sample per cycle. The results of the test points from the work are provided in Table III-III.

TABLE III-II.
FLICKER TEST POINTS

CPM	P_{st}
1	1.0013
2	1.0175
7	0.9837
39	0.9884
110	1.0328
1620	0.9714
4800	0.9716

TABLE III-III.
FLICKER TEST POINTS WITH RMS INPUT FROM [9]

CPM	P_{st}
1	0.9999
2	1.0019
7	1.0170
39	1.0183
110	1.0018
1620	1.0105
4000	0.9013

The work in [9] suggests that it is permissible to utilize a full-cycle RMS value as the input to the flickermeter. Each of the test points were reprocessed for the exact same flickermeter implementation that was used to generate the results in Table III-I except the input was RMS values. These RMS values of the AM test point signals were calculated on a fundamental frequency full cycle time window and applied to the input of the flickermeter. Each RMS value was held constant at the input of the flickermeter for the

duration of time for which it was calculated. This concept is illustrated in Fig. 3-1. The resulting RMS value for each cycle of the fundamental is presented by the stem plots. There are 16 samples per cycle in this example that were utilized in each RMS calculation. The signal that is applied to the flickermeter is represented by the "x" marks. There are 16 samples in a cycle, thus the RMS value is used 16 times with the flickermeter input because it expects a time domain function and then the next RMS value is used 16 times and so on. This implementation method is fundamentally different from the method that is utilized in [9] because nothing in the digital flickermeter implementation is changed to account for the type of data that is applied to the meter's input.

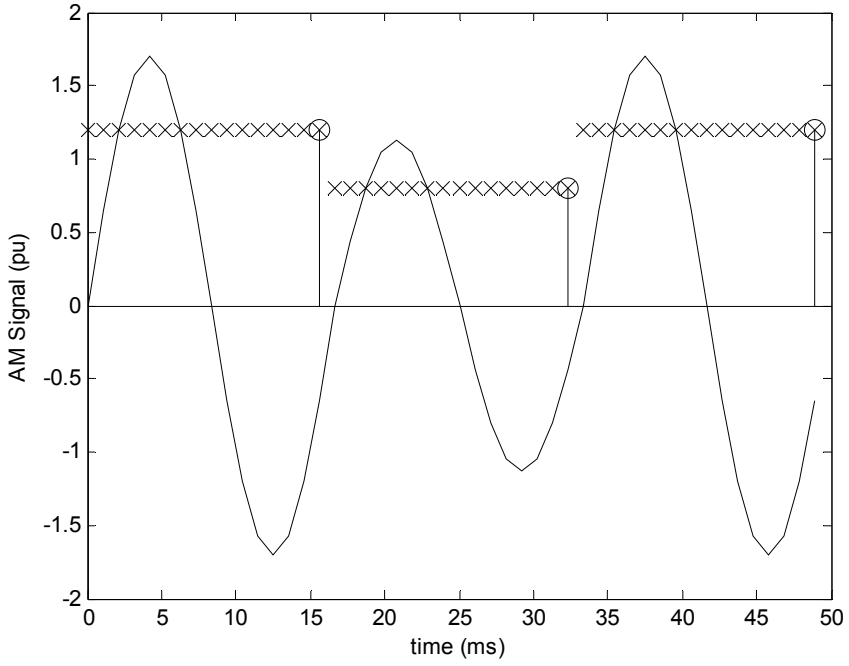

Figure 3-1. Example RMS Input to the Flickermeter

The P_{st} results for the flickermeter with full cycle RMS values as the input are provided in Table III-IV. Notice that the flickermeter passes the low frequency test points but not the highest frequency test point. This is similar to the results presented in Table III except the 4000 CPM (33.33 Hz) test point in Table III fails low and the 4800 CPM (40 Hz) test point fails high in Table III-IV.

TABLE III-IV.
FLICKER TEST POINTS WITH RMS INPUT

CPM	P_{st}
1	0.9985
2	1.0159
7	0.9503
39	0.9684
110	0.9821
1620	0.9714
4800	1.7269

These results suggest that it is acceptable to use RMS values as the input to the flickermeter if the voltage fluctuations are low frequency. It seems reasonable to expect the P_{st} results to decrease as the frequency of the fluctuation increases when full cycle RMS values are utilized with the flickermeter. This is because the RMS calculation will smooth (average) the voltage fluctuations that are present such that the flickermeter would calculate a lower P_{st} value. The data provided in Table III-III and Table III-IV seems to support this hypothesis except for the highest frequency test point in Table III-IV. It is appropriate to consider field test data to evaluate whether or not the analytical inconsistencies are significant in practice.

3.3: Flickermeter Field Measurements

Two identical software flickermeters were used to collect field measurements, but time-domain voltage samples were processed with one meter and RMS values were processed in the other meter. It is necessary to use identical meters operating in parallel for comparison so that any observed differences in the P_{st} outputs will be due only to the type of input data that is utilized. The need for this comparison is why it is essential to use a fundamentally different digital flickermeter implementation than [9]. The two digital flickermeters were connected to three different load types to measure the short term flicker severity.

The first load is a 12.47 kV substation that is supplying residential and industrial loads. The industrial load includes significant fluctuating motor load. This type of load has low frequency fluctuations, thus using full cycle RMS voltages as the input to the flickermeter should give similar P_{st} results to the P_{st} results that use time-domain voltage samples. A plot of the P_{st} results for this load are provided in Fig. 3-2, where the "TI" label represents the P_{st} results from using time-domain voltage samples with the flickermeter and the "RI" label represents the P_{st} results from using full cycle RMS voltages with the flickermeter. The maximum percent difference between the P_{st} results for the time-domain and RMS inputs is 4.65%. Because the percent difference is within the 5% tolerance specified in IEEE 1453, the difference between time-domain P_{st} results and RMS P_{st} results is indistinguishable. These results support the idea that RMS values will fluctuate in a similar manner to the time domain waveform for low frequency voltage fluctuations.

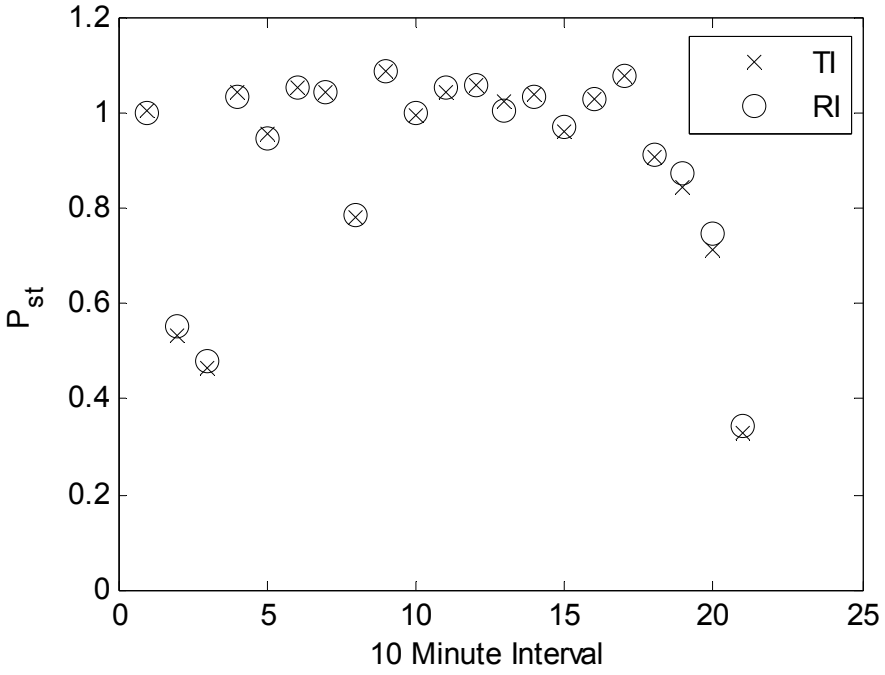

Figure 3-2. Residential and Industrial Load

The second load is a 60 MW DC arc furnace with a PCC voltage of 115 kV. An arc furnace also produces low frequency voltage fluctuations. Therefore it is expected that the P_{st} results for both the full cycle RMS voltages and the instantaneous voltage samples will be similar. A comparison of the short term flicker severity for the DC arc furnace load is provided in Fig. 3-3. The maximum percent difference is 5.5% for the P_{st} results presented in Fig. 3-3. Although a 5.5% percent difference is not within the 5% requirement in IEEE 1453, it is likely that this level of minor variation is acceptable given the potential benefits of using RMS type input data with the flickermeter.

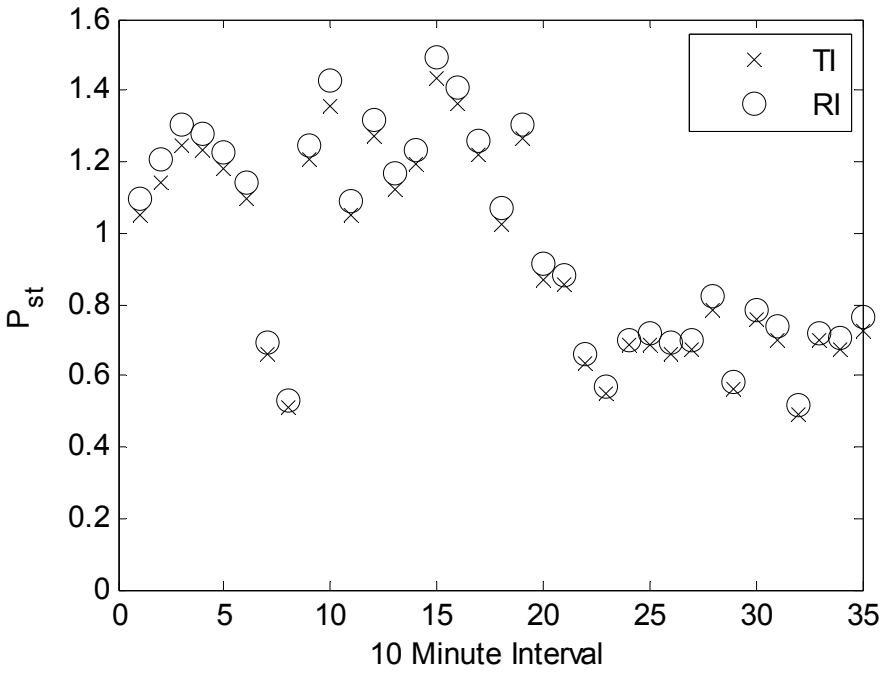

Figure 3-3. DC Arc Furnace

The third type of load that was considered is an industrial welding facility. There were multiple three-phase and single-phase spot welder loads fed by an ungrounded three-phase 13.8 kV delta connection. The controllers for the welders produced high frequency fluctuations in the range of 30-45 Hz. It is expected that the RMS calculation will smooth (average) the input signal such that the P_{st} result will be less than the time sample input result when full cycle RMS voltage data is utilized (as the flickermeter input) and high frequency voltage fluctuations are present. The short-term flicker severity measurements for the welding facility with both full cycle RMS voltages and instantaneous voltage samples are provided in Fig. 3-4. The P_{st} results from the RMS input are significantly higher than the results that use the time-domain samples; the

maximum percent difference for the P_{st} results is 56.2%. This field data result, while unexpected, is consistent with the result from the 4800 CPM test point in Table III-IV.

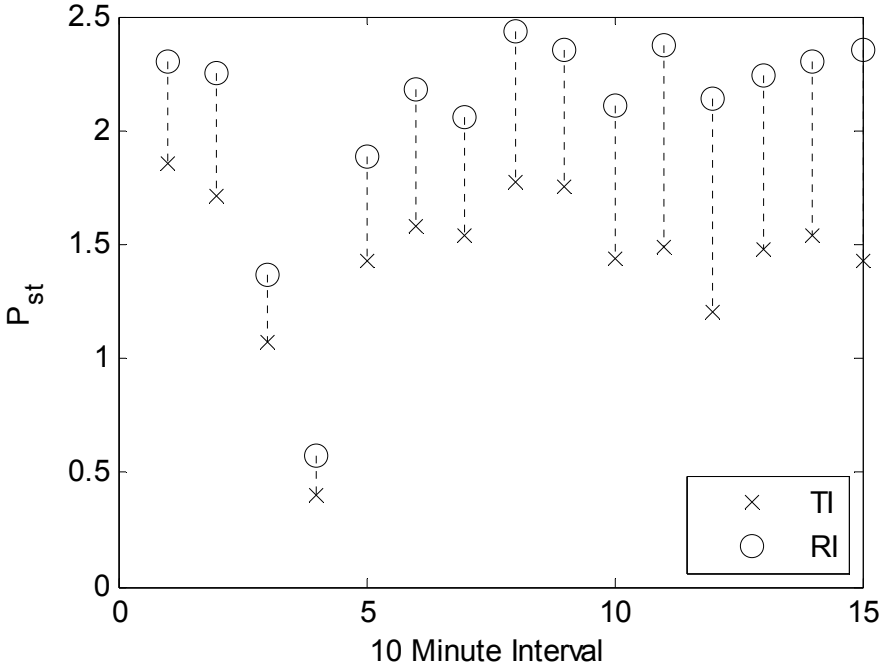

Figure 3-4. Welder Loads

Based on the field test results it does appear that the analytical inconsistencies described in section III are indeed experienced in reality when using RMS values as the input to the flickermeter. It is necessary to further consider the nature of the process used to calculate RMS values to fully understand the reasons for these inconsistencies.

3.4: RMS Input Operation Conditions

At some higher frequency there are inconsistencies that begin to appear in the flicker results, however there is a gap in the test points which represents a significant portion of the higher frequency range of interest. The frequency gap exists between the 1620 CPM

and 4800 CPM test points in Table III-IV. At some frequency between these test points, the flickermeter begins to give erroneous results when full cycle RMS voltage values are used as the input. A detailed flicker test point table is provided in [10] that has additional test points over the frequency range of interest. These additional test points will help determine when the use of RMS inputs breaks down. The results of these test points when using RMS values as the input are provided in Table III-V. Notice that the 1620 CPM test point is the highest frequency that passes; the test points after 1620 CPM all fail low except for the 4800 CPM test point.

TABLE III-V.
FLICKER TEST POINTS WITH RMS INPUT

CPM	P_{st}	CPM	P_{st}	CPM	P_{st}
0.1	1.0175	22	0.9717	682	0.9714
0.2	0.9652	39	0.9710	796	0.9714
0.4	0.9649	48	0.9985	1020	0.9714
0.6	0.9675	68	0.9880	1055	0.9714
1	0.9939	110	0.9768	1200	0.9714
2	1.0169	176	0.9567	1390	0.9714
3	1.0587	273	0.9714	1620	0.9714
5	0.9699	375	0.9714	2400	0.9317
7	0.9508	480	0.9714	2875	0.6794
10	0.9835	585	0.9714	4800	1.7269

There are multiple issues that pertain to this phenomenon of low and high P_{st} results when utilizing RMS voltages as the input to the flickermeter. These issues manifest such that the full-cycle RMS values of an AM signal with square wave modulation could introduce new signal characteristics even though nothing about the AM signal is changing. The presence of any combination of the following list of issues can affect the P_{st} result in a negative way. The issues are as follows:

1. RMS Fluctuations due to RMS Window Location,
2. Repeating RMS Fluctuations of AM Signals,
3. Signal Aliasing due to the RMS Calculation, and
4. Short Term Flicker for Complex Modulations.

The consequence of these issues is that there is no consistently over- or under-conservative pattern in the P_{st} results for voltage fluctuations higher than 1620 CPM. It is appropriate to consider these issues to understand the implications of how they impact the P_{st} results in an inconsistent manner.

3.4.1: RMS Fluctuations due to RMS Window Location

Consider a general square wave modulated AM signal f(t) as illustrated in Fig. 3-5 where the windows denote the samples of the waveform that are utilized to calculate the corresponding RMS value. In the case of the RMS window on the top line, the result of this calculation will be the same as other RMS values whose window only includes samples from when the modulation signal is high. Similarly, the RMS window on the bottom line will result in an RMS value that will match other RMS values whose window only includes samples from when the modulation signal is low. The noteworthy RMS window is on the middle line in the figure. There are samples included in the window from when the modulation signal is high and samples from when it is low that will be included in the calculation. This calculated RMS value will not be the same as the RMS value calculated in the top window or in the bottom window and its actual value will vary based on the amount of the modulation signal that is included when it is high versus when it is low.

In order to use the RMS values with the flickermeter, an assumption is made that the RMS values will fluctuate in much the same way as the time domain waveform. The RMS value calculated in the middle window of Fig. 3-5 is going to change the fluctuation pattern that is presented by the RMS values when compared to the fluctuation present in the original time domain waveform. In effect, this represents some additional content in the modulation signal which could have unexpected consequences when demodulated internally by the flickermeter. This is problematic because the flickermeter is going to calculate a P_{st} value that is based on this new fluctuation pattern that is different from what is actually present in the time domain waveform. Unfortunately, this varying RMS calculation will occur anytime the RMS calculation window includes the transition from high to low or low to high of the square wave modulation signal.

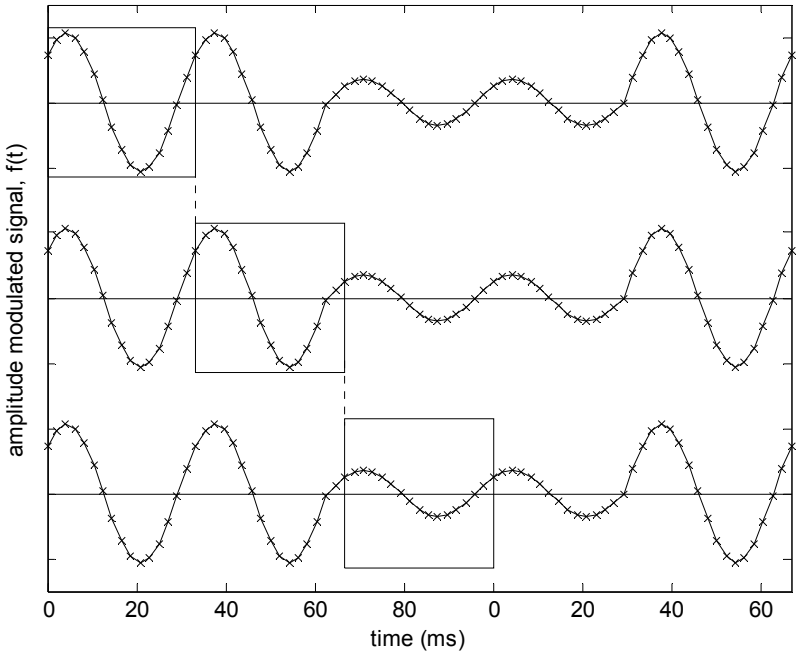

Figure 3-5. Amplitude Modulated Signal

The varying nature of the RMS value that is calculated from the middle window in Fig. 3-5 is dependent upon the location of the change from high to low or low to high of the square wave modulation in the RMS window. This is verified by considering how the RMS values fluctuate for a sinusoidal AM signal. It is appropriate to consider how the RMS value fluctuates for sinusoidal modulation because rectangular modulation can be written as a sum of sinusoids from a Fourier Series [11].

It is possible to calculate full cycle RMS values of an AM signal with sinusoidal modulation in closed form. The general form of the AM signal is provided in (3-2) with the following variable definitions:

A: Amplitude of the carrier signal,

B: Amplitude of the modulating signal,

ω_1: Radian frequency of the carrier signal (e.g. $2\pi 60$ rad/s),

ω_2: Radian frequency of the modulating signal,

α: Phase angle of the carrier signal, and

β: Phase angle of the modulating signal.

$$f(t) = A\cos(\omega_1 t + \alpha)\big(1 + B\cos(\omega_2 t + \beta)\big) \tag{3-2}$$

The RMS of (3-2) is calculated by using (3-3) and the result, provided in (3-4), will have 8 terms that are summed under the square root function and it is valid for any RMS time window. One of the terms will be a constant value and the remaining seven terms all have sinusoidal expressions that are a function of the RMS window times, T_1 and T_2.

$$RMS = \sqrt{\frac{1}{T_2 - T_1}\int_{T_1}^{T_2} f^2(t)} \tag{3-3}$$

$$RMS = \sqrt{\frac{1}{T_2 - T_1}\left(\begin{array}{c}
\left(\frac{2A^2 + A^2B^2}{4\omega_1}\right)\sin\left(\omega_1(T_2 - T_1)\right)\cos(\omega_1(T_2 + T_1) + 2\alpha) \quad (3\text{-}4a)\\
+\frac{2A^2B}{\omega_2}\sin\left(\frac{(\omega_2(T_2 - T_1))}{2}\right)\cos\left(\frac{(\omega_2(T_2 + T_1) + 2\beta)}{2}\right) \quad (3\text{-}4b)\\
+\frac{A^2B}{(2\omega_1 - \omega_2)}\sin\left(\frac{((2\omega_1 - \omega_2)(T_2 - T_1))}{2}\right)\cos\left(\frac{((2\omega_1 - \omega_2)(T_2 + T_1) + 4\alpha - 2\beta)}{2}\right) \quad (3\text{-}4c)\\
+\frac{A^2B}{(2\omega_1 + \omega_2)}\sin\left(\frac{((2\omega_1 + \omega_2)(T_2 - T_1))}{2}\right)\cos\left(\frac{((2\omega_1 + \omega_2)(T_2 + T_1) + 4\alpha + 2\beta)}{2}\right) \quad (3\text{-}4d)\\
+\frac{A^2B^2}{4\omega_2}\sin\left(\omega_2(T_2 - T_1)\right)\cos(\omega_2(T_2 + T_1) + 2\beta) \quad (3\text{-}4e)\\
+\frac{A^2B^2}{8(\omega_1 + \omega_2)}\sin\left((\omega_1 + \omega_2)(T_2 - T_1)\right)\cos\left((\omega_1 + \omega_2)(T_2 + T_1) + 2\alpha + 2\beta\right) \quad (3\text{-}4f)\\
+\frac{A^2B^2}{8(\omega_1 - \omega_2)}\sin\left((\omega_1 - \omega_2)(T_2 - T_1)\right)\cos\left((\omega_1 - \omega_2)(T_2 + T_1) + 2\alpha - 2\beta\right) \quad (3\text{-}4g)\\
+\left(\frac{A^2B^2}{4} + \frac{A^2}{2}\right)(T_2 - T_1) \quad (3\text{-}4h)
\end{array}\right)}$$

It is difficult to predict if the RMS value described in (3-4) will be constant or if it will vary from cycle to cycle just by examining the equation. The term (3-4h) is a constant, thus it will not fluctuate as the RMS time window changes. All of the remaining terms have sinusoidal parts that are a function of the RMS window times, T_1 and T_2. The sinusoidal parts of the terms in (3-4) that are a function of $(T_2–T_1)$ will not fluctuate with time because $(T_2–T_1)$ is a constant. This is not the case for the other sinusoidal parts that are a function of (T_2+T_1). As the RMS calculation window moves from one cycle of the fundamental to the next, the result of (T_2+T_1) will increase because T_1 and T_2 are increasing. This means that all of the terms in the RMS calculation, except for (3-4h), will fluctuate because they have sinusoidal parts that will vary as (T_2+T_1) increases. These fluctuating terms are part of the entire RMS calculation. When the terms in the RMS calculation fluctuate, the result of the RMS calculation will fluctuate with time even though the amplitudes, frequencies, and phases in (3-2) are constant. This variation in the

RMS calculation will introduce fluctuations to the flickermeter that are not actually present in the power system. The fluctuations are inherent to the RMS calculation that analytically describes the RMS window synchronization issue that is demonstrated graphically in Fig. 3-5 and they will impact the P_{st} result from the flickermeter. It is of interest to determine if these RMS fluctuations will be cyclical because of the sinusoidal terms that are present in (3-4).

3.4.2: Repeating RMS Fluctuations of AM Signals

It has been determined that the RMS values will fluctuate from cycle to cycle because the RMS calculation is a function of the sum of the times T_1 and T_2. Eventually these calculations will begin to repeat because the RMS calculation window will comprise the exact same portion of the time domain signal as it did in previous RMS calculations. Consider the following examples of AM signals with sinusoidal modulation from (3-2) with different frequencies f_2 where f_1 is 60 Hz. The cycle-by-cycle RMS values for each of the AM signals are calculated based on a 60 Hz time window and presented with the corresponding AM signal. The first example has f_2 equal to 9 Hz and is provided in Fig. 3-6 and the cycle-by-cycle RMS results are provided in Fig. 3-7. Notice that the first 20 RMS results are all different, but the 21st result is the same as the very first result.

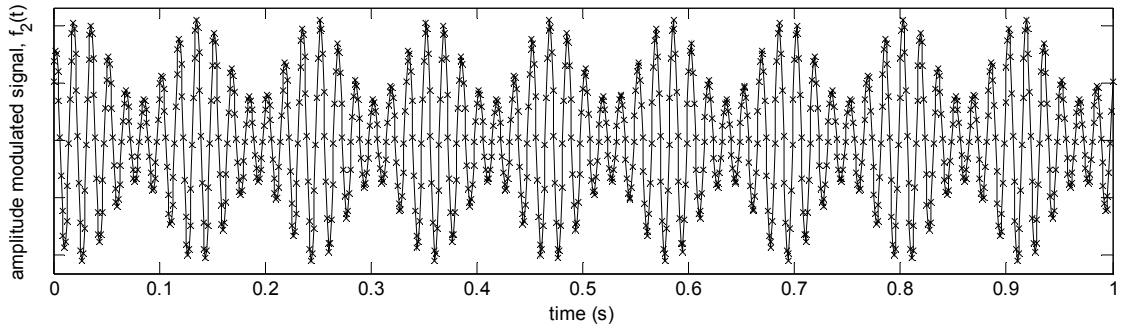

Figure 3-6. AM Signal with 9 Hz Sinusoidal Modulation

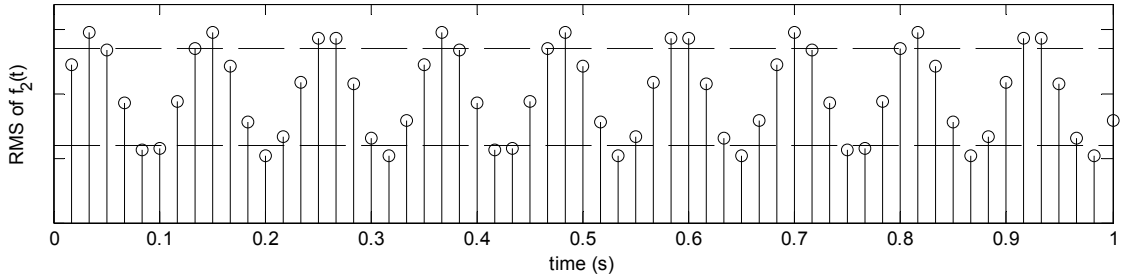

Figure 3-7. RMS of AM Signal with 9 Hz Sinusoidal Modulation

The second example has f_2 equal to 20 Hz and is provided in Fig. 3-8 and the cycle-by-cycle RMS results are provided in Fig. 3-9. Notice that the first 3 RMS results are all different, but the 4th result is the same as the very first result.

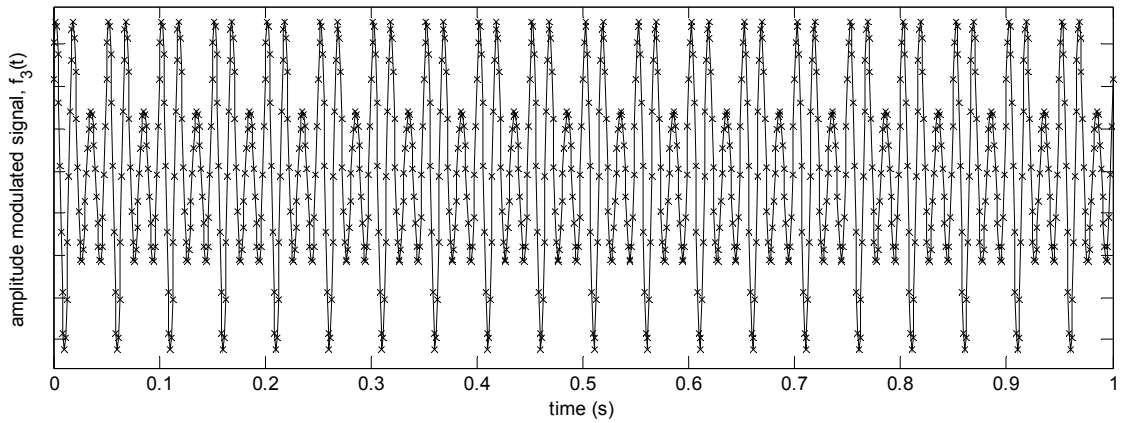

Figure 3-8. AM Signal with 20 Hz Sinusoidal Modulation

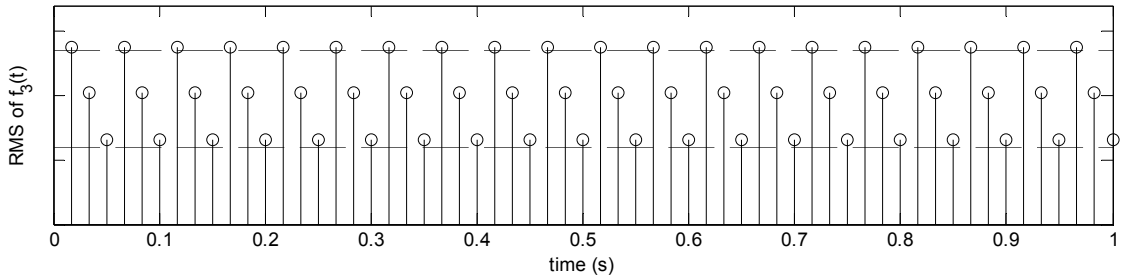

Figure 3-9. RMS of AM Signal with 20 Hz Sinusoidal Modulation

The third example has f_2 equal to 7 Hz and is provided in Fig. 3-10 and the cycle-by-cycle RMS results are provided in Fig. 3-11. Notice that none of the RMS values repeat for the one second block, but the next second of RMS values will be the same as the first second.

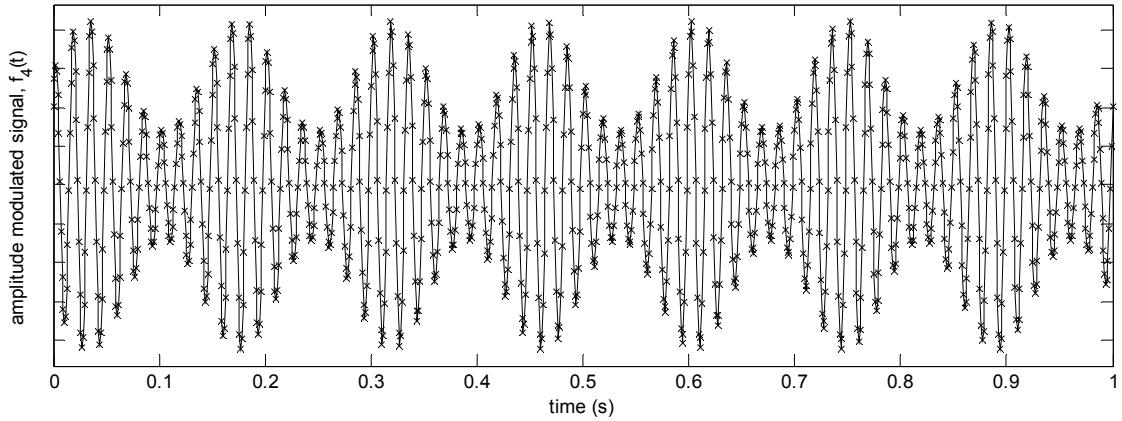

Figure 3-10. AM Signal with 7 Hz Sinusoidal Modulation

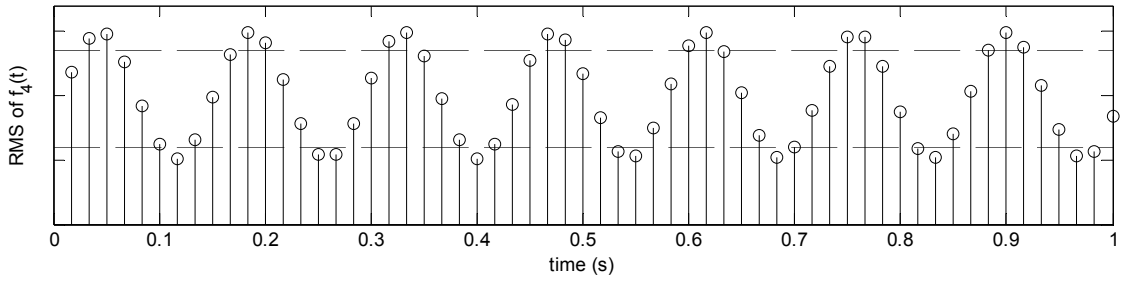

Figure 3-11. RMS of AM Signal with 7 Hz Sinusoidal Modulation

After 20 RMS calculations for the first example, the results will begin to repeat. The same repetition occurs in the second example, but it is after 3 RMS calculations. A repetition also occurs for the third example, but it repeats every second. These repetitions correspond to a frequency of how often the blocks of RMS values repeat. It is possible to calculate the frequency of the repeating blocks of RMS values by utilizing (3-5). The calculation involves determining the greatest common divisor (GCD) of f_1, f_2, and the RMS calculation frequency (f_{RMS_Calc}). The GCD for the first example (f_1=60 Hz, f_2=9 Hz, and f_{RMS_Calc}=60 Hz) will result in a value of 3. Similarly, for the second example

(f_1=60 Hz, f_2=20 Hz, and f_{RMS_Calc}=60 Hz), the GCD is 20. And finally for the third example (f_1=60 Hz, f_2=7 Hz, and f_{RMS_Calc}=60 Hz), the GCD is 1. This means that the frequency of repetition of the blocks of RMS values for the examples is 3 Hz, 20 Hz, and 1 Hz, respectively. By using (3-6) it is possible to calculate the number of RMS values that make up each block of values. Based on the numbers in this example it can be shown that that there are 20 RMS values in each block that repeats 3 times each second based on (3-5) and (3-6) for the first example, 3 RMS values at 20 times per second for the second example, and 60 RMS values at 1 time per second for the third example.

$$f_{RMS\_block} = GCD(f_1, f_2, f_{RMS\_Calc}) \tag{3-5}$$

$$RMS_{values} = \frac{f_{RMS\_Calc}}{f_{RMS\_block}} \tag{3-6}$$

Equations have been presented that describe the periodic nature of the RMS values that are produced from the RMS calculation of an AM signal. However, this is not the only issue associated with the RMS calculation. The RMS calculation will also alias frequency content that is present in the AM signal that is greater than 30 Hz into a frequency that is less than 30 Hz. This aliasing changes the signal and could negatively impact the P_{st} results. It is necessary to determine how aliasing of the signal due to the RMS calculation can affect the P_{st} results from the flickermeter.

3.4.3: Signal Aliasing due to the RMS Calculation

In section 3.3.1 it was shown that the RMS value that is calculated when the RMS window overlaps a change in state of the square wave modulation will not exactly correspond to the fluctuation that is present in the time domain waveform. As shown in

section 3.3.2, these differences will vary over time in a periodic way. If the flickermeter utilizes RMS inputs, the fluctuation characteristic that the meter processes will therefore be different than the actual fluctuation that is present in the time domain waveform. This new fluctuation content introduced by the RMS calculation could result in an invalid flicker calculation. It is possible to assess the amount of new frequency content that is introduced by the RMS calculation to determine if it will impact the flickermeter result.

Consider the RMS values that are presented in Fig. 3-7 that are calculated from the signal from Fig. 3-6 every 16.67 milliseconds. Notice that the modulation envelope of the original AM signal is captured in the RMS values. However, there is additional content present because the peaks of the modulation in the RMS waveform are not exactly the same from one cycle of the 9 Hz modulation to the next. An FFT was performed on the RMS signal and the magnitude results are provided in Table III-VI. The majority of the content is at 9 Hz and there is negligible content (relative to 9 Hz) at the harmonic multiples of the 9 Hz modulation. There is also 3 Hz content due to the frequency of RMS blocks from (3-5), but this content is also negligible relative to the 9 Hz content. The 9 Hz harmonic content accounts for the fluctuations that can be seen in the varying peaks in Fig. 3-7, but this content is not significant enough to lead to an invalid result from the flickermeter. This is expected because the RMS waveform will capture the low frequency fluctuations that are present in the time domain signal.

TABLE III-VI.
FFT RESULTS OF THE RMS SIGNAL IN FIG. 3-7

Hz	Mag	Hz	Mag	Hz	Mag	Hz	Mag
DC	1.00416	8	3.5E-16	16	3.3E-16	24	0.00026
1	6.3E-16	9	0.483	17	2.2E-16	25	3.3E-16
2	3.5E-16	10	7.5E-16	18	0.00381	26	4.2E-16
3	4.9E-06	11	5.8E-16	19	1.8E-16	27	0.00098
4	2.6E-16	12	1.4E-06	20	1.6E-16	28	3.3E-16
5	1.1E-15	13	4.1E-16	21	3.5E-07	29	2.4E-16
6	1.8E-05	14	4.3E-16	22	3.1E-16	30	1.7E-08
7	4.1E-16	15	6.8E-05	23	2.9E-16		

Aliasing of the input signal is problematic for higher frequency modulation when using RMS values as the input to the flickermeter. The sampling frequency of the RMS data is the same as the power system operating frequency because the data is calculated on a cycle-by-cycle basis. By applying the sampling theorem, the highest frequency content that can be properly represented will be half of the power system frequency and any higher frequency content will be aliased to some other frequency in the valid range [11]. There is content at frequencies presented in Table III-VI that are not harmonics of 9 Hz. For example, content exists at 6 Hz, 15 Hz, and 24 Hz because the 54 Hz, 45 Hz, and 36 Hz harmonics were aliased to those respective frequencies. However, the flickermeter does not "know" that this information has been aliased. It is going to calculate a flicker level based on the content that is present in the signal that is applied to its input, but this aliased content is not an issue for 9 Hz modulation harmonics. The reason that this is not an issue is because, as a rule of thumb, the magnitude of the modulation harmonics will decrease by the inverse of the harmonic number (i.e. *1/n* - where n is the harmonic number).

Aliasing is an issue if RMS values are calculated from an AM signal with square wave modulation where the modulation harmonics are greater than 30 Hz. Consider the

signal where the modulation frequency is 40 Hz. An AM signal with 40 Hz square wave modulation with a fluctuation magnitude that gives $P_{st}=1.0$ is provided in Fig. 3-12. The harmonic multiples of 40 Hz are 80 Hz, 120 Hz, 160 Hz, etc. The 40 Hz, 80 Hz, and 160 Hz frequencies will be aliased to 20 Hz and 120 Hz will alias to DC. Cycle-by-cycle RMS values are calculated for the signal presented in Fig. 3-12 and the results are presented in Fig. 3-13. An FFT is performed on the RMS values in Fig. 3-13 and the results are presented in Table III-VII. Notice that the only non-negligible content, besides DC, is the 20 Hz component that has a value of 0.01396, which is 0.02792 for the fluctuation magnitude. The fluctuation magnitude for 20 Hz sinusoidal modulation that gives a $P_{st}=1.0$ result is 0.01421. The 40 Hz modulation input that the flickermeter operates on is aliased to 20 Hz and it has a magnitude that is almost twice the corresponding $P_{st}=1.0$ magnitude at 20 Hz. This means that a large P_{st} result is expected from the flickermeter for cycle-by-cycle RMS input with 40 Hz modulation and is in accordance with the high 4800 CPM (40 Hz) test point result in Table III-IV.

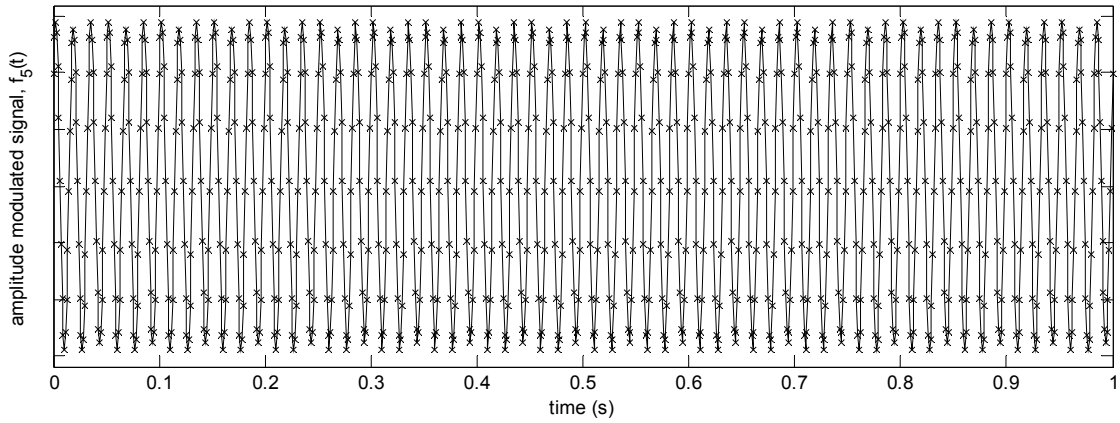

Figure 3-12. AM Signal with 40 Hz Square Wave Modulation

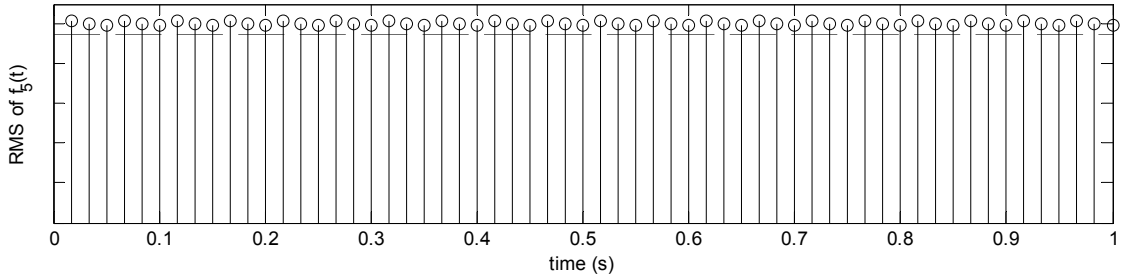

Figure 3-13. RMS of AM Signal with 40 Hz Square Wave Modulation

TABLE III-VII.
FFT RESULTS OF THE RMS SIGNAL IN FIG. 3-13

Hz	Mag	Hz	Mag	Hz	Mag	Hz	Mag
DC	1.001569	8	8.09E-05	16	1.70E-04	24	5.10E-04
1	8.68E-04	9	7.71E-04	17	1.42E-04	25	3.45E-04
2	7.52E-04	10	5.35E-04	18	6.72E-04	26	5.40E-04
3	3.98E-04	11	7.54E-04	19	6.24E-04	27	1.71E-05
4	4.07E-04	12	2.69E-04	20	0.01396	28	3.01E-04
5	7.41E-04	13	2.81E-04	21	6.93E-04	29	1.93E-04
6	6.77E-04	14	2.26E-04	22	2.02E-04	30	9.80E-05
7	2.98E-04	15	4.58E-04	23	5.32E-04		

In the previous example, the 40 Hz modulation content and the 40 Hz modulation harmonic content was aliased to the 20 Hz frequency. For known signal types, it seems possible to introduce an additional weighting filter at the input of the flickermeter to scale the frequencies that are over 30 Hz such that the aliasing issue is removed. This in effect fixes the aliasing problem that is illustrated in the previous example such that the flickermeter results would be $P_{st}=1.0$ when cycle-by-cycle RMS values are used as the input. However, it is not possible to do this because the cycle-by-cycle RMS values are the only data values that are available. Once the cycle-by-cycle RMS calculation is performed, the sampling frequency is forced to 60 Hz because there are now only 60 data values in a second. According to the sampling theorem, the new sampling frequency of

60 Hz means that the highest frequency that can be accurately represented is 30 Hz [11]. Because the highest frequency that can be represented is 30 Hz, this means that any content that is higher than 30 Hz is aliased by the RMS calculation. Also, in actual field data, the frequency content that is present before the cycle-by-cycle RMS calculation is performed is unknown. This means that once the signal is aliased by the cycle-by-cycle RMS calculation, it is not possible to determine whether content at a particular frequency was previously at that frequency before the cycle-by-cycle RMS calculation or if it was aliased to that frequency after the calculation. Thus, it is not possible to correctly weight content that is higher than 30 Hz because the RMS calculation has already aliased the signal content and it is not possible to adjust the aliased data after the RMS calculation because the aliased frequencies are unknown in actual field data.

It has been shown that performing the cycle-by-cycle RMS calculation on a signal will alias frequency content that is greater than 30 Hz to some frequency less than 30 Hz. This aliased frequency content could easily be aliased into the more sensitive flicker frequencies (around 8 Hz) or into the same frequency (e.g. aliasing of 40 Hz modulation). The result of this aliased content could produce inaccurate and inflated P_{st} results. Also, another complication is when the aliased content is to different frequencies that are less than 30 Hz. This resultant signal will be a signal with complex modulations. An example of a signal with complex modulations is a carrier signal that has two modulation waveforms instead of only one as illustrated in (3-7). It is tempting to calculate the individual P_{st} result that corresponds to each frequency and then sum up the individual P_{st} results to calculate the total P_{st} result. It will be shown that the P_{st} results for each

frequency that comprise a signal with complex modulations cannot be summated individually to calculate the total P_{st} result.

$$f_6(t) = Acos(\omega_1 t + \alpha)\big(1 + Bcos(\omega_2 t + \beta) + Ccos(\omega_3 t + \gamma)\big) \tag{3-7}$$

3.4.4: Short Term Flicker for Complex Modulations

Consider the AM signal presented in (3-8) where M_1, f_1, M_2, and f_2 are the test point modulation magnitude and frequency values that correspond to the 110 CPM and 480 CPM square wave modulation test points respectively.

$$f_7(t) = \sqrt{2}sin(377t)\begin{pmatrix} 1 \\ +\frac{M_1}{100} * 0.5 * sign(\sin(\omega_1 t)) \\ +\frac{M_2}{100} * 0.5 * sign(\sin(\omega_2 t)) \end{pmatrix} \tag{3-7}$$

If this signal is applied to the input of the software flickermeter with time domain voltage samples, then a P_{st} result of 2.0 is expected because each of the test points give a result of 1.0 when they are the only modulation content in the AM signal. The result from the flickermeter for this test signal that has complex flicker modulations is P_{st} = 1.47, which is not the expected result of 2.0. This is because it is easy to confuse the linear nature of the flickermeter with the concept of superposition; the flickermeter is only linear in that a doubling of the fluctuation magnitude results in a doubling of the P_{st} result. This means that in general it is not possible to calculate the total flicker level that an AM signal with complex modulations will produce by directly summing the flicker values that each individual component will produce if they were the only component in the AM signal.

This is important because if superposition could be applied to the flickermeter, then the FFT results that are presented in Table III-VI could be used to calculate a P_{st} result that would correspond to each magnitude and frequency in the table. Once a P_{st} result has been calculated for each individual component, then the P_{st} results could be summated to calculate the total P_{st} result that is the same as the output of the flickermeter. But, this method of calculating the P_{st} result will not work because superposition is not a suitable method to account for complex flicker modulations. A summary of the previously discussed issues that involve utilizing cycle-by-cycle RMS voltage data as the input to the flickermeter is appropriate.

3.5: Summary of Issues

Any combination of the issues that were explored in section 3.3.1 through section 3.3.4 can create a problem that impacts the P_{st} result when RMS values are used as the input to the flickermeter. It was found in section 3.3.1 and section 3.3.2 that the incorrect RMS values are due to the RMS calculation and that the values are periodic. In section 3.3.3 it was found that the RMS calculation aliases the frequency content that is present in the original signal into some frequency that is less than 30 Hz and that it is not possible to correct for the aliased content. It was determined in section 3.3.4 that the aliased content could lead to a signal with complex modulations and that it is not possible to use the summation law to calculate a P_{st} result based on the frequency content present in the signal. For these reasons, it does not appear, in general, to be possible to predict over- or under-conservative P_{st} results with RMS input for high frequency fluctuations.

It has been found that it acceptable to utilize cycle-by-cycle RMS values as the input to the flickermeter defined in IEEE 1453 for low frequency voltage fluctuations. A power flow calculation is going to be utilized to calculate an equivalent cycle-by-cycle voltage for the load installation of interest. These values will be processed by the flickermeter to calculate the flicker level for that specific load installation.

Chapter 4: Calculating the Equivalent Load Voltage

A method to calculate the cycle-by-cycle RMS equivalent load voltage values is necessary in order to be able to calculate the flicker level for the load installation of interest. The Thévenin equivalent circuit for the load of interest is provided in Fig. 4-1. The Thévenin equivalent impedance is calculated using the algorithm that is described in Chapter 2. The load voltage, $\bar{V}_L$, and load current, $\bar{I}_L$, are measured values at the load terminals on a cycle-by-cycle basis. It is possible to process the measured cycle-by-cycle RMS voltage values at the load with the flickermeter, but the flicker result will be based on the flicker due to all flicker producing sources that are connected electrically close together. A two bus power flow problem will be used to calculate the equivalent cycle-by-cycle RMS voltage values at the terminals of the load of interest.

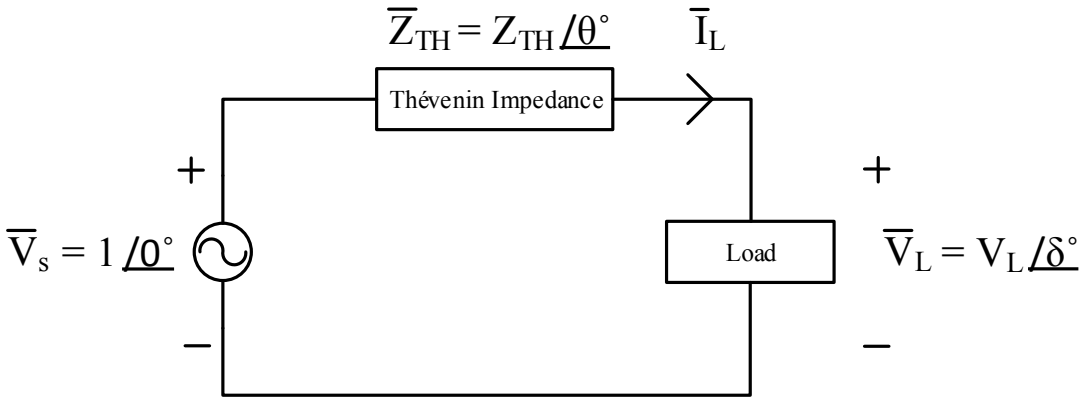

Figure 4-1. Thévenin Equivalent Circuit for the Load of Interest

The two bus power flow problem applied to the circuit presented in Fig. 4-1 involves solving two non-linear equations. These non-linear equations will be solved using the Newton-Raphson iterative method. The cycle-by-cycle measured load voltage and load current values are used to calculate the cycle-by-cycle complex power of the load of interest. It is necessary to determine the complex power of the load because this information is used in the non-linear equations to calculate the equivalent load voltage. The complex load power for the load in Fig. 4-1 is calculated using (4-1). By using substitution and various algebraic manipulations, it is possible to derive (4-2) and (4-3), where V_L and δ are the unknowns.

$$\bar{S}_L = \bar{V}_L \bar{I}_L^* = P_L + jQ_L \tag{4-1}$$

$$P_L = \frac{V_L}{Z_{TH}}\cos(\delta + \theta) - \frac{V_L^2}{Z_{TH}}\cos(\theta) \tag{4-2}$$

$$Q_L = \frac{V_L}{Z_{TH}}\sin(\delta + \theta) - \frac{V_L^2}{Z_{TH}}\sin(\theta) \tag{4-3}$$

The Newton-Raphson method is used to solve (4-2) and (4-3) every cycle to produce a set of cycle-by-cycle RMS voltage values. These RMS values will be used with the flickermeter to calculate the equivalent flicker level that a load of interest is producing independent of other flicker producing sources that are connected electrically near. It is appropriate to consider how this approach of calculating a particular load's flicker level performs with theoretical data.

Chapter 5: Device Implementation with Theoretical Data

A device that is able to implement the processes described in chapters 2-4 to calculate the flicker level that is produced by a particular load of interest has been developed in software. A test system was built that has two parallel loads connected to the power system through a Thévenin impedance. The test system is provided in Fig. 5-1, where the Thévenin impedance is 0.01+j0.05 per-unit. The first load is a constant impedance of 1+j0.3 per-unit and the second load fluctuates between 1+j0.3 per-unit and some fraction of the base impedance for some number of CPM. This test system is used to calculate the total flicker level of the parallel loads and then the equivalent flicker level for each of the loads.

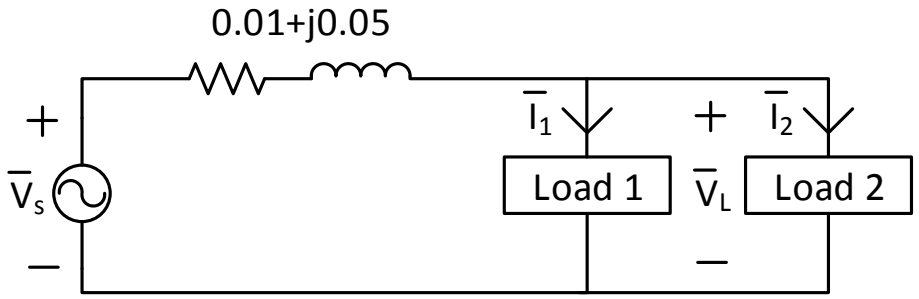

Figure 5-1. Thévenin Equivalent Circuit for the Load of Interest

5.1: Example 1

The first test involves setting the load 2 fluctuating impedance between 1+j0.3 per-unit and 0.5+j0.15 per-unit at 20 CPM or 0.167 Hz. A plot of the cycle-by-cycle RMS

voltages of the loads is provided in Fig. 5-2. The load voltage has a rectangular fluctuation from 0.953 to 0.929 per-unit, which is a change of 2.4%. The cycle-by-cycle RMS voltage values are processed by a software implemented flickermeter to calculate the flicker level. The total flicker level for the loads is calculated to be 2.15 based on the RMS voltage input. The total flicker level for the loads based on time sampled voltage data was calculated to be 2.15. The fact that the flicker results for the time sampled voltage data and the cycle-by-cycle RMS voltage data are the same is expected because the cycle-by-cycle RMS values are valid inputs to the flickermeter for low frequency fluctuations.

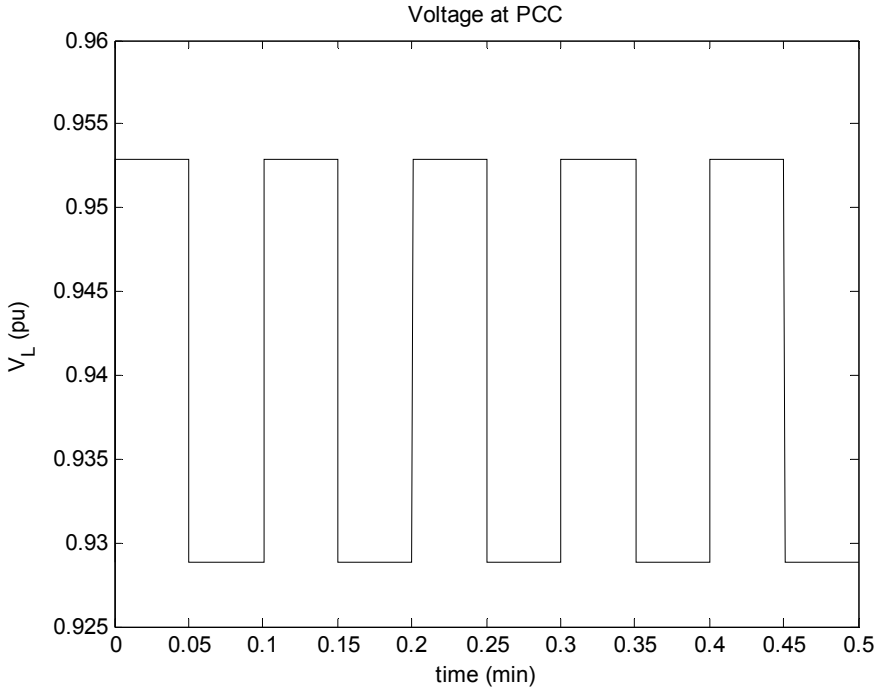

Figure 5-2. Voltage at the Parallel Load's Terminals

It is possible to calculate the Thévenin impedance at the terminals of load 2 by computing the parallel combination of the power system Thévenin impedance

(0.01+j0.05) with the impedance of Load 1 (1+j0.3). The Thévenin impedance at the load 2 terminals can be calculated analytically to be 0.0118+j0.0484 per-unit. The impedance estimation algorithm described in chapter 2 must calculate this impedance. The time constant and power threshold that were chosen for the algorithm were 5 seconds and 0.2 per-unit, respectively. A plot of the resistance is provided in Fig. 5-3 and a plot of the reactance is provided in Fig. 5-4. Notice that the initial condition for the Thévenin impedance at the load 2 terminals is 0.01+j0.04 per-unit. The impedance estimation algorithm reaches 5% of the analytical 0.0118 per-unit resistance at 22.15 minutes and it reaches 5% of the analytical 0.0484 per-unit reactance at 16.55 minutes.

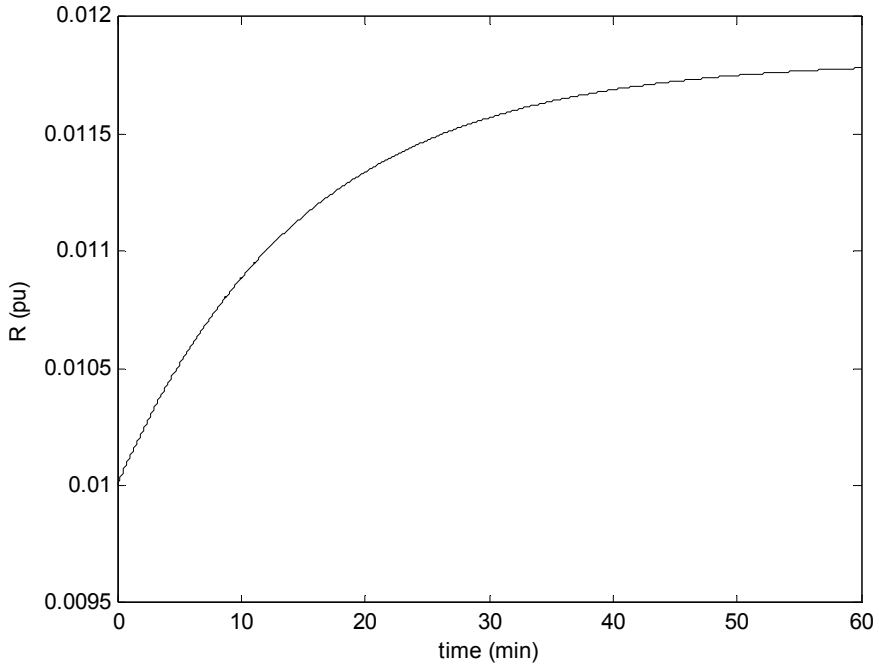

Figure 5-3. Thévenin Estimated Resistance at Load 2

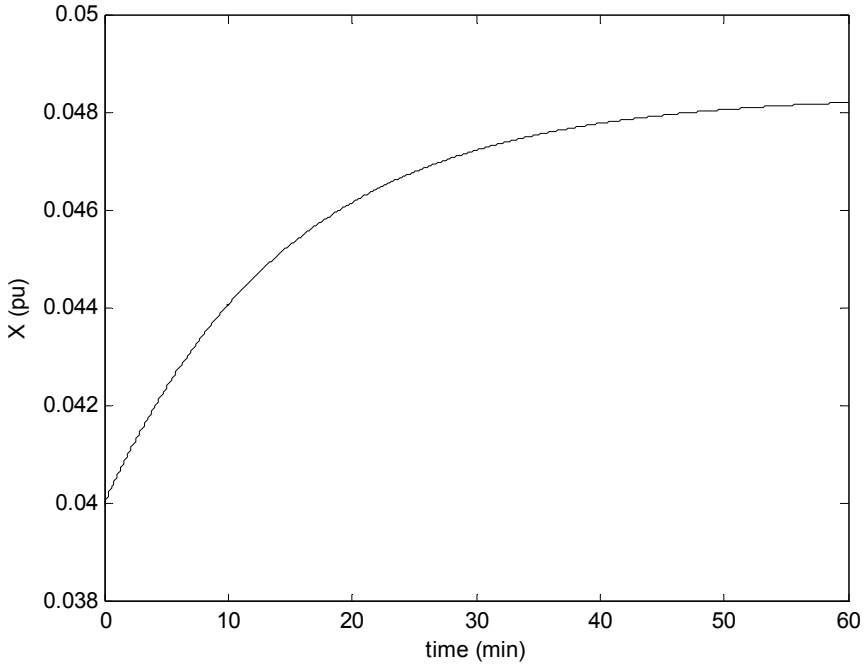

Figure 5-4. Thévenin Estimated Reactance at Load 2

The calculated voltage for load 2 from the power flow calculation discussed in chapter 4 is provided in Fig. 5-5. A zoomed in look at the load voltage after the transient due to the impedance estimation algorithm reaches steady state is provided in Fig. 5-6. There is a fluctuation from 0.977 to 0.954 per-unit, which is a change of 2.3%. This change of 2.3% is expected because load 2 is driving the voltage fluctuations and it is 0.1% from the total 2.4% measured fluctuation. A software implemented flickermeter can process the calculated cycle-by-cycle RMS values for load 2 to determine its flicker level; the flicker level for load 2 is calculated to be 2.07.

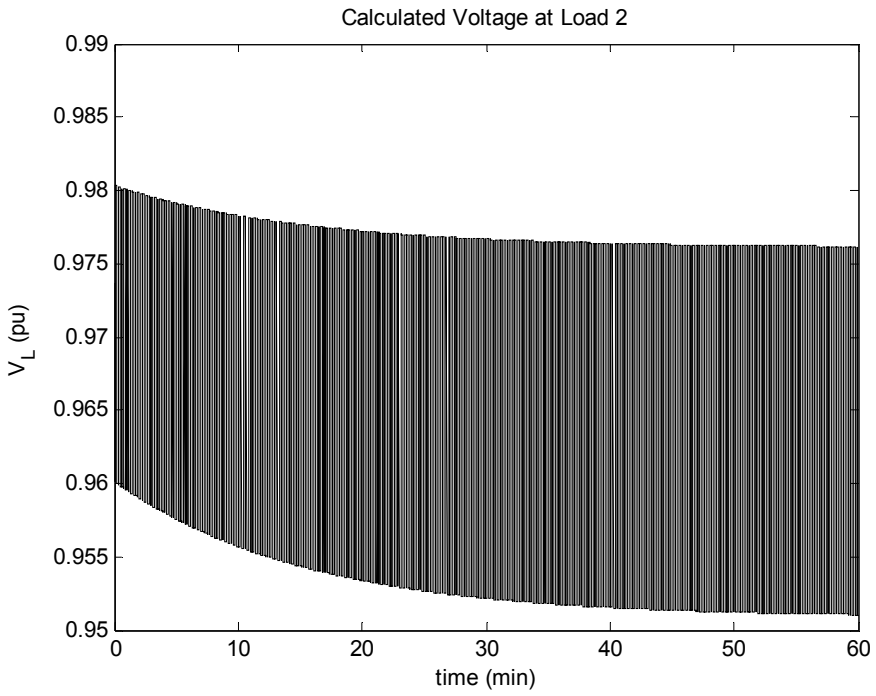

Figure 5-5. Load 2 Calculated Equivalent Voltage

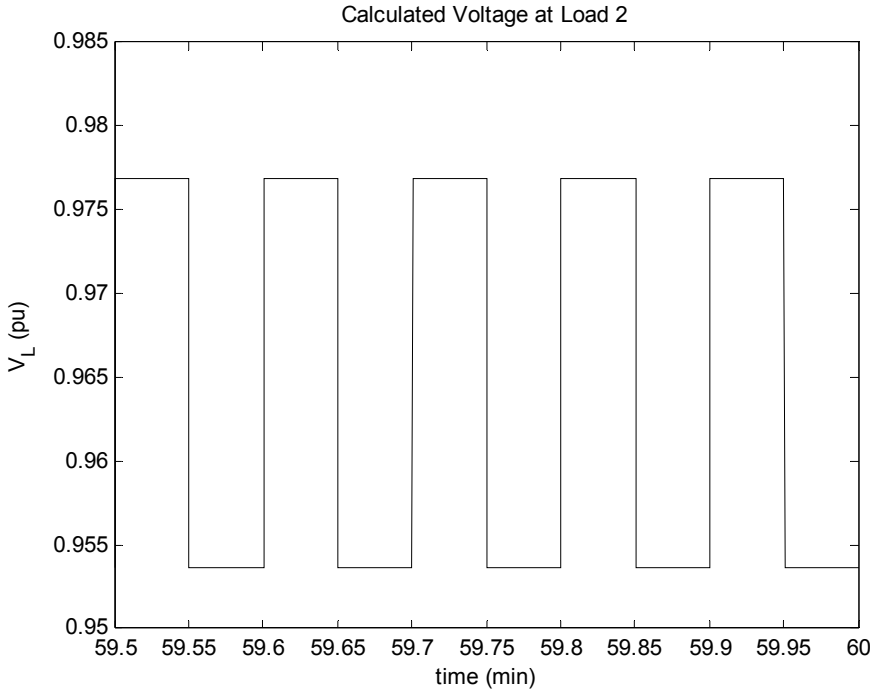

Figure 5-6. Load 2 Calculated Equivalent Voltage at Steady State

The same process was performed on load 1. The Thévenin impedance estimation algorithm does not calculate a new impedance; it holds the initial conditions constant. This is expected because load 1 is a constant impedance load with small power variations, any power changes are due to the voltage fluctuations produced by load 2. The calculated voltage for load 1 from the same power flow calculation is provided in Fig. 5-7. A zoomed in plot of the calculated voltage for load 1 is provided in Fig. 5-8. This calculated voltage fluctuates from 0.982 to 0.981, which is a change of 0.1%. The calculated cycle-by-cycle RMS voltage values were processed with the flickermeter and the flicker level was calculated to be 0.084. As expected, the calculated voltage for load 1 has a voltage fluctuation magnitude that is significantly less than load 2 and results in a flicker level that is significantly less than load 2 because load 2 is producing the voltage fluctuations.

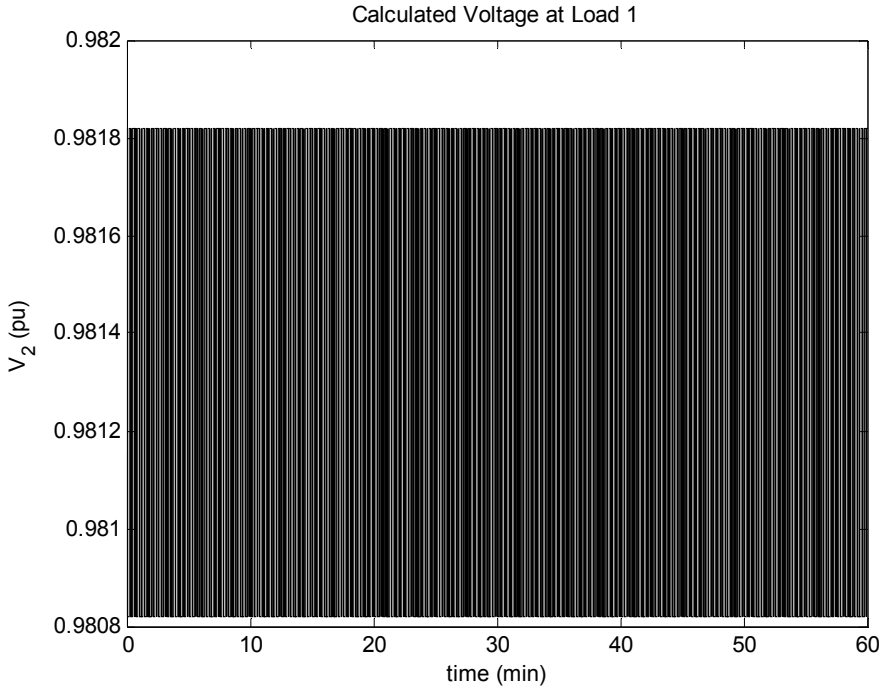

Figure 5-7. Load 1 Calculated Equivalent Voltage

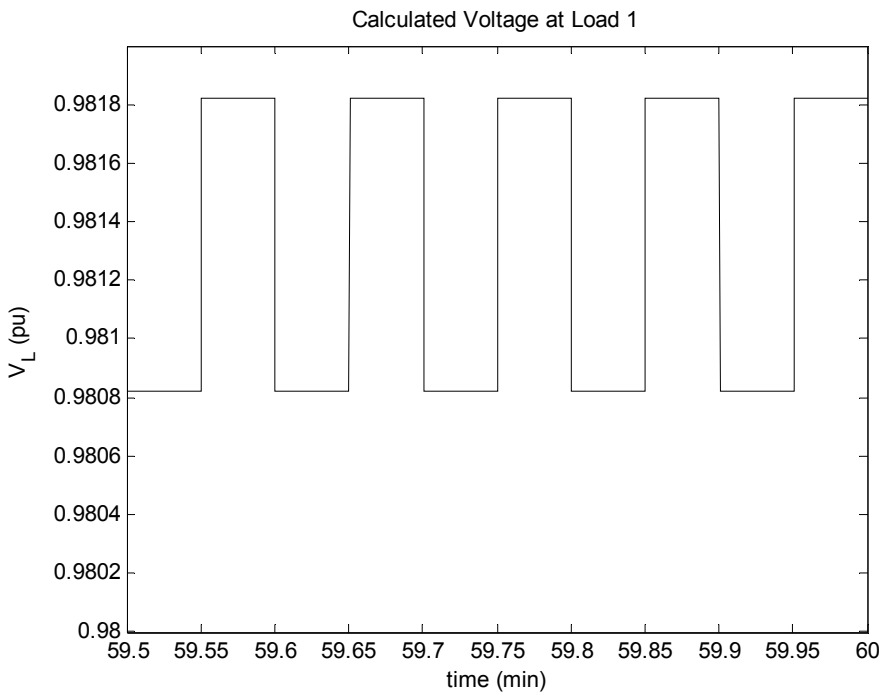

Figure 5-8. Adjusted View of Load 1 Calculated Equivalent Voltage

5.2: Example 2

The second test involves setting the load 2 fluctuating impedance from 1+j0.3 to 0.75+j0.225 per-unit at 240 CPM or 2 Hz. A plot of the cycle-by-cycle RMS voltages at the terminals of the loads is provided in Fig. 5-9. The load voltage fluctuations are from 0.953 to 0.945 with a rectangular fluctuation pattern that has a change of 0.8%. The flicker level for this amount of voltage fluctuation is calculated to be 1.26. The total flicker level for the loads based on time sampled voltage data was calculated to be 1.25. There is a 0.8% difference between the time sampled voltage data and the cycle-by-cycle RMS voltage data. A small difference is reasonable because the fluctuation frequency is higher in this example than in the previous example.

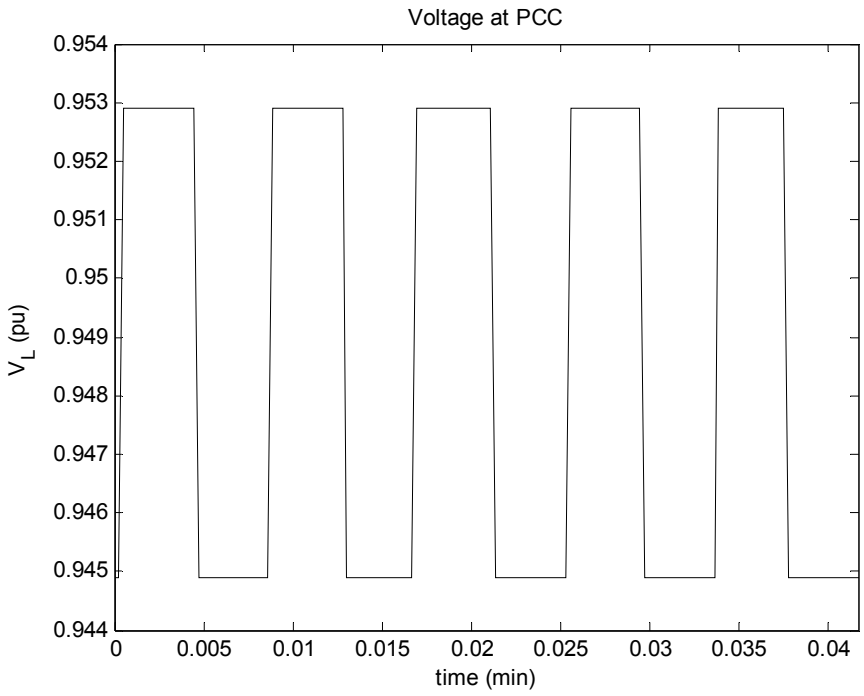

Figure 5-9. Voltage at the Parallel Load's Terminals

The Thévenin impedance at the terminals of load 2 is the same as the previous example because load 1 and the Thévenin impedance of the power system are unchanged. Also, the time constant and power threshold that were chosen for the impedance estimation algorithm are the same as the previous example: 5 seconds and 0.2 per-unit, respectively. Plots of the estimated Thévenin equivalent resistance and reactance are provided in Fig. 5-10 and Fig. 5-11, respectively. Each initial condition for both the resistance and reactance are the same from the first example. The impedance estimation algorithm reaches 1% of the 0.0118 per-unit resistance at 3.3 minutes and it reaches 1% of the 0.0484 per-unit reactance at 3.6 minutes.

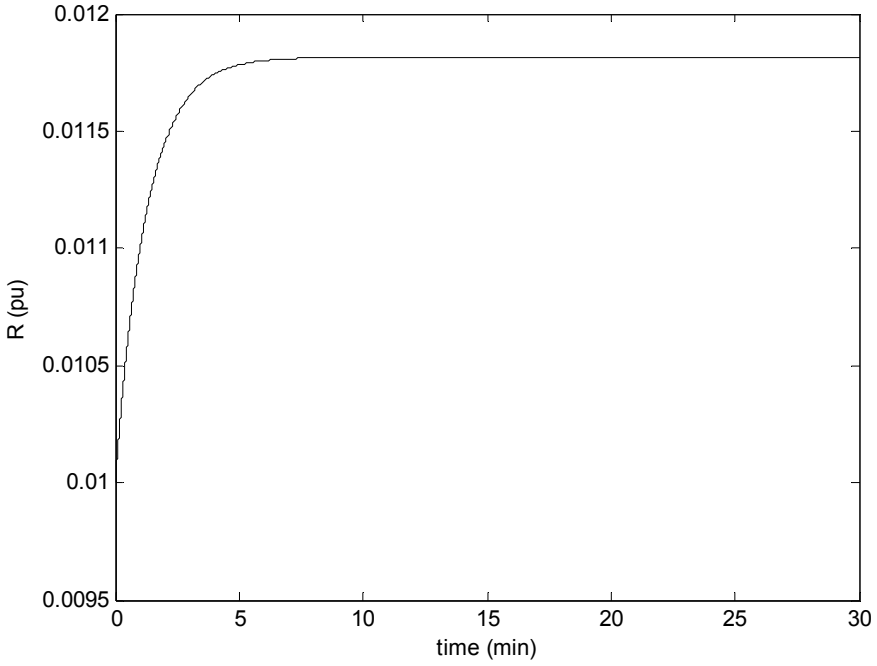

Figure 5-10. Thévenin Estimated Resistance at Load 2

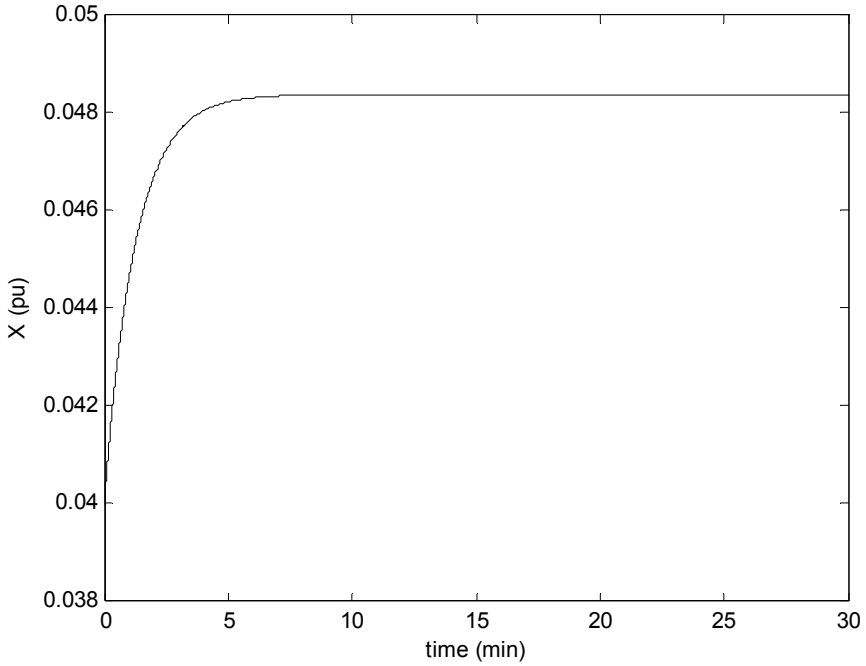

Figure 5-11. Thévenin Estimated Reactance at Load 2

The calculated load voltage for load 2 from the same power flow calculation used in example 1 is provided in Fig. 5-12. A zoomed in look at the load voltage after the initial transient reaches steady state is provided in Fig. 5-13. There is a voltage fluctuation from 0.9768 to 0.969, which is a change of 0.78%. This result is very close to the 0.8% change from the measured voltage presented in Fig. 5-9. A flicker value of 1.18 was calculated for load 2 by using the same software implemented flickermeter as in the first example.

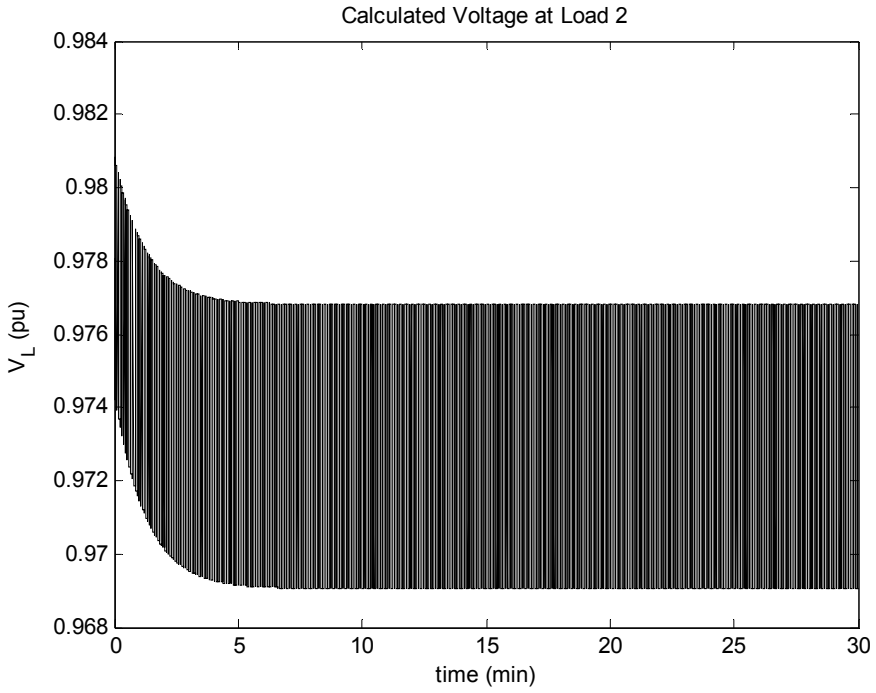

Figure 5-12. Load 2 Calculated Equivalent Voltage

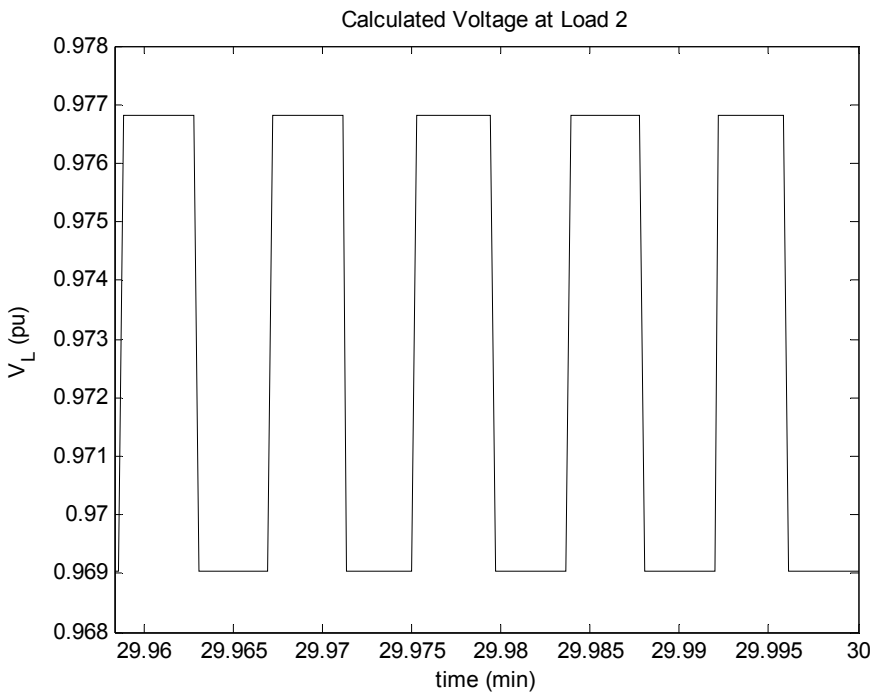

Figure 5-13. Load 2 Calculated Equivalent Voltage at Steady State

An identical process is used to calculate the flicker level of load 1. Similar to the first example, the Thévenin impedance estimation algorithm does not estimate a new impedance for load 1. The calculated voltage for load 1 is provided in Fig. 5-14. A zoomed in plot of the calculated voltage for load 1 is provided in Fig. 5-15. This calculated voltage fluctuates from 0.9812 to 0.9808, which is a change of 0.04%. The flicker level for load 1 was calculated to be 0.05 for this fluctuation level. Similarly to the first example, the flicker level for load 1 is significantly less than load 2 because load 2 is producing the voltage fluctuations.

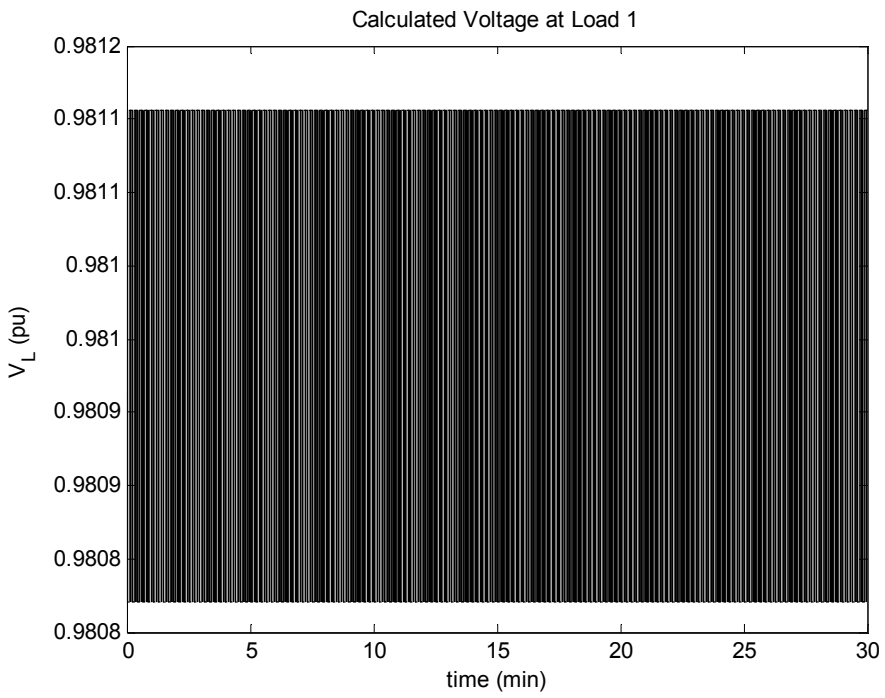

Figure 5-14. Load 1 Calculated Equivalent Voltage

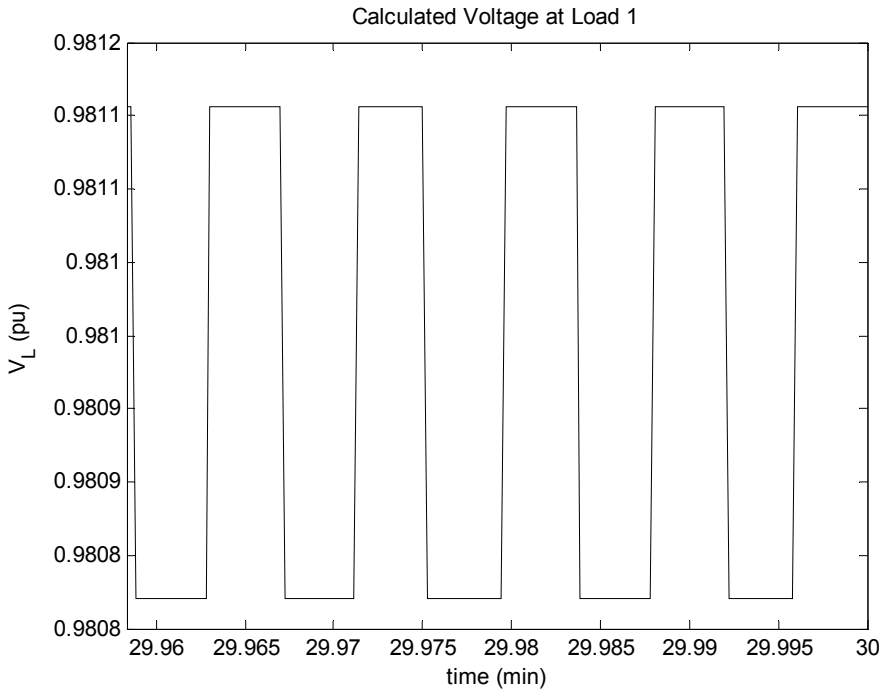

Figure 5-15. Adjusted View of Load 1 Calculated Equivalent Voltage

5.3: Example 3

The third test is a high frequency test where the CPM is expected to give an invalid flicker result because of the discussion presented in chapter 3. The same fluctuation magnitude for example 2 is now applied at 2400 CPM or 20 Hz for load 2. A plot of the cycle-by-cycle RMS voltages of the loads is provided in Fig. 5-16. Notice that the voltage fluctuation magnitude is the same as the previous example (0.8%), but the fluctuation shape is triangular rather than square because of the high rate of fluctuation relative to sampling frequency. The total flicker level for the loads based on time sampled voltage data was calculated to be 0.97. There are 1.5 hours of flicker results provided in Table V-I that are based on cycle-by-cycle RMS voltage data. Notice that the flicker results are greater than 0.97 from the time sampled voltage data input and that each value is different even though the fluctuation pattern is the same. The flicker results should be 0.97, but they are all larger and fluctuate from 1.01 to 1.185. These flicker results are invalid because of the high frequency limitations of calculating flicker using cycle-by-cycle RMS values.

TABLE V-I.
FLICKER RESULTS FOR THE PARALLEL LOADS

10 Minute Interval	P_{st}
1	1.1291
2	1.0718
3	1.0155
4	1.1437
5	1.1529
6	1.0857
7	1.1653
8	1.1854
9	1.1481

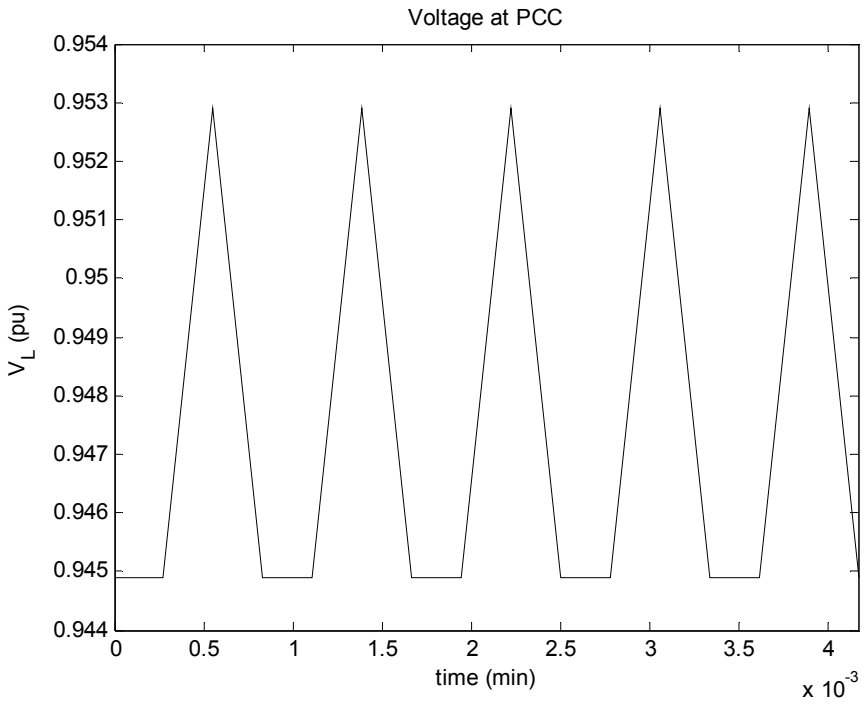

Figure 5-16. Voltage at the Parallel Load's Terminals

The Thévenin impedance at the terminals of load 2 will be the same as the previous examples. Also, the time constant and power threshold that were chosen for the impedance estimation algorithm are the same as the previous examples: 5 seconds and 0.2 per-unit, respectively. Plots of the estimated Thévenin equivalent resistance and reactance are provided in Fig. 5-17 and Fig 5-18, respectively. Notice that the estimated resistance and reactance reach 1% of the expected values after 20 seconds and 21.5 seconds, respectively. This is expected because load 2 fluctuates at 2400 CPM in this example whereas it fluctuates at 240 CPM in the previous example which results in more impedance calculations that meet the requirement of (2-25) in a shorter amount of time.

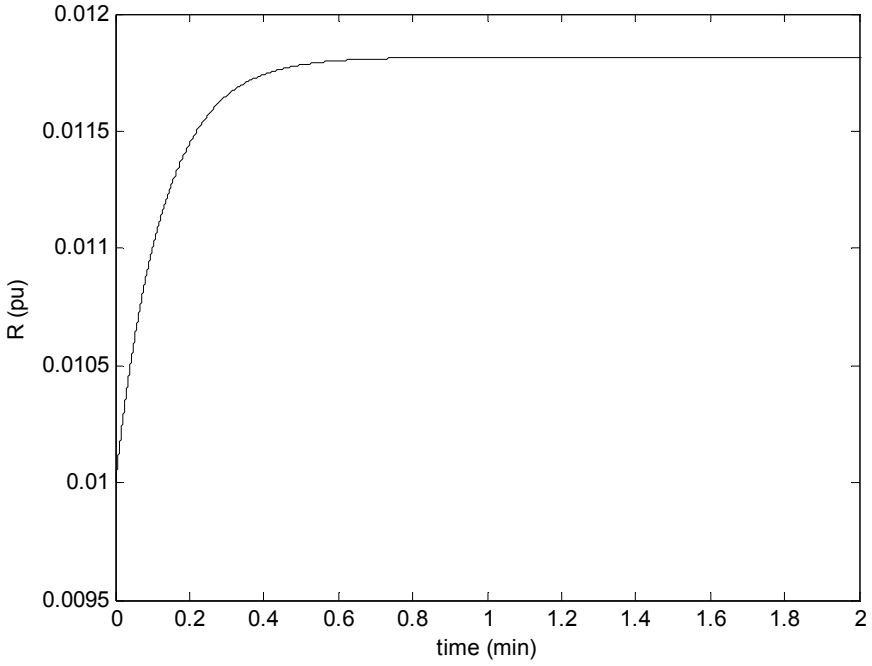

Figure 5-17. Thévenin Estimated Resistance at Load 2

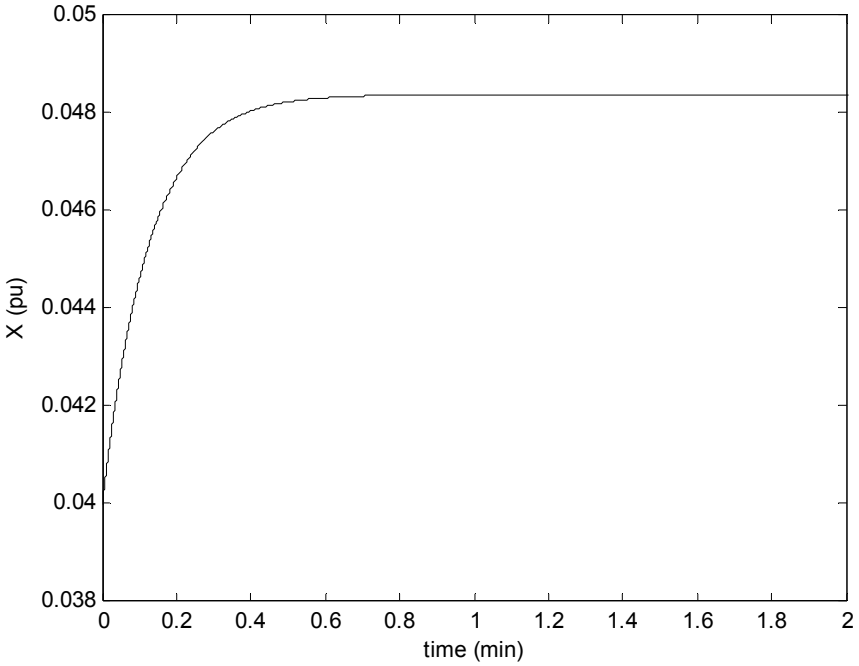

Figure 5-18. Thévenin Estimated Reactance at Load 2

The calculated load voltage for load 2 from the same power flow calculation used in the previous examples is provided in Fig. 5-19. A zoomed in look at the steady state portion of the calculated load voltage is provided in Fig. 5-20. The calculated load voltage fluctuates from 0.9768 to 0.969 for a change of 0.78%, which is the same as example 2. There are 1.5 hours of flicker results for load 2 provided in Table V-II. These flicker levels also fluctuate from one 10 minute period to the next because of using cycle-by-cycle RMS values as the input to the flickermeter for high frequency fluctuations. However, notice that the flicker values using the calculated cycle-by-cycle RMS values for load 2 are about the same as the values in Table V-I. This is expected because load 2 is producing the flicker that is present for the parallel loads.

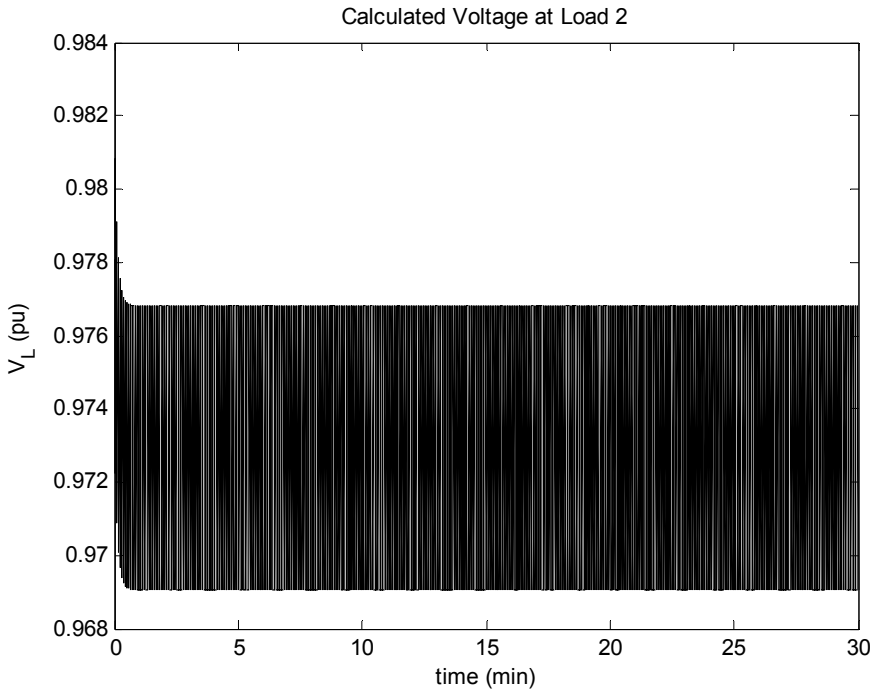

Figure 5-19. Load 2 Calculated Equivalent Voltage

TABLE V-II.
FLICKER RESULTS FOR LOAD 2

10 Minute Interval	P_{st}
1	1.0639
2	0.9935
3	0.9827
4	1.0934
5	1.0984
6	1.0251
7	1.1299
8	1.1358
9	1.08

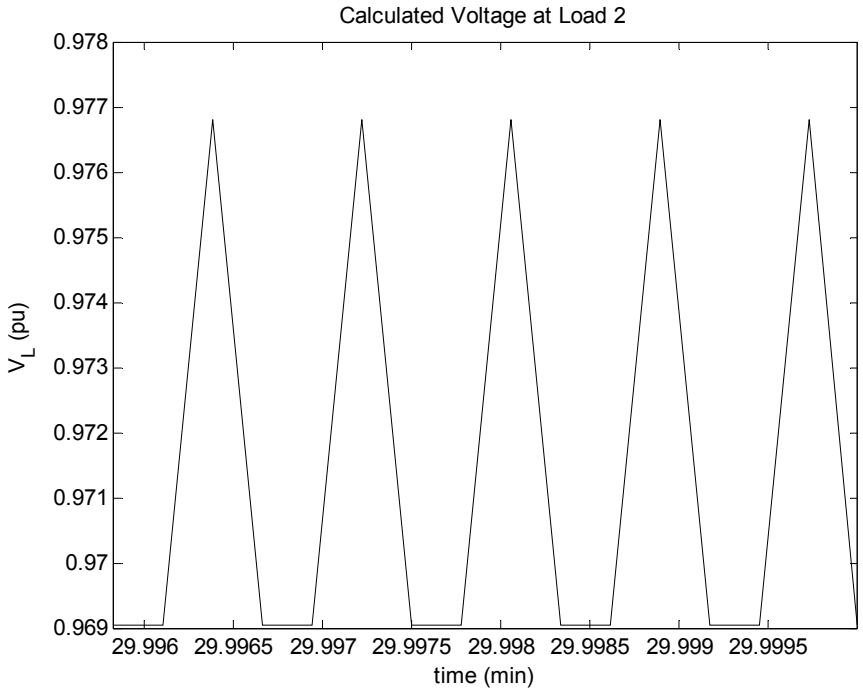

Figure 5-20. Load 2 Calculated Equivalent Voltage at Steady State

The same process is used to calculate the flicker level of load 1. As expected, based on the previous examples, the calculated Thévenin impedance algorithm holds the initial values constant for load 1. The calculated voltage for load 1 is provided in Fig. 5-21 and

a zoomed in plot is provided in Fig. 5-22. This calculated voltage for load 1 has the exact same fluctuation magnitude as example 2 (0.04%). There are 1.5 hours of flicker results for load 1 provided in Table V-III. These results also fluctuate from one 10 minute interval to the next even though the fluctuation magnitude does not change. However, these results are significantly less than the results that are provided in Table V-II. While it is not possible to calculate a valid flicker result using cycle-by-cycle RMS voltage values for a particular load of interest, it is still possible to identify which load is producing the majority of the flicker even though there are high frequency voltage fluctuations.

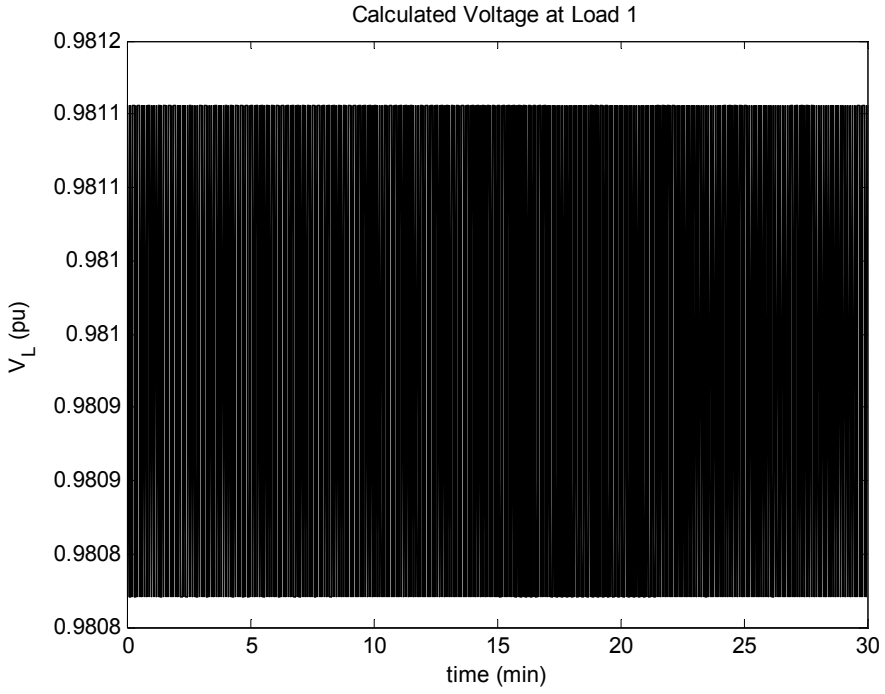

Figure 5-21. Load 1 Calculated Equivalent Voltage

TABLE V-III.
FLICKER RESULTS FOR LOAD 1

10 Minute Interval	P_{st}
1	0.0443
2	0.0426
3	0.0404
4	0.0446
5	0.0449
6	0.0429
7	0.0461
8	0.0459
9	0.0446

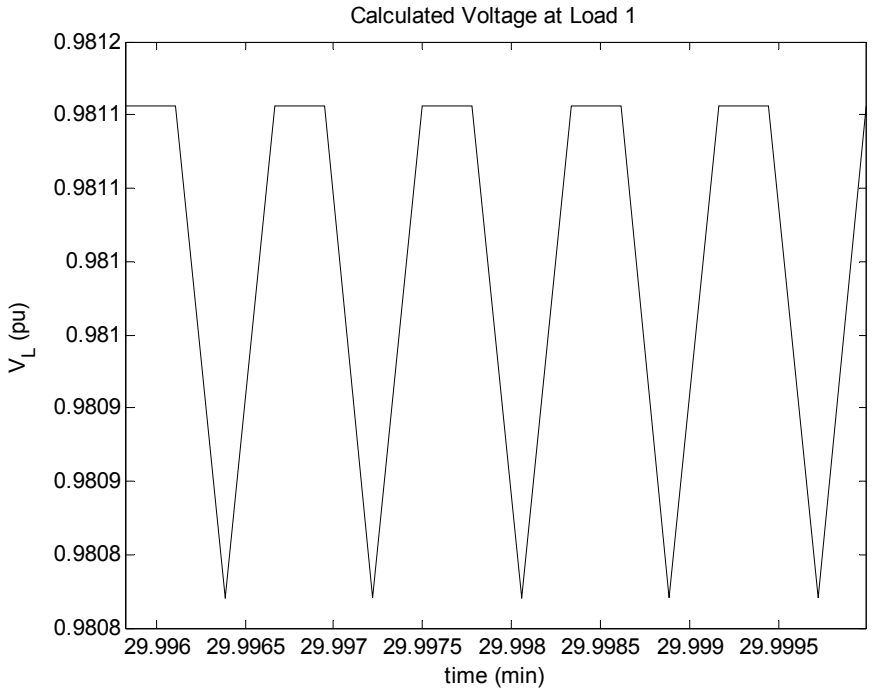

Figure 5-22. Adjusted View of Load 1 Calculated Equivalent Voltage

5.4: Example 4

The fourth test involves setting the load 2 fluctuating impedance from 1+j0.3 to 0.75+j0.225 per-unit at 240 CPM or 2 Hz and the system Thévenin equivalent impedance fluctuates from 0.01+j0.05 to 0.005+j0.025 every 30 minutes or 0.278 mHz. A plot of the cycle-by-cycle RMS voltages at the loads for the system Thévenin impedance of 0.01+j0.05 is provided in Fig. 5-23 and another plot of the load cycle-by-cycle RMS voltages for the system Thévenin impedance of 0.005+j0.025 is provided in Fig. 5-24. The load voltage fluctuations are from 0.953 to 0.945 with a rectangular fluctuation pattern that has a change of 0.8% when the system Thévenin impedance is 0.01+j0.05 and 0.977 to 0.973 for a change of 0.4% when the system Thévenin impedance is 0.005+j0.025.

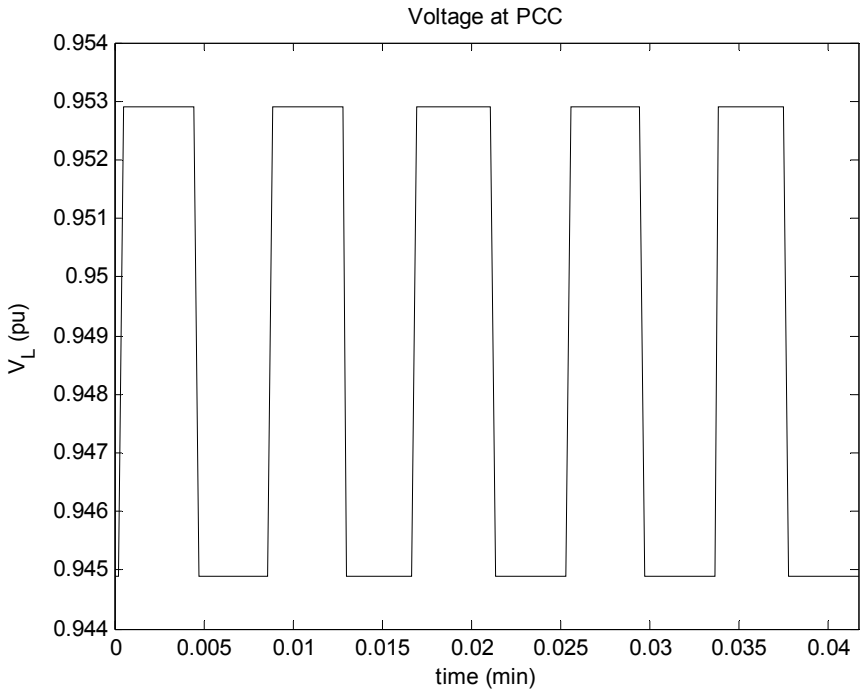

Figure 5-23. Voltage at the Parallel Load's Terminals

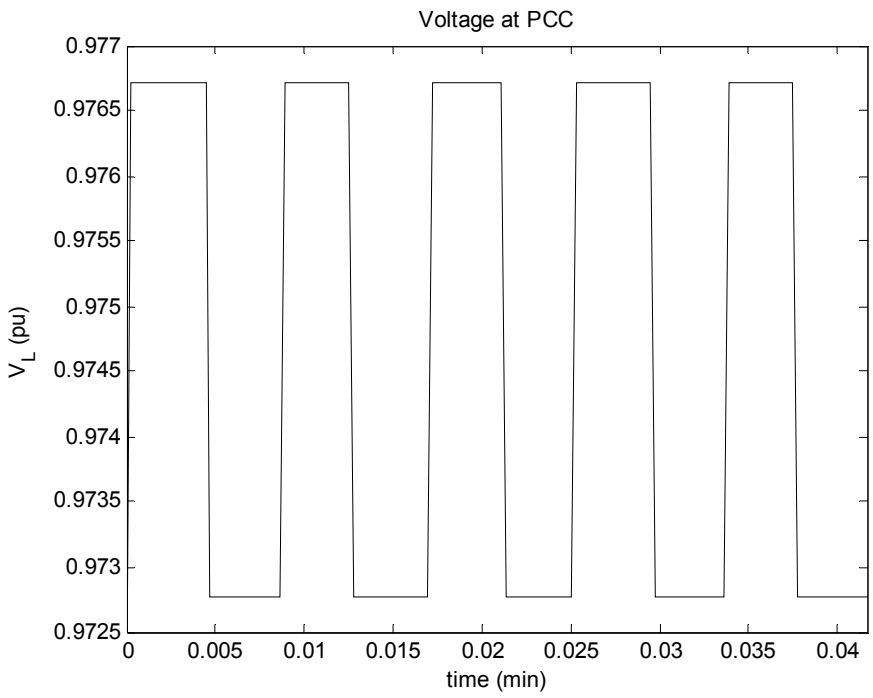

Figure 5-24. Voltage at the Parallel Load's Terminals

The Thévenin impedance at the terminals of load 2 is going to fluctuate between 0.0118+j0.0484 per-unit and 0.00547+j0.0246 per-unit because the system Thévenin impedance is fluctuating. Plots of the estimated Thévenin equivalent resistance and reactance are provided in Fig. 5-25 and Fig. 5-26, respectively. The time constant and power threshold that were chosen for the impedance estimation algorithm are the same as the previous examples: 5 seconds and 0.2 per-unit, respectively. The impedance estimation algorithm tracks both of the Thévenin equivalent impedances at the terminals of the second load as the system Thévenin equivalent impedance varies.

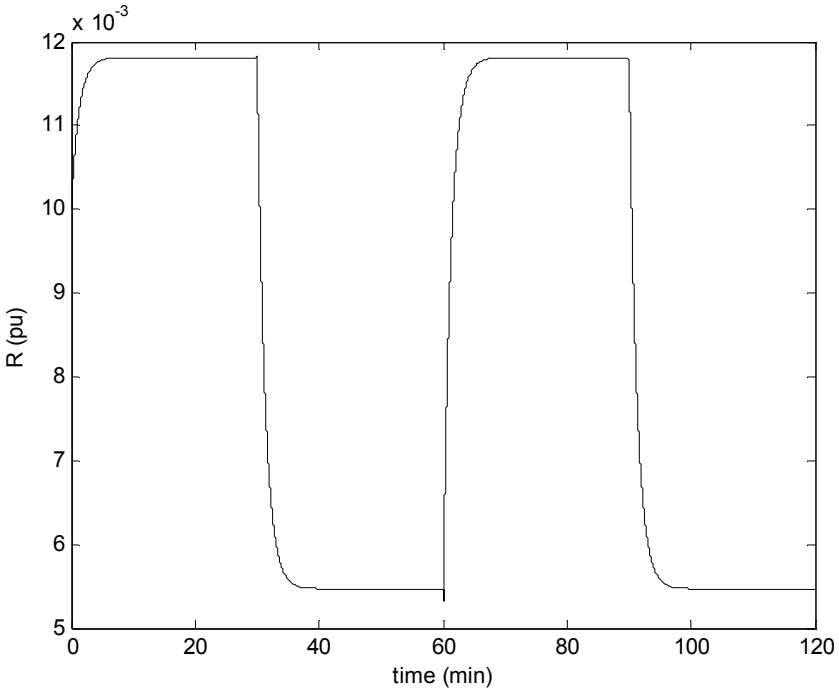

Figure 5-25. Thévenin Estimated Resistance at Load 2

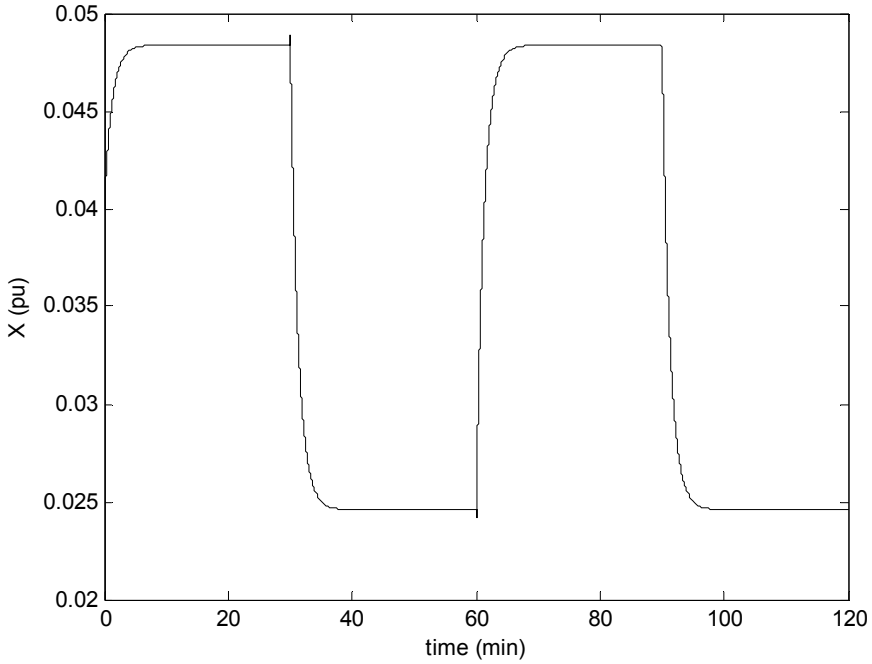

Figure 5-26. Thévenin Estimated Reactance at Load 2

The calculated load voltage for load 2 from the power flow calculation used in example 1 is provided in Fig. 5-27. Notice that the calculated voltage fluctuations have a transient when the system Thévenin impedance changes because the Thévenin equivalent estimation algorithm has to estimate the new impedance before the correct voltage fluctuations are calculated. These "incorrect" transient cycle-by-cycle RMS values are going to affect the corresponding flicker whose window includes these RMS values. This is of particular interest because the flicker result that is based on these calculated RMS values is expected to be approximately the same as or slightly less than the total flicker level for the parallel loads. This expectation has been verified in examples 1 and 2. The flicker results that are based on time sampled voltage data for when the system Thévenin impedance is 0.01+j0.05 per-unit and 0.005+j0.025 are 1.25 and 0.58, respectfully. The total flicker level results for the parallel loads from the measured cycle-by-cycle RMS values are provided in Table V-IV. The flicker results that are based on the calculated cycle-by-cycle RMS values for the second load are provided in Table V-V. Notice that the calculated flicker results for load 2 are lower than the flicker results for the parallel loads except for when the system Thévenin impedance switches from 0.01+j0.05 per-unit to 0.005+j0.025 per-unit. Both the fourth and the tenth 10 minute intervals for the calculated flicker results for load 2 are about 13% larger than the corresponding total flicker results for the parallel loads. This issue of the calculated cycle-by-cycle RMS values producing larger P_{st} results than the measured cycle-by-cycle RMS voltages is due to the transient that is produced in the impedance estimation algorithm as it tracks the new Thévenin equivalent impedance at the load 2 terminals.

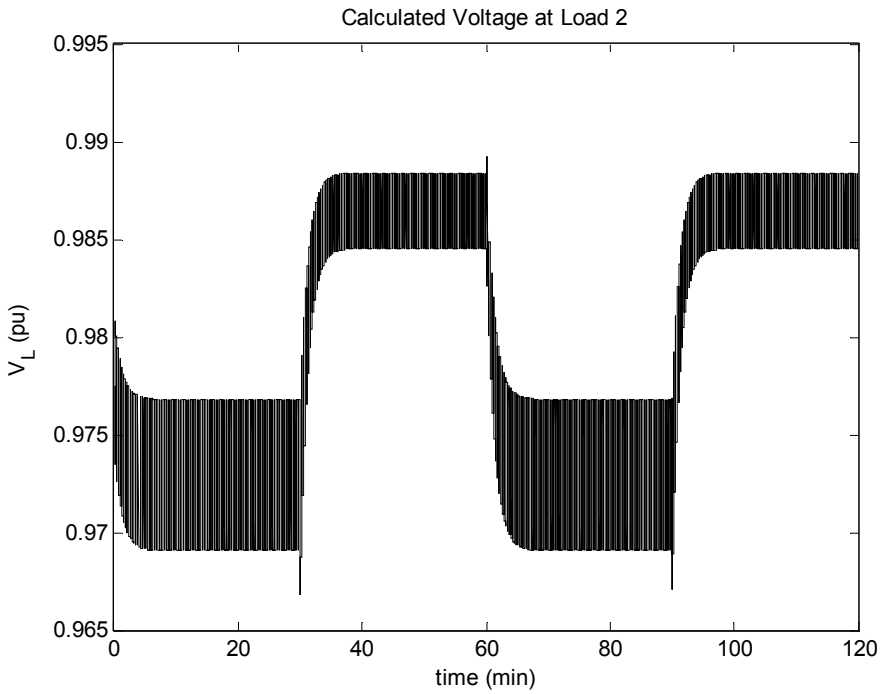

Figure 5-27. Load 2 Calculated Equivalent Voltage

TABLE V-IV.
FLICKER RESULTS FOR THE PARALLEL LOADS

10 Minute Interval	P_{st}
1	1.2552
2	1.2554
3	1.2635
4	0.5823
5	0.5829
6	0.8988
7	1.2556
8	1.2559
9	1.2598
10	0.5836
11	0.5831
12	0.8986

TABLE V-V.
FLICKER RESULTS FOR LOAD 2

10 Minute Interval	P_{st}
1	1.1742
2	1.1774
3	1.1806
4	0.7101
5	0.5709
6	0.6529
7	1.1669
8	1.1774
9	1.1781
10	0.7079
11	0.5709
12	0.6529

5.5: Examples Summary

Theoretical examples have been provided that support the acceptability of the discriminating flickermeter for low frequency voltage fluctuations. It is possible to calculate the amount of flicker that a particular load of interest is producing when there are multiple loads connected electrically close together. This was verified by varying a load by some amount for some number of CPM and holding the other load constant. The flicker results were calculated for each load and it was the fluctuating load that was producing the flicker in each case. Based on the discussion in chapter 3, it is known that using cycle-by-cycle RMS voltage values with the flickermeter is not valid for high frequency fluctuations. It was seen in example 3 that this is validated, but it is still possible to determine which load is producing flicker even though the flicker value is invalid. Each of the four examples is based on theoretical data for theoretical loads with controlled fluctuations. It is appropriate to process field data to determine if this method gives reasonable results with data that is encountered in an uncontrolled environment.

Chapter 6: Device Implementation with Field Measurements

Theoretical data has been presented in chapter 5 that supports the idea of a device that is able to determine the amount of flicker that a load of interest is producing when there are multiple loads connected electrically close to each other. While it is important to establish that the device will work with theoretical data, it is critical to look at the device's performance in the field. Field applications rarely, if ever, have data that resemble the theoretical data that was processed in chapter 5. The goal of the flicker discriminator is to use it in field applications, thus it is necessary to test the device in the field and determine if the results are reasonable given known operating conditions for the loads that are measured. Multiple field data examples are going to be presented that have results that are reasonable based on the expected operation of the flicker discriminator and the known operating conditions of the loads that are measured.

A device that implements the requirements described in chapter 2 through chapter 4 has been built using a dell laptop and a NI USB-6356 data acquisition unit. The discriminator was connected to two EAFs at the first location in the power system and to another two EAFs at a second location in the power system. At each location, the two EAFs are connected electrically near to each other. This was done to see if it possible to discriminate between the total flicker amount that is due to all flicker producing sources that are connected electrically near and the amount that is due to a particular load in the same area.

6.1: Flicker Discriminator connected to EAF 1 and EAF 2

The first location that was selected has two flicker producing loads that are both EAFs. A single line diagram of a portion of the power system where the two EAFs are connected is provided in Fig. 6-1. The first EAF of interest has equipment installed to aid in mitigating the flicker impact on the power system. Because of this, the flicker contribution by this EAF is expected to be less than the total flicker level that is measured. The total flicker level and the discriminated flicker level results were calculated for 6 hours for the first EAF and they are provided in Fig. 6-2. The figure label "DFL" corresponds to the discriminated flicker results and the figure label "TFL" corresponds to the total flicker level. Notice that the DFL results are less than the TFL results. This is expected because of the flicker mitigating equipment that is connected to this EAF.

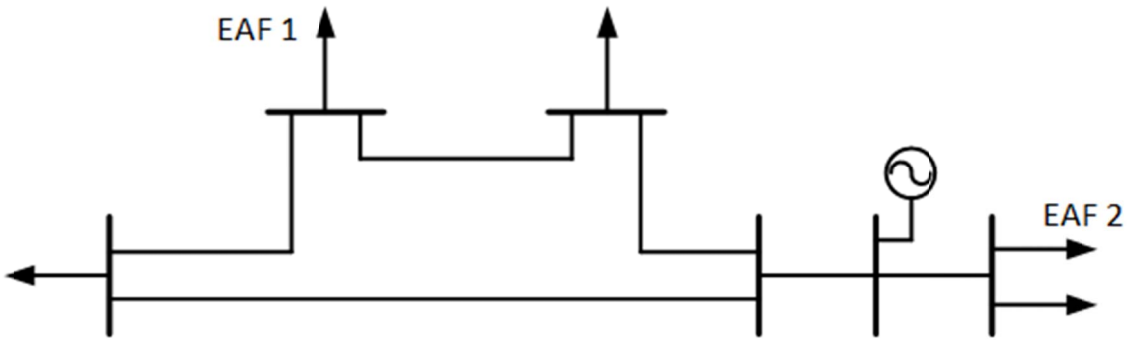

Figure 6-1. Power System Single Line Diagram of EAF Locations

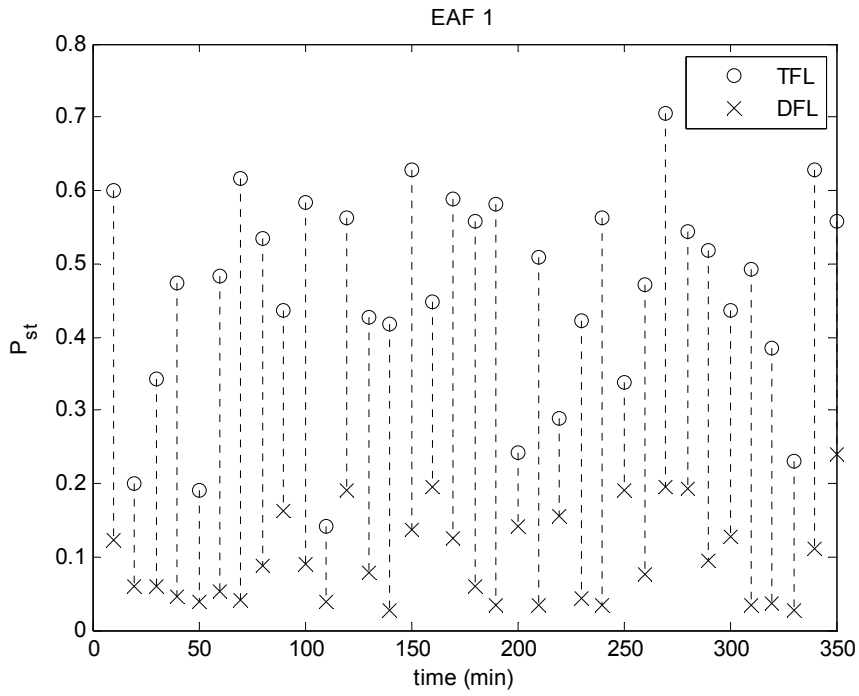

Figure 6-2. Discriminated Flicker Results for EAF 1

The flicker level for the second EAF that is connected electrically near to the first EAF is now calculated using the flicker discriminating device. The device is connected for 16.5 hours and the flicker results are provided in Fig. 6-3. Notice that the DFL results have a maximum percent difference of 6.25% of the TFL results. This means that the second EAF is producing the majority of the flicker level. This is expected because this EAF does not have a flicker mitigating device connected to limit its flicker impact to the power system.

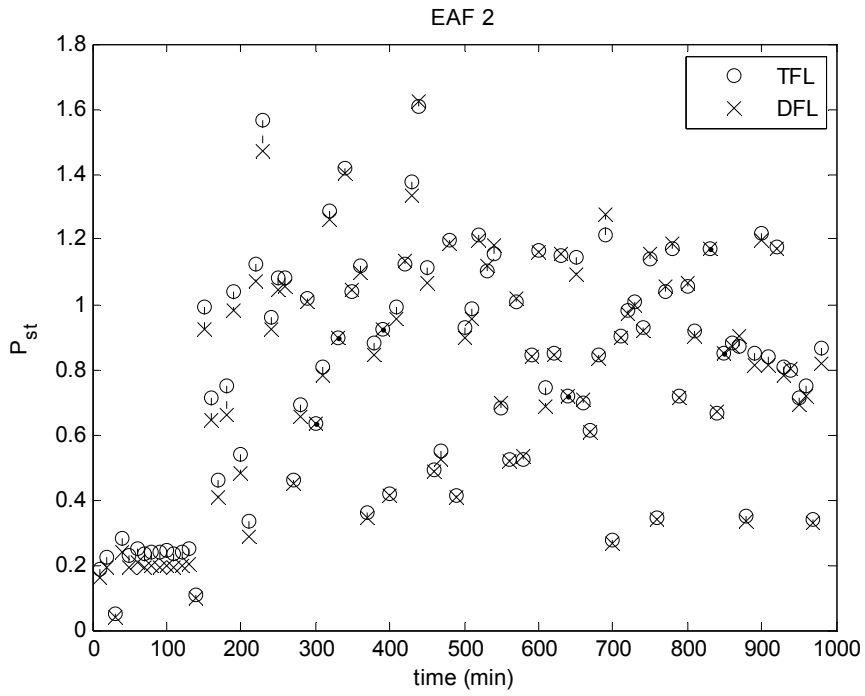

Figure 6-3. Discriminated Flicker Results for EAF 2

The two previous sets of data suggest that the flicker discriminator works as expected, but the amount of field data is only hours and the device must work for months. Next the flicker discriminating device collected flicker data for the first EAF, but for 3 weeks instead of a few hours. This data includes the total flicker level and the amount of flicker due to the first EAF that would be expected if there were not any other flicker producing sources connected electrically near. A plot of the flicker results are provided in Fig. 6-4. The ninety-fifth percentile flicker value for each of the 3 weeks was calculated and the results are provided in Table VI-I. As expected, the ninety-fifth percentile flicker values for EAF 1 are less than the total flicker values for each week.

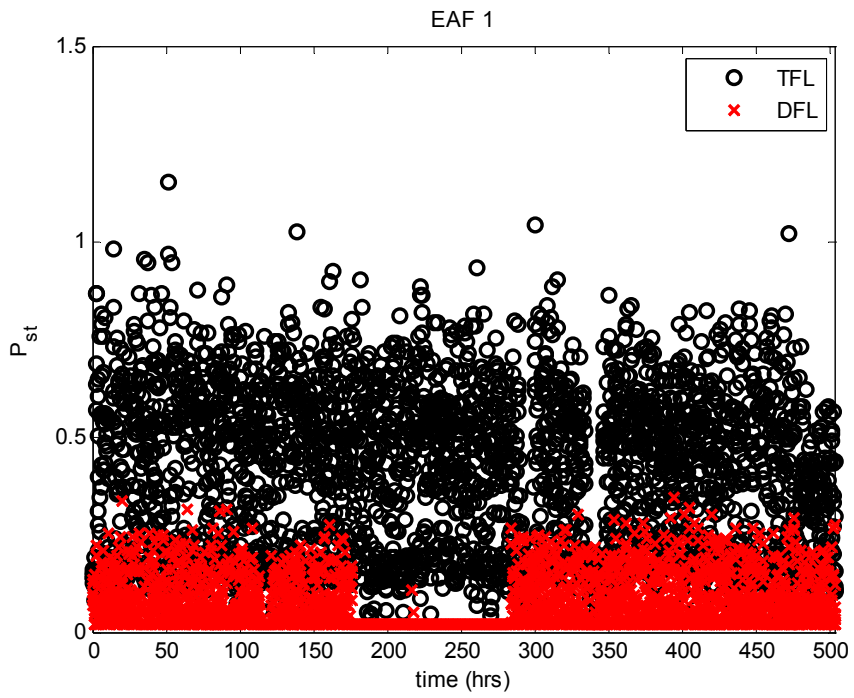

Figure 6-4. Discriminated Flicker Results for EAF 1 for 3 Week Data Set

TABLE VI-I.
95% FLICKER RESULTS FOR THE EAF

Flicker	Week 1	Week 2	Week 3
TOTAL	0.7463	0.7241	0.7170
EAF	0.2017	0.1775	0.2176

The results of the data collected with the two EAFs suggests that the device is able to discriminate between the amount of flicker that is present at the terminals of the EAFs that are connected electrically close and the amount that is due to the EAF of interest. It would be appropriate to utilize the flicker discriminating device at another location to determine if it still operates as expected.

6.2: Second Test Location with EAF 3 and EAF 4

The second location that the flicker discriminator was connected too has two EAFs that are connected electrically near to each other. A single line diagram of a section of the power system where the EAFs are connected is provided in Fig. 6-5. The flicker discriminator device was connected to both EAF 3 and EAF 4 for months to collect the TFL and DFL at each EAF.

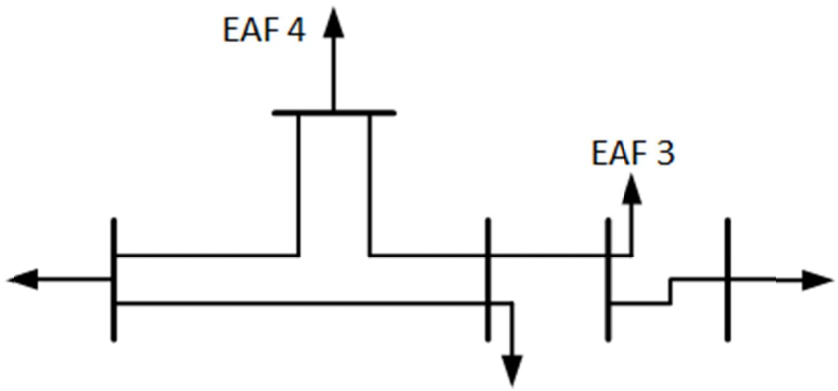

Figure 6-5. Power System Single Line Diagram of EAF Locations

Additionally, the EAF operating data has been collected for each EAF to compare the flicker levels based on when the EAFs were operating. There are four operating conditions that are of interest to compare to the flicker levels calculated by the flicker discriminator. These operating conditions are:

1. Both EAFs are operating,
2. The EAF at the measurement site is operating and the other EAF is not operating,
3. The EAF at the measurement site is not operating and the other EAF is operating,
4. Both EAFs are not operating.

Each of these four operating conditions will be considered when the flicker discriminator is connected to EAF 3 and then again when it is connected to EAF 4. It is expected that the DFL level will be slightly less than the TFL level for the first operating condition because the TFL will include the flicker produced by both EAFs, whereas the DFL is for only one of the EAFs. In the second operating condition, the TFL and DFL levels should be very close together because only the EAF to which the flicker discriminator is connected is operating. During the third operating condition, the TFL level should be much larger than the DFL level because the EAF that the flicker discriminator is not connected too is operating. For the fourth operating condition, the TFL and DFL levels will be similar and they will be small because both of the EAFs are not operating, thus they will not be producing flicker in the power system. These conditions will be applied to EAF 3 first and then these same conditions will be applied to EAF 4.

6.3: Flicker Discriminator connected to EAF 3

The flicker discriminator device was connected to EAF 3 in Fig. 6-5 to determine the TFL and DFL for various operating conditions of both EAF 3 and EAF 4. The first operating condition is when both EAF 3 and EAF 4 are operating. A plot of the total demand power for each of the EAFs for 12 hours is provided in Fig. 6-6; notice that each EAF is operating during this time interval. The TFL and DFL results measured by the flicker discriminator are provided in Fig. 6-7. Notice that the DFL result is typically less than the TFL result at EAF 3 for this operating condition. The DFL results exceed the TFL results six times in this 12 hour window by a maximum of 6.8%. A DFL result that is a few percent higher than the TFL is most likely due to the impedance estimation

technique transient that is produced for changes in the power system Thévenin impedance as discussed in chapter 5.4. The Thévenin impedance at the terminals of EAF 3 has most likely changed and incorrect voltage values are calculated from the power flow calculation that produces a slightly larger DFL result than the TFL result.

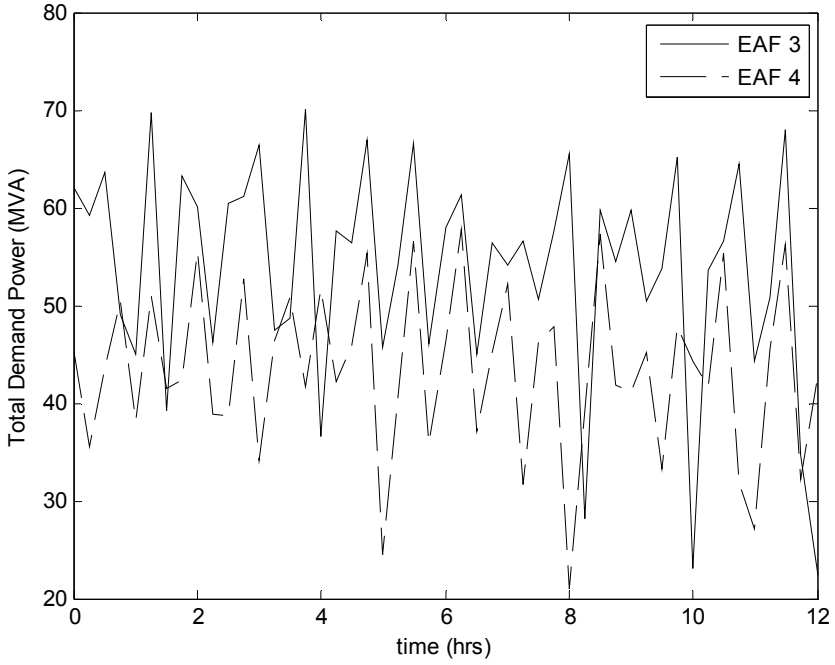

Figure 6-6. Total Demand Power for each EAF for the First Operating Condition

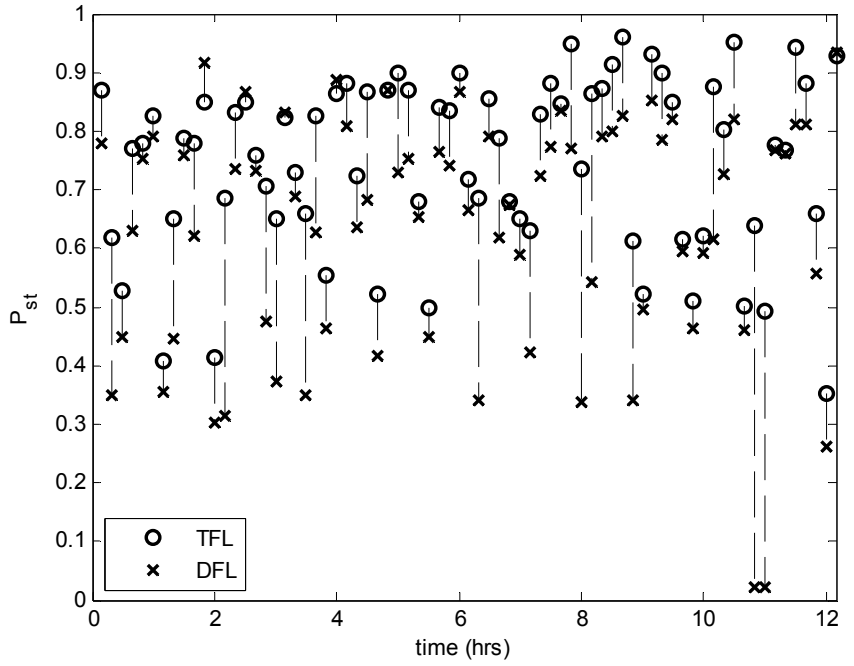

Figure 6-7. Flicker Levels Measured at EAF 3 for the First Operating Condition

The second operating condition for consideration involves EAF 3 operating and EAF 4 not operating. Under this operating condition, the DFL and TFL results should be very similar because EAF 3 is the only flicker producing source that is operating. The total demand power for each of the EAFs is provided in Fig. 6-8. Notice that the power level for EAF 3 is similar to the level in Fig. 6-6 and the power level for EAF 4 is significantly less than the level in Fig. 6-6 because it is not operating. A plot of the DFL and TFL results measured by the flicker discriminator are provided in Fig. 6-9. As expected, the DFL and TFL results are very similar.

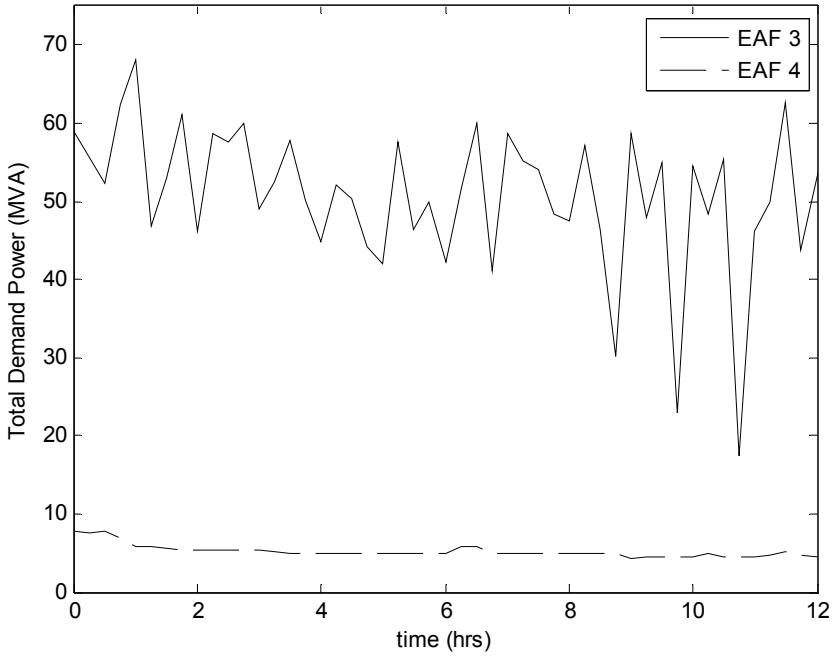

Figure 6-8. Total Demand Power for each EAF for the Second Operating Condition

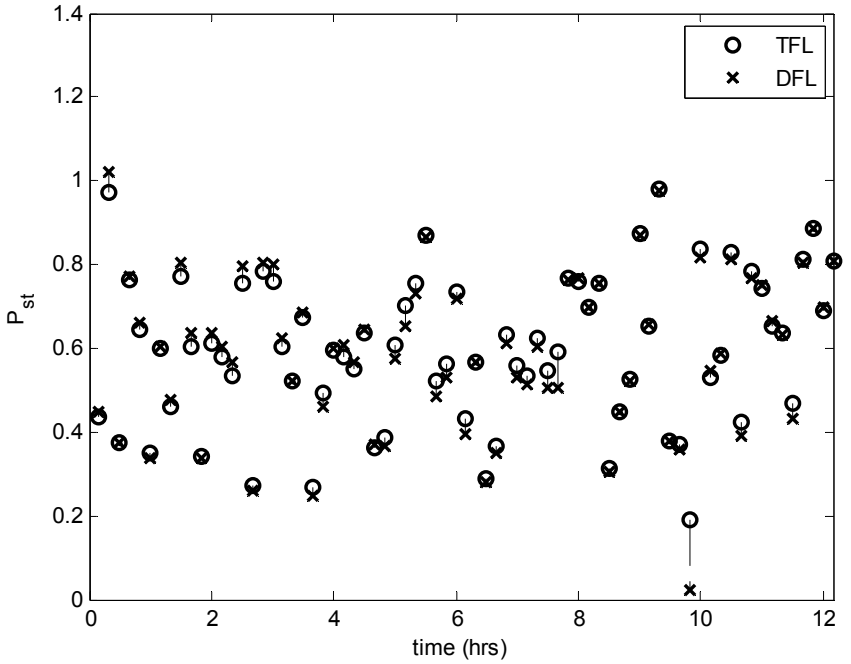

Figure 6-9. Flicker Levels Measured at EAF 3 for the Second Operating Condition

The third operating condition to consider is when EAF 3 is not operating, but EAF 4 is operating. During this operating condition, the DFL results will be significantly less than the TFL results because EAF 3 is not producing any flicker. The total demand power for each of the EAFs is provided in Fig. 6-10. Notice that the power level for EAF 3 is much less than the level provided in Fig. 6-6 and the power level for EAF 4 is similar to the level provided in Fig. 6-6. A plot of the DFL and TFL results measured by the flicker discriminator are provided in Fig. 6-11. As expected, the DFL results are all less than the TFL results because EAF 3 is not operating.

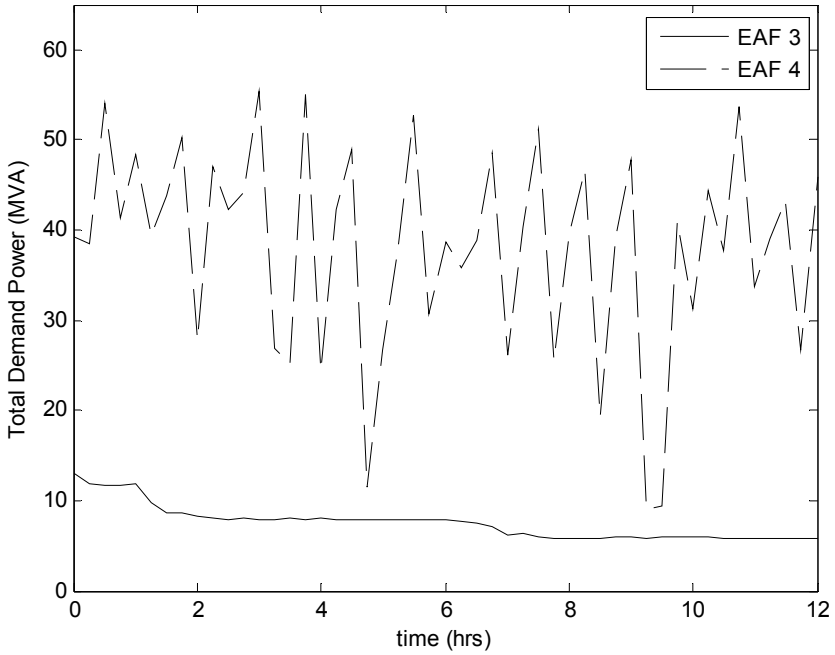

Figure 6-10. Total Demand Power for each EAF for the Third Operating Condition

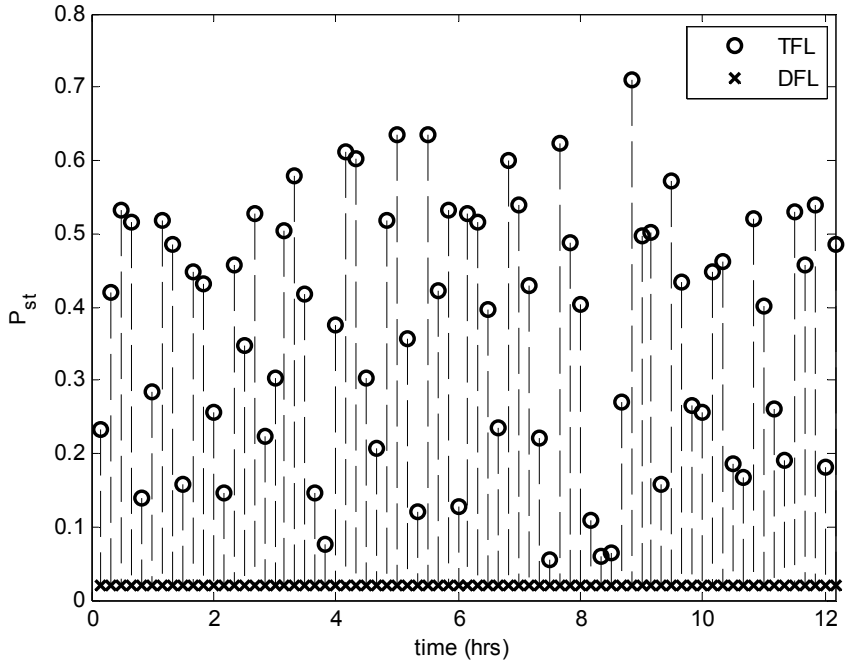

Figure 6-11. Flicker Levels Measured at EAF 3 for the Third Operating Condition

The fourth case to consider is when both EAF 3 and EAF 4 are not operating. It is expected that the DFL and TFL results will be low because neither flicker producing source is operating. The total demand power for each of the EAFs is provided in Fig. 6-12. Notice that the power level for each of the EAFs is significantly less than the levels provided in Fig. 6-6. A plot of the DFL and TFL results measured by the flicker discriminator are provided in Fig. 6-13. As expected, the DFL results and the TFL results have low flicker values.

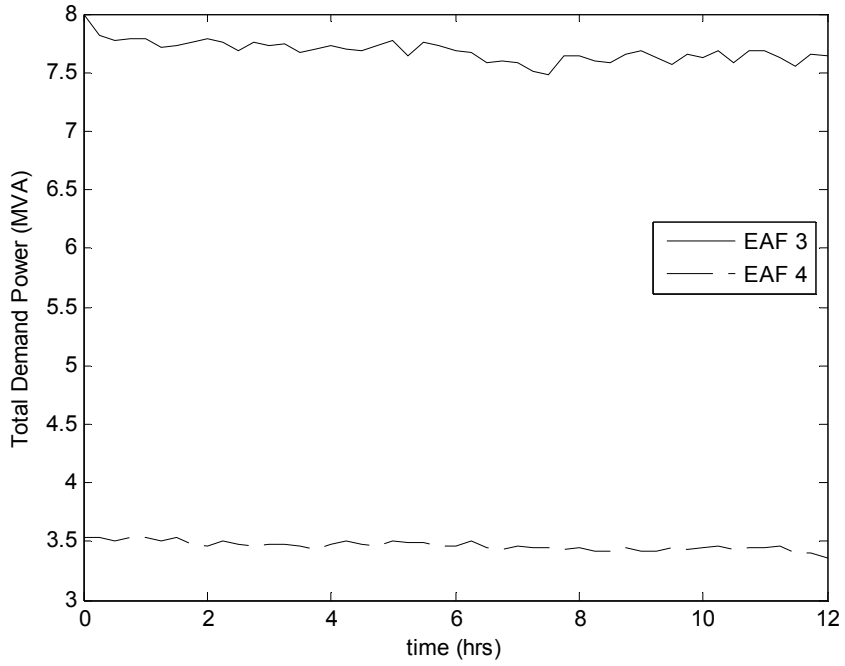

Figure 6-12. Total Demand Power for each EAF for the Fourth Operating Condition

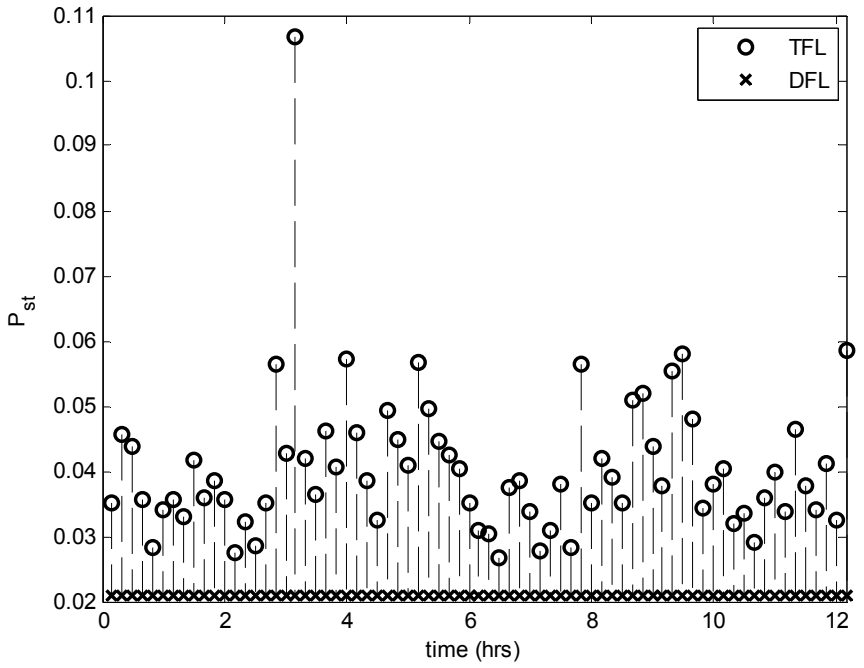

Figure 6-13. Flicker Levels Measured at EAF 3 for the Fourth Operating Condition

Each of these four cases represents different operating conditions for both EAF 3 and EAF 4 such that comparisons of the DFL and TFL results could be made. There are expectations about the relationship between the DFL and TFL results based on the operating conditions of both EAFs. The expected relationships between the DFL and TFL results were all substantiated in each operating case for when the flicker discriminator was connected to EAF 3. These results support correct operation of the flicker discriminator in that it is possible to determine the flicker level at a load of interest when there are other flicker producing sources that are connected electrically close. It is appropriate to connect the flicker discriminator to EAF 4 and repeat the analysis to verify that the flicker discriminator continues to operate as expected.

6.4: Flicker Discriminator connected to EAF 4

The flicker discriminator device was connected to EAF 4 in Fig. 6-5 to determine the TFL and DFL for various operating conditions of both EAF 3 and EAF 4. There is a 115 kV to 13.8 kV transformer that connects EAF 4 to the 115 kV transmission system as illustrated in Fig. 6-14.

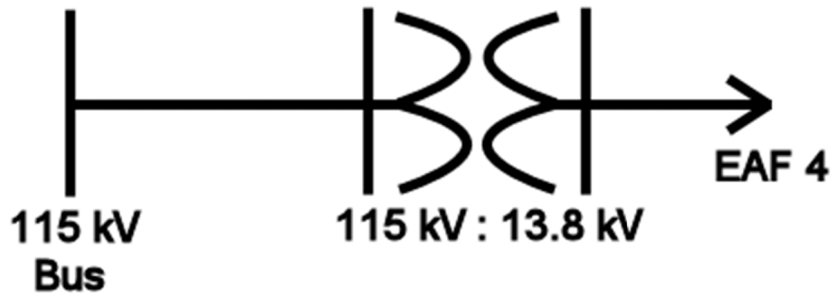

Figure 6-14. Single Line Diagram of Transformer Connecting EAF 4 to 115 kV Bus

The measurement point at EAF 4 is on the low voltage (LV) side of the transformer because there are not any potential transformers connected to the 115 kV side of the transformer to use to make measurements. The local utility company provided the flicker transfer coefficient of 0.0854 that is based on a short-circuit study to transfer the flicker values to the high voltage (HV) side (115 kV) of the transformer. The first operating condition for consideration is when both EAF 3 and EAF 4 are operating. A plot of the total demand power for each of the EAFs for 12 hours is provided in Fig. 6-15; notice that each EAF is operating during this time interval. The TFL and DFL results measured by the flicker discriminator and transferred to the high voltage side of the transformer are provided in Fig. 6-16. When the DFL values were reflected to the high voltage side of the transformer, the information about the background flicker due to EAF 3 and other flicker producing sources was lost. The flicker level at the measurement point when EAF 4 is not operating will be the same as the background flicker at the high voltage side of the transformer because a voltage drop is not produced in the transformer from the load current of EAF 4. The average background flicker level was found to be 0.27 from Fig. 6-17. The cubic summation law in (6-1) was utilized to calculate the TFL results from the average background flicker level and the DFL results at the high voltage side of the transformer. As expected, the DFL results are a little less than the TFL results.

$$P_{st} = \sqrt[3]{\sum_i P_{st,i}^3} \tag{6-1}$$

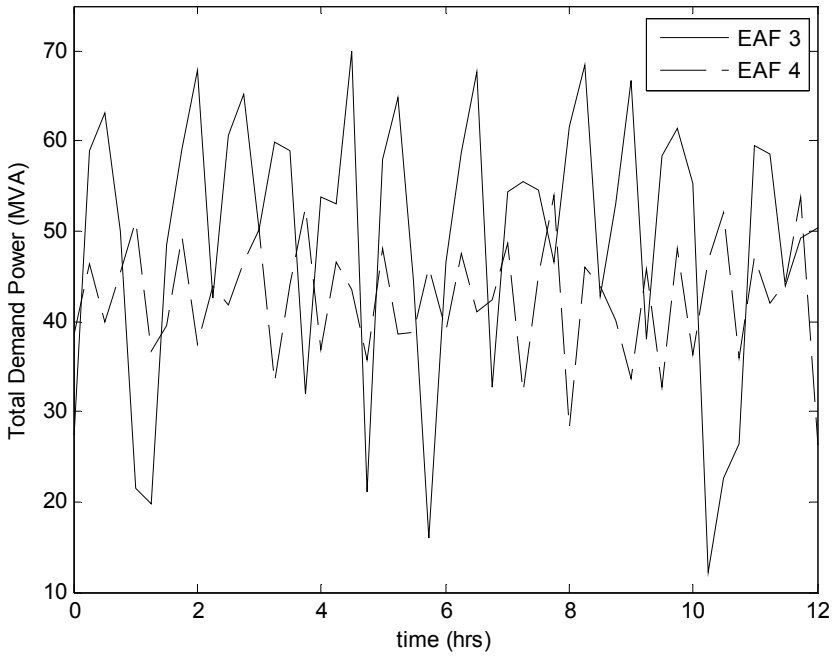

Figure 6-15. Total Demand Power for each EAF for the First Operating Condition

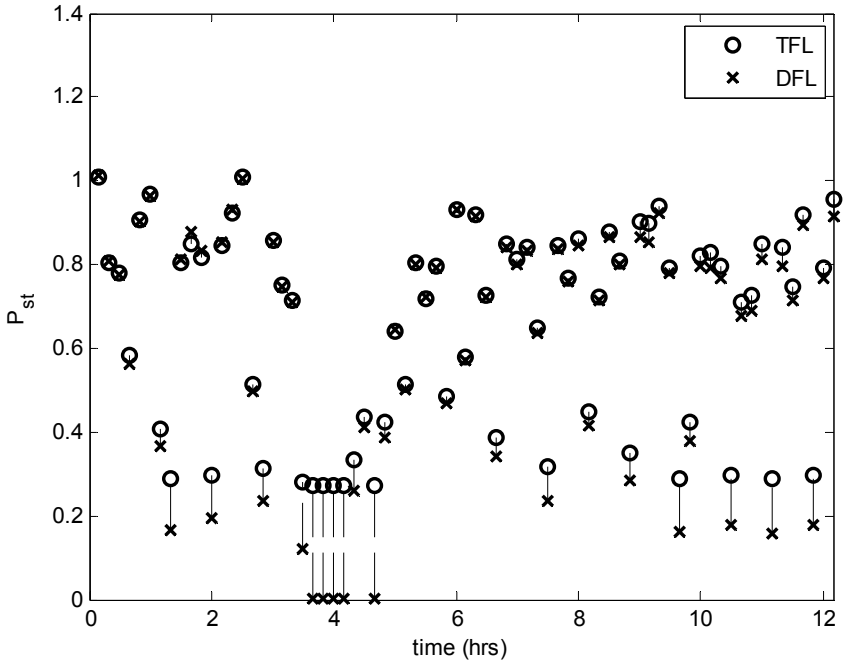

Figure 6-16. Flicker Levels Measured at EAF 4 for the First Operating Condition

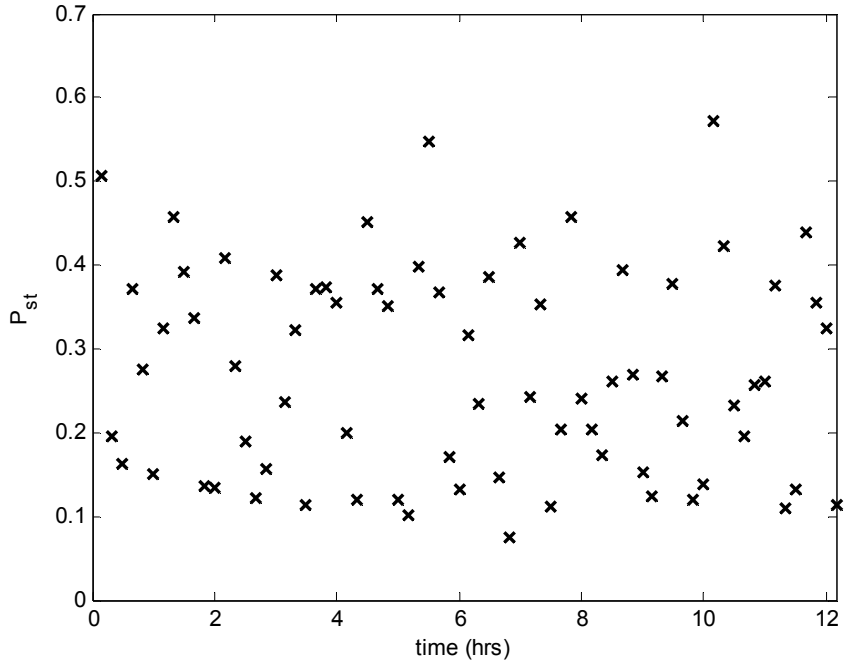

Figure 6-17. Background Flicker Levels Measured at EAF 4

The second operating condition for consideration involves EAF 3 not operating and EAF 4 operating. The information necessary to evaluate this operating condition is not available because the flicker discriminator was connected to the LV side of the transformer at EAF 4. Any background flicker that is present on the HV side of the transformer is lost at the LV side because of the extremely large flicker values at the LV side when EAF 4 is operating. This means that the TFL and DFL results will be the same at the LV side of the transformer where the flicker discriminator is connected. It is possible to transfer both the TFL and DFL results to the HV side using the 0.0854 transfer coefficient, however the results will still be the same because the transfer coefficient does not account for the fact that the background flicker is the same at both voltage levels.

The third operating condition to consider is when EAF 3 is operating, but EAF 4 is not operating. During this operating condition, the DFL results will be significantly less than the TFL results because EAF 4 is not producing any flicker. The total demand power for each of the EAFs is provided in Fig. 6-18. Notice that the power level for EAF 4 is much less than the level provided in Fig. 6-15 and the power level for EAF 4 is similar to the level provided in Fig. 6-15. A plot of the DFL and TFL results measured by the flicker discriminator are provided in Fig. 6-19. As expected, the DFL results are all less than the TFL results because EAF 4 is not operating.

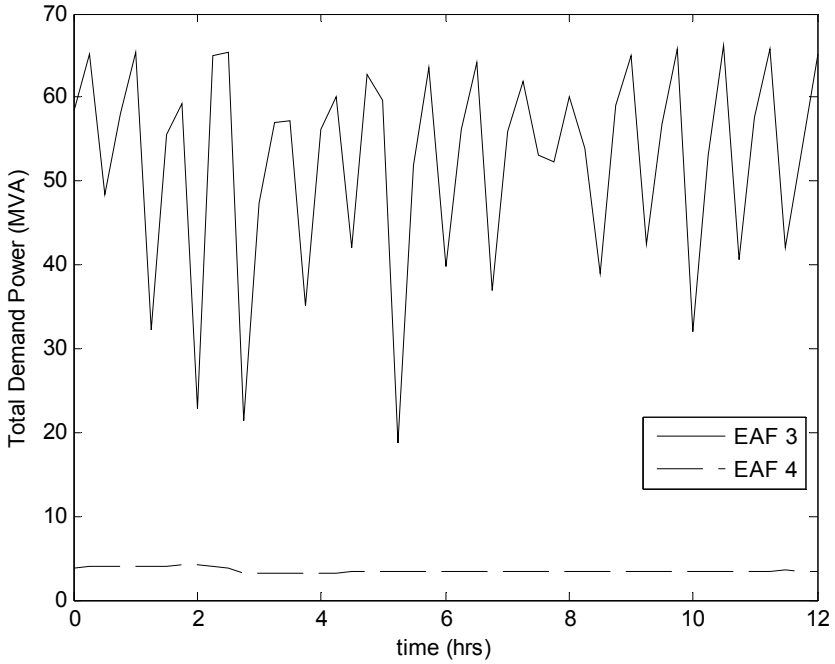

Figure 6-18. Total Demand Power for each EAF for the Third Operating Condition

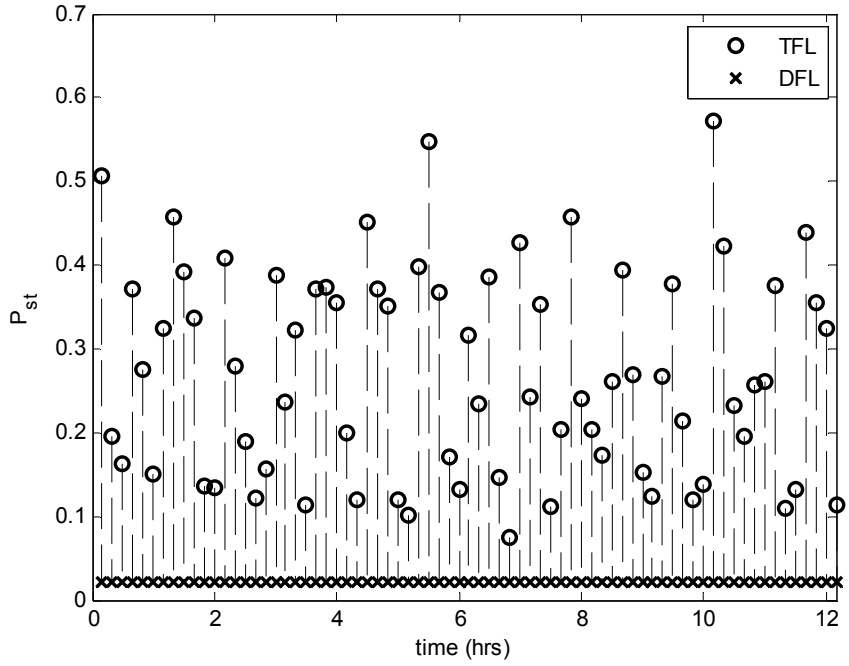

Figure 6-19. Flicker Levels Measured at EAF 4 for the Third Operating Condition

The fourth case to consider is when both EAF 3 and EAF 4 are not operating. It is expected that the DFL and TFL results will be low because neither flicker producing source is operating. The total demand power for each of the EAFs is provided in Fig. 6-20. Notice that the power level for each of the EAFs is significantly less than the levels provided in Fig. 6-15. A plot of the DFL and TFL results measured by the flicker discriminator are provided in Fig. 6-21. As expected, the DFL results and the TFL results have low flicker values (less than 0.1) because both flicker producing sources are off.

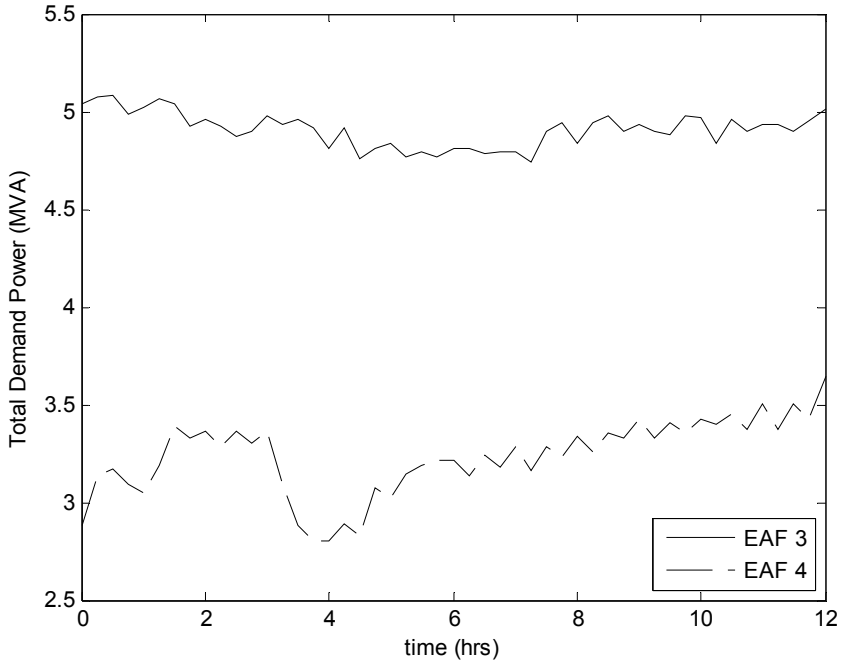

Figure 6-20. Total Demand Power for each EAF for the Fourth Operating Condition

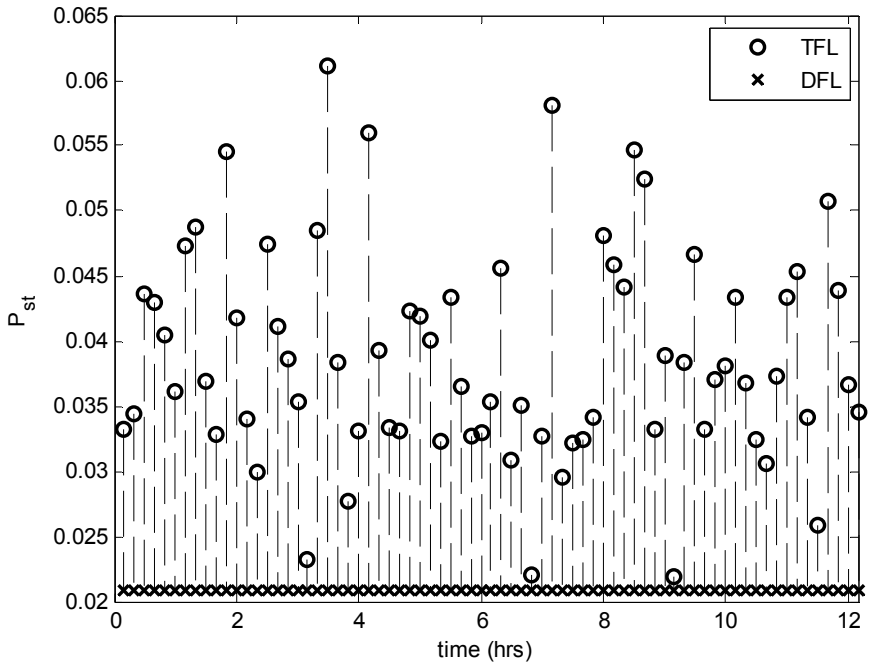

Figure 6-21. Flicker Levels Measured at EAF 3 for the Fourth Operating Condition

6.5: Flicker Discriminator with Field Data Conclusions

The discriminator was connected to two EAFs at the first location in the power system and to another two EAFs at a second location in the power system. At each location, the two EAFs are connected electrically near to each other. Data was collected at each of the EAFs that supports that the flicker discriminator is operating properly. This is because the collected flicker values are reasonable based on known operating conditions for each of the EAFs.

The flicker discriminator was connected to each of the first two EAFs for a few hours to see if reasonable flicker values were obtained. It was known that the first EAF has flicker mitigating equipment connected to decrease the flicker impact of the EAF, whereas the second EAF did not have any such equipment. The discriminated results for each EAF support that the second EAF produces the majority of the flicker for the area. This is a reasonable result because the EAF does not have the flicker mitigating equipment. Next the flicker discriminator was connected to the first EAF for three weeks. The results from the three weeks are also reasonable because the weekly ninety-fifth percentile discriminated flicker values are less than the ninety-fifth percentile total flicker values for each week.

Next, the flicker discriminator was connected to two different EAFs that are connected electrically close together for months at a time. There were four different cases that represent different operating conditions for each of the EAFs that were considered when the flicker discriminator was connected to EAF 3 and again when it was connected to EAF 4. There are expectations about the relationship between the DFL and TFL results based on the operating conditions of both EAFs. The expected relationships

between the DFL and TFL results were all substantiated in each operating case for when the flicker discriminator was connected to EAF 3 and when it was connected to EAF 4. These results support correct operation of the flicker discriminator in that it is possible to calculate the amount of flicker that a particular load of interest is producing when there are other flicker producing sources connected electrically close to the load of interest.

Chapter 7: Conclusion

A flickermeter is a device that is used to assess the amount of voltage fluctuation that is present at a measurement point. In the case where there are multiple loads connected electrically close to each other, the flickermeter is not able to determine an individual load's flicker level; it can only measure the total level for the area. It is possible that there is one particular load that is connected that is producing significant voltage fluctuations that are negatively impacting other loads that are connected electrically close. But, a device is not available to determine which load is producing the issue. By having a device that is able to determine the flicker level that a particular load is producing, the utility will be able to enforce limits so that loads do not negatively impact the power system.

A device that can determine the flicker level of a particular load works by first calculating the equivalent voltage at a particular load of interest's terminals on a cycle-by-cycle basis. Calculating the voltage is a well understood problem and it is accomplished by performing a two bus power flow. In order to calculate a valid voltage, it is necessary to have a valid Thévenin equivalent impedance at the load of interest's terminals. Once the cycle-by-cycle voltage values are calculated, the device then processes these calculated voltages with the flickermeter that is described in IEEE 1453. The flicker result applies specifically to the load of interest and is independent of any other loads that are connected electrically near to the load of interest.

In chapter 2, a discussion as to how to calculate a valid Thévenin impedance was presented. It was found that using a change in power as a threshold to calculate an impedance value will minimize the number of invalid impedance calculations because the power system will be sufficiently excited. However, some invalid impedance calculations will still be calculated even though the power threshold is met. A low pass filter is used to prevent any one invalid impedance calculation from significantly affecting the estimated impedance.

A discussion is presented in chapter 3 as to the validity of using cycle-by-cycle RMS voltage values as the input to the flickermeter. This is necessary because time sampled voltage data is specified as the flickermeter input in IEEE 1453. A thorough investigation is provided and it is found that it is acceptable to utilize cycle-by-cycle RMS voltage data as the input to the flickermeter defined in IEEE 1453 as long as the voltage fluctuations are known to be low frequency. There were several issues presented that impact the flicker result for high frequency fluctuations, but do not negatively impact low frequency fluctuations. Because of the discussed issues, it does not appear, in general, to be possible to predict over- or under-conservative flicker results with RMS input for high frequency fluctuations.

A device that is able to determine the amount of flicker that a particular load of interest is producing where there are multiple loads connected close by has been presented. The device requirements and limitations have been presented to build a device that is able to discriminate flicker for multiple flicker producing sources. A software implementation of the device was designed to test with theoretical parallel loads in chapter 5. The theoretical data that was collected supports the idea that the device can

calculate a flicker level for a specific load connected to a location with other loads connected electrically near. However, by verifying that the device works for theoretical data does not mean that the device will operate properly in the field.

The flicker discriminator was connected to various load types for weeks and months. It was connected to an EAF that has a flicker mitigating device for three weeks. Next it was connected to another load for several months and the flicker levels were correlated to when the load was operating. Then it was connected to a third load for several months and the flicker levels were again correlated to when the load was operating. The months of field data that was collected from the flicker discriminator verifies that it is possible to determine the actual flicker level that a particular load of interest is producing when there are other loads connected electrically near.

In conclusion, an algorithm has been provided that is able to track the Thévenin equivalent impedance at the terminals of a load. Next, a thorough investigation has been provided to show that it is acceptable to utilize cycle-by-cycle RMS voltage data as the input to the flickermeter described in IEEE 1453 for low frequency voltage fluctuations. This is a huge advancement to the field because it allows for offline processing of data that is collected by voltage recorders. Finally, the flicker discriminator device was tested with theoretical data and months of field data was collected that supports proper device operation.

References

[1] IEEE Recommended Practice--Adoption of IEC 61000-4-15:2010, Electromagnetic compatibility (EMC)--Testing and measurement techniques--Flickermeter--Functional and design specifications," *IEEE Std 1453-2011*, pp.1-58, Oct. 21 2011.

[2] M. Sumner, D.W.P Thomas, A. Abusorrah, and P. Zanchetta, "Power System Impedance Estimation for Improved Active Filter Control, using Continuous Wavelet Transforms," *Proc. IEEE Power Eng. Soc. Transmission Distribution Conf. Exhibit.*, pp.653-658, May 21-24, 2006.

[3] M. Bahadornejad and G. Ledwich, "System Thevenin impedance estimation using signal processing on load bus data," in *Pro. 6th Int. Conf. Advances in Power System Control, Operation and Management (APSCOM)*, Nov. 2003, pp.274-279.

[4] R.W. Wilson, G.A. Zevenbergen, D.L. Mah, and A.J. Murphy, "Calculation of transmission line parameters from synchronized measurements," *Electric Power Components and Systems*, vol.27, no.12, pp.1269-1278, 1999.

[5] I. Kim and R.K. Aggarwal, "A study on the on-line measurement of transmission line impedances for improved relaying protection," *Int. J. Elect. Power & Energy Syst.*, vol. 28, no.6, pp.359, 2006.

[6] M. Bahadornejad and N.K.C. Nair, "System Thevenin Impedance Estimation Through On-Load Tap Changer Action," *Universities Power Engineering Conference (AUPEC)*, Dec. 2010, pp.1-5.

[7] S.A. Arefifar, and W. Xu, "Online Tracking of Power System Impedance Parameters and Field Experiences", *IEEE Transactions on Power Delivery*, Vol. 24, No. 4, October 2009.

[8] Eidson, B.L.; Geiger, D.L.; Halpin, M., "Equivalent power system impedance estimation using voltage and current measurements," *Power Systems Conference (PSC), 2014 Clemson University* , vol., no., pp.1,6, 11-14 March 2014.

[9] Yang, X.X.; Kratz, Maurice, "Power System Flicker Analysis by RMS Voltage Values and Numeric Flicker Meter Emulation," *Power Delivery, IEEE Transactions on*, vol.24, no.3, pp.1310-1318, July 2009.

[10] Electromagnetic compatibility (EMC)—Part 3-7: Limits — Assessment of emission limits for the connection of fluctuating installations to MV, HV and EHV power systems—Basic EMC Publication IEC Tech. Rep. 61000-3-7, 2008, Ed. 2.0.

[11] E. W. Kamen and B. S. Heck, *Fundamentals of Signals and Systems Using the Web and Matlab*, 3rd ed., Upper Saddle River, New Jersey: Prentice Hall, 2006.